POLYTECHNIQUE MONTRÉAL

affiliée à l'Université de Montréal

Seismic Behaviour and Design of Two-Bay Steel Multi-Tiered Braced Frames and Other Special Steel Concentrically Braced Frames in Single-Storey Buildings

CHRISTOPHE COMEAU

Département des génies civil, géologique et des mines

Mémoire présenté en vue de l'obtention du diplôme de *Maîtrise ès sciences appliquées*

Génie Civil

Août 2020

© Christophe Comeau, 2020.

POLYTECHNIQUE MONTRÉAL

affiliée à l'Université de Montréal

Ce mémoire intitulé :

Seismic Behaviour and Design of Two-Bay Steel Multi-Tiered Braced Frames and Other Special Steel Concentrically Braced Frames in Single-Storey Buildings

présenté par **Christophe COMEAU**

en vue de l'obtention du diplôme de *Maîtrise ès sciences appliquées*

a été dûment accepté par le jury d'examen constitué de :

Sanda KOBOEVIC, présidente
Robert TREMBLAY, membre et directeur de recherche
Ali IMANPOUR, membre et codirecteur de recherche
Colin ROGERS, membre

DÉDICACE

À Fritz,

Pour l'étincelle

À Papa,

Pour m'avoir appris la place de l'Art dans le monde

REMERCIEMENTS

Je tiens tout d'abord à remercier mon directeur de recherche, Robert Tremblay, pour son soutien et son encadrement au cours des dernières années. Je suis extrêmement reconnaissant d'avoir eu l'opportunité de travailler sur ce projet de recherche, d'échanger avec vous et de commencer à bâtir un bagage d'ingénieur à vos côtés. Les apprentissages que j'aurai réalisés, autant sur le plan technique qu'humain, me seront perpétuellement utiles. Merci pour vos encouragements et pour votre regard critique, et surtout pour soutien moral que vous avez su m'apporter durant les hauts et les bas de ce projet de recherche. Merci également à Ali Imanpour, qui a su m'épauler avec brio en tant que co-directeur de recherche. Merci pour votre expertise et vos conseils. Je garde de bons souvenirs de nos échanges et discussions sur les meilleures hypothèses et méthodes à considérer.

Paul, merci à toi pour tous ces merveilleux moments passés au bureau et ailleurs. Je n'aurais jamais pu souhaiter un meilleur collègue de travail. Au-delà de cela, évidemment, ton amitié m'est véritablement très chère. Ton écoute, ton soutien et tes conseils auront été primordiaux à mon cheminement et à ma réussite au plan personnel. J'espère simplement qu'un jour tu amèneras tes connaissances géographiques au même niveau que ton expertise des répliques des classiques du cinéma français.

Merci à Pablo, dont j'ai fait la connaissance en même temps que je découvrais mon sujet de recherche. Nos longs échanges sur le comportement sismique des charpentes d'acier et sur les procédures optimales de conception m'auront permis de perfectionner ma compréhension de mon sujet de recherche. Je sais que tu vis la même excitation que moi quand les spécimens d'essais sont livrés au laboratoire, et j'ai hâte de partager avec toi la suite de ce projet expérimental

Je souhaite remercier tout le personnel du GRS avec qui j'ai interagi au cours des dernières années. L'encadrement et les activités organisées par le département sont essentielles à la cohésion du groupe. Un merci particulier à Simon Bourget, Martin Leclerc, Julie Dallaire et Patrice Bélanger pour leurs conseils et soutien au cours de ce projet.

À l'extérieur du cadre de recherche, merci évidemment à tous mes amis qui, de près ou de loin, m'auront entendu parler de ma maîtrise et m'auront écouté et encouragé. Autant à PolyPhoto qu'au Rosemont, merci du fond du cœur; vous savez qui vous êtes.

Un merci tout particulier à ma famille, qui m'aura apporté un soutien inébranlable durant ces trois années. Vos accolades, vos regards ébahis et vos airs intéressés m'auront insufflé énormément de motivation. Merci à Papa et Ilan, pour m'avoir écouté discuter de systèmes structuraux avec intérêt.

Merci enfin au FRQNT, pour m'avoir octroyé cette bourse d'études durant mon parcours aux études supérieures. Celle-ci m'aura permis de me concentrer sur l'achèvement de ma maîtrise, en diminuant largement le poids financier présent sur les épaules de tout étudiant.

RÉSUMÉ

Pour les structures de bâtiments en acier de grande hauteur comme les centres sportifs, les hangars d'avions, les bâtiments industriels ou les entrepôts, il est courant d'utiliser des contreventements concentriques en treillis à segments multiples (CCSM). Ces CCSM sont constitués de plusieurs panneaux contreventés superposés sur la hauteur de l'étage. Chacun de ces panneaux est appelé un segment. Cette configuration de contreventements résulte en l'utilisation de diagonales plus courtes, ce qui permet généralement de minimiser l'aire des sections choisies et de respecter plus facilement les critères d'élancement et de rapport largeur sur épaisseur. Des bielles intermédiaires sont placées entre chaque segment contreventé, afin de résister aux efforts axiaux débalancés des diagonales qui surviennent lorsque les diagonales flambent en compression. La redistribution de ces efforts axiaux débalancés au moyen des bielles permet d'éviter un comportement de cadre contreventé en « K », pour lequel les colonnes doivent résister d'importantes sollicitations flexionnelles dans le plan du cadre. Dans des CCSM, les colonnes sont généralement constituées de profilés en I orientés de tel manière à ce que le flambement hors plan survienne autour de l'axe fort du profilé, sur toute la hauteur de l'étage. Les bielles permettent de contreventer latéralement les colonnes à la hauteur de chaque segment contre le flambement autour de l'axe faible. Les résultats d'études antérieures ont démontré que les déformations inélastiques dans les CCSM sont concentrées dans un segment, appelé le segment critique. Deux considérations majeures découlent de ce constat. Tout d'abord, d'importantes déformations inélastiques peuvent survenir dans la diagonale en tension du segment critique, ce qui peut donner lieu à une rupture prématurée par fatigue. Ensuite, la concentration des déplacements inélastiques dans le segment critique entraine des moments de flexion dans les colonnes dans le plan du cadre, ce qui peut mener à des phénomènes d'instabilité. Les codes canadien et américain requièrent que ce comportement soit explicitement considéré lors du dimensionnement de CCSM.

Ce projet de recherche porte sur la réponse sismique de systèmes de contreventements pouvant à priori montrer un comportement similaire à ce qui est décrit ci-haut. Le premier type de contreventement étudié est le CCSM à deux baies, où deux CCSM sont placés côte à côte dans des baies adjacentes. Le deuxième système de cadre contreventé à l'étude est le contreventement concentrique en treillis sur deux baies. Celui-ci correspond à un cadre contreventé typique, où les diagonales sont étendues sur deux baies, faisant intersection avec une colonne intermédiaire. Le

troisième système à l'étude est le cadre contreventé en X séparé. Celui-ci comporte une bielle à mi-hauteur du cadre permettant de contreventer latéralement les colonnes.

L'objectif de ce projet de recherche est d'étudier le dimensionnement et le comportement sismique des systèmes de cadre contreventé susmentionnés, pour des bâtiments situés à Vancouver en Colombie-Britannique. Cet objectif fut mené à bien en développant un modèle numérique à l'aide du logiciel *OpenSees*, lequel permet de simuler adéquatement le comportement inélastique des diagonales de contreventement et des colonnes. La conception d'un CCSM à deux segments a été réalisée selon les codes canadien et américain. Finalement, des analyses temporelles non-linéaires ont été complétées pour les trois systèmes à l'étude.

La conception d'un CCSM à deux segments a permis de mettre en évidence des différences clés entre les approches de conception canadienne et américaine. La variation de la demande anticipée en ductilité mène à un poids sismique et un cisaillement à la base différent pour une même section de diagonales. De plus, la conception des colonnes diffère entre les deux codes. La norme canadienne requiert qu'une analyse progressive de la plastification soit réalisée, alors que la norme américaine requiert que la colonne soit suffisamment résistance en flexion pour accommoder le cisaillement débalancé provenant de la résistance probable des panneaux contreventés adjacents. Cela mène à une colonne plus lourde pour la conception américaine.

Des analyses temporelles non-linéaires des CCSM à deux baies adjacentes ont été réalisées. Les résultats montrent que la plastification progressive des panneaux contreventés survient de manière analogue à ce qui est observés pour des CCSM à une seule baie. Cette plastification progressive se produit dans différents panneaux, mais également dans différentes baies. La méthode de conception utilisée fut en mesure de prédire adéquatement la séquence de plastification des panneaux, ainsi que la demande flexionnelle en plan des colonnes. Des différences entre les valeurs de conception et les résultats d'analyses pour ce dernier paramètre furent observées en raison des valeurs supposées d'efforts axiaux dans les diagonales durant la conception. Ensuite, il a été déterminé que les déplacements inélastiques au toit sont systématiquement sous-estimés en conception. À contrario, la demande flexionnelle hors-plan des colonnes est surestimée par la méthode de conception, basée sur la norme CSA S16-19.

Des analyses temporelles non-linéaires sur les cadres contreventés en X à deux baies ont montré que le comportement des cadres est adéquat, avec ou sans l'utilisation d'une bielle intermédiaire.

Le comportement des diagonales de contreventement était similaire pour le haut et le bas du cadre, et reflétait les caractéristiques typiques d'un cadre contreventé classique. Lorsqu'une bielle intermédiaire était introduite, les colonnes extérieures développaient une demande en flexion dans le plan du cadre significative, lesquels étaient prédits par la méthode de conception. De plus, lorsque la variation inhérente de la contrainte de plastification de l'acier des diagonales était considérée, il a été déterminé que la colonne intérieure pouvait également être soumise à des efforts de flexion dans le plan du cadre.

Finalement, des analyses temporelles non-linéaires ont été menées pour un modèle de contreventement en X séparé. La bielle intermédiaire permettait aux colonnes d'être contreventées latéralement contre le flambement autour de leur axe faible. Par contre, après la plastification des diagonales en tension, le point d'intersection des diagonales subissait des déplacements horizontaux dans le plan du cadre conséquents. Ceux-ci résultaient en un effort axial dans la bielle intermédiaire et dans en des moments de flexion dans les colonnes, supérieurs aux valeurs anticipées en conception. La réponse du cadre montrait des caractéristiques typiques aux CCSM, puisque des déformations inélastiques étaient concentrées dans la partie supérieure des colonnes.

ABSTRACT

In tall single-storey steel structures such as sports facilities, airplane hangars, industrial buildings or warehouses, multi-tiered concentrically braced frames (MT-CBFs) are commonly used. MT-CBFs consist of a bracing system where multiple braced panels are stacked over each other along the storey height. Each panel is referred to as a *tier*. This bracing configuration results in shorter braces, which typically leads to minimized brace sections and easier compliance with slenderness and width-to-thickness requirements. Intermediate struts are provided at tier levels, to resist unbalanced brace axial loads that develop after the compression braces have buckled. This redistribution of unbalanced axial loads through struts prevents undesirable K-braced frame behaviour, where the columns must resist large in-plane flexural demands. The columns typically consist of I-shaped members oriented such that strong-axis bending is utilized to resist out-of-plane bending moments over the frame height. Struts allow the columns to be laterally braced at tier levels for weak-axis buckling. Results from previous studies showed that under seismic loading inelastic deformations in MT-CBFs tend to concentrate in one critical tier. Two major concerns arise from this phenomenon. On one hand, significant inelastic deformations can occur in the bracing members of the critical tier, which may result in brace fracture due to low cycle fatigue. On the other hand, concentration of inelastic drifts in one tier leads to in-plane bending demands in the columns, which may cause instability. Both Canadian and American seismic design provisions require MT-CBFs to be designed for seismic loading assuming a concentration of inelastic deformations in one tier.

This research project focuses on the seismic response of bracing systems that can presumably exhibit behaviour similar to the one described above. The first studied bracing system is two-bay MT-CBFs, where two multi-tiered braced frames are placed side by side in adjacent bays. The second studied bracing system consists of two-bay X-CBFs, where a standard braced frame spans over two column bays, intersecting with a middle column. The third and last studied bracing system is a split-X braced frame, where struts are placed at mid height of a standard CBF to laterally brace the columns against in-plane buckling.

The objective of this research project is to study the design and the seismic behaviour of the aforementioned bracing systems, for prototype buildings located in Vancouver, British Columbia. This objective was achieved by developing and refining an *OpenSees* numerical model, capable of

simulating the inelastic behaviour of bracing members and columns. The design of a two-tiered MT-CBF was carried out, following both Canadian and American seismic provisions. Finally, nonlinear response history analyses were realized for all three studied bracing systems.

The design of a two-tiered CBF allowed to point out key differences in the Canadian and American design approaches. Variation in anticipation of the ductility demand led to different building seismic weight and design base shears for the same brace selection. Additionally, column design differs in the two codes. The Canadian standard requires progressive analysis of the frame to be realized, whereas the American standard requires the columns to be sufficiently resistant in bending to accommodate the unbalanced probable shear resistance occurring between tiers.

Nonlinear response history analyses (NLRHA) of six two-bay MT-CBFs were conducted. The results show that progressive yielding of tiers occurs in this system, in a similar manner to what is observed in single-bay MT-CBFs. Progressive yielding can occur in various tiers, as well as in various bays. The implemented design procedure was able to predict the yielding sequence of the tiers, as well as the in-plane flexural demand on columns. Discrepancies in this prediction were noted because of the assumed brace forces in design. It was found that design inelastic drifts were consistently underestimated. On the contrary, the out-of-plane bending moments on columns were largely overestimated by the design procedure, based on CSA S16-19.

NLRHA on the two studied two-bay X-CBFs showed that frame behaviour was satisfactory, regardless whether an intermediate strut was included or not. Brace behaviour resembled what is typically observed in traditional CBFs. When an intermediate strut was used, the exterior columns developed significant in-plane bending moments, which were anticipated and considered in design. Furthermore, when accounting for the inherent variability of brace yield stress, it was determined that the interior column can also be subject to in-plane flexure.

Finally, NLRHA was conducted for a split-X CBF. The intermediate strut allowed the column to be laterally braced in the in-plane direction. However, after tension brace yielding, the brace intersection point exhibited in-plane displacements resulting in strut axial force and in-plane bending moments on the columns. These were larger than anticipated in design, and the frame response showed inelastic demand concentrated in the upper half of the column members.

TABLE OF CONTENTS

DÉDICACE III

REMERCIEMENTS IV

RÉSUMÉ VI

ABSTRACT IX

TABLE OF CONTENTS XI

LIST OF TABLES XIV

LIST OF FIGURES XV

LIST OF SYMBOLS AND ABBREVIATIONS XX

LIST OF APPENDICES XXIII

CHAPTER 1 INTRODUCTION 1

1.1 Background 1

1.2 Objectives 4

1.3 Research methodology 5

1.4 Thesis organization 5

CHAPTER 2 LITERATURE REVIEW 7

2.1 Seismic behaviour of steel CBFs 7

2.2 Seismic behaviour of steel MT-CBFs 9

2.3 Seismic design requirements for steel MT-CBFs 12

2.3.1 CSA S16-19 12

2.3.2 AISC 341-16 16

2.4 Available numerical studies on MT-CBFs 18

CHAPTER 3 DESIGN OF TWO-TIERED CBFS ACCORDING TO CSA S16-19 AND AISC 341-16 21

3.1 Design according to CSA S16-19 21
3.1.1 Building selected 21
3.1.2 Seismic loading 22
3.1.3 Braced frame design 23
3.2 Design according to AISC 341-16 27
3.2.1 Building selected 27
3.2.2 Braced frame design 28
3.3 Comparison between the braced frame designs 30
CHAPTER 4 NUMERICAL MODEL 32
4.1 *OpenSees* numerical model 32
4.1.1 End conditions 34
4.1.2 Model limitations 35
4.1.3 Calculation of response parameters 35
4.2 Ground motions 36
4.3 Validation of the *OpenSees* numerical model 38
4.3.1 Frame geometry used for the validation 38
4.3.2 *Abaqus* numerical model 39
4.3.3 Comparison of the *OpenSees* numerical model with the *Abaqus* numerical model 41
CHAPTER 5 SEISMIC BEHAVIOUR OF A TWO-TIERED CBF 47
5.1 Nonlinear response history analysis 47
CHAPTER 6 SEISMIC BEHAVIOUR OF TWO-BAY MT-CBFS 53
6.1 Studied geometries 53
6.2 Design of the braced frames 55
6.3 Initial geometric imperfections 58

6.4 Nonlinear response history analysis of two-bay two-tiered CBFs 59

6.4.1 Uniform configuration: 7-meter bays 60

6.4.2 Non-uniform configuration: 6-m and 8-m bays 69

6.4.3 Non-uniform configuration: 7-meter and 8-meter bays 72

6.5 Nonlinear response history analysis of two-bay three-tiered CBFs 74

6.5.1 Comparison of NLRH analyses of two-bay three-tiered CBFs with design predictions 79

CHAPTER 7 SEISMIC BEHAVIOUR OF TWO-BAY X-CBFS 81

7.1 Two-bay X-CBFs studied 81

7.2 Nonlinear response history analysis 84

7.2.1 Two-bay X-CBF without strut 85

7.2.2 Two-bay X-CBF with strut 88

7.2.3 Accounting for brace yield strength variability in two-bay X-CBFs 92

CHAPTER 8 SEISMIC BEHAVIOUR OF A SPLIT-X CBF 94

8.1 Split-X CBF design 94

8.2 Nonlinear response history analysis 95

CHAPTER 9 CONCLUSIONS AND RECOMMENDATIONS 101

9.1 Summary 101

9.2 Limitations of the study 101

9.3 Conclusions 102

9.4 Recommendations for future research 106

BIBLIOGRAPHY 108

APPENDICES 113

LIST OF TABLES

Table 3.1 Braces characteristics for the Canadian 2T-CBF 23

Table 3.2 Design parameters for the braced frame columns according to CSA S16-19.....26

Table 3.3 Seismic design parameters according to ASCE 7-16.....27

Table 3.4 Braces characteristics for the American 2T-CBF 28

Table 3.5 Tier 1 braces (HSS 102x102x6.4) parameters for the Canadian and American frame..31

Table 4.1 Steel02 calibration parameters used in the OpenSees model.....34

Table 4.2 Material model assumption of the the Abaqus model.....39

Table 5.1 Peak frame response for 2T-CBF.....52

Table 6.1 Peak frame response from NLRHA for the two-bay 2T-CBF uniform configuration with the same column sections.....64

Table 6.2 Peak frame response from NLRHA for the two-bay 2T-CBF uniform configuration using different column sections 66

Table 6.3 Peak frame response from NLRHA for the two-bay 2T-CBF non-uniform 6- and 8-meter bays.....69

Table 6.4 Peak frame response parameters for two-bay 2T-CBF non-uniform 7- and 8-m bays configuration 74

Table 6.5 Average ratios between in-plane bending moments from NLRHA and design in columns for all three studied two-bay 3T-CBFs.....79

Table 7.1 Peak frame response for the two-bay X-CBF without strut.....85

Table 7.2 Peak frame response parameters for the two-bay X-CBF with strut 89

Table 7.3 Peak response from NLRHA of the two-bay X-CBF with and without strut when using 90% of R_yF_y in bottom braces 92

Table 8.1 NLRHA mean values for the studied split-X CBF 96

Table A.9.1 List of the ground motion records used in NLRH analyses 113

LIST OF FIGURES

Figure 1.1 Examples of MT-CBFs: a) construction of an industrial building using two-tiered concentrically braced frames in Varennes, QC; and b) example of a multi-storey MT-CBF..1

Figure 1.2 Example of a two-bay two-tiered CBF 3

Figure 1.3 Other special concentrically braced frames studied in this project: a) two-bay X-CBF on an industrial building; and b) geometric representation of a split-X CBF 4

Figure 2.1 Example of an inverted-V steel CBF in Varennes, Qc 7

Figure 2.2 Typical MT-CBF configurations (American Institute of Steel Construction, 2016a).10

Figure 2.3 Pushover analysis of a 2T-CBF: a) drift in braced panels and column in-plane bending moments; and b) brace axial forces (tension and compression forces are positive to ease comparison) (Imanpour & Tremblay, 2012) 11

Figure 2.4 Critical tier scenarios for a three-tiered CBF (Auger, 2017) 14

Figure 2.5 Progressive brace buckling and yielding in MT-SCBFs (American Institute of Steel Construction, 2016a) 17

Figure 2.6 Bending moments in column and strut coming from brace buckling (American Institute of Steel Construction, 2016a).....18

Figure 2.7 Numerical model of a three-tiered CBF: a) initial geometric imperfections; b) residual stresses and fiber discretization (Auger, 2017) 19

Figure 3.1 Building geometry of the designed 2T-CBF.....22

Figure 3.2 Deformed shape of the SAP2000 model for: a) tier 1 critical; and b) tier 2 critical....25

Figure 4.1 Undeformed shape of a typical 2T-CBF modeled with OpenSees (leaning column not shown) 33

Figure 4.2 Determination of the period range for ground motion scaling (NRCC, 2017).....37

Figure 4.3 Scaled spectral acceleration of the selected ground motions in Vancouver, soil type E: a) mean spectral accelerations; b) crustal earthquakes; c) in-slab subduction earthquakes; and d) interface subduction earthquakes 37

Figure 4.4 Two-tiered CBF geometry and sections used for OpenSees and Abaqus comparison 38

Figure 4.5 Geometry of the two-tiered CBF in *Abaqus* 40

Figure 4.6 Comparison of OpenSees and Abaqus models for pinned conditions under the 1989 Loma Prieta earthquake, Gilroy array #2: a) drifts; b) brace forces in tier 1; and c) brace forces in tier 2 42

Figure 4.7 Comparison of *OpenSees* and *Abaqus* models for pinned conditions under the 1989 Loma Prieta earthquake Gilroy array #2: a) *OpenSees* deformed shape at column buckling; and b) *Abaqus* deformed shape at column buckling 43

Figure 4.8 Comparison of OpenSees and Abaqus models for fixed conditions under the 1989 Loma Prieta earthquake Gilroy array #2: a) drifts; b) brace forces in tier 1; c) brace forces in tier 2; and d) in-plane bending moment in columns 44

Figure 4.9 Comparison of OpenSees and Abaqus models for fixed conditions under the 1989 Loma Prieta earthquake Gilroy array #2: a) *OpenSees* deformed shape at yielding of tier 1; and b) *Abaqus* deformed shape at yielding of tier 1 45

Figure 5.1 Geometry and selected members for the studied two-tiered CBF 47

Figure 5.2 2T-CBF deformed shape of the OpenSees numerical model at the verge of brace yielding in Tier 1: a) elevation view; b) side view; and c) isometric view 48

Figure 5.3 Frame drifts for the 2T-CBF under Loma Prieta 1989 earthquake, Hollister Differential Array.....49

Figure 5.4 2T-CBF response under 1989 Loma Prieta, Hollister Differential Array record: a) drifts; b) normalized brace forces; c) normalized in-plane column moment; and d) normalized out-of-plane column moment 50

Figure 6.1 Geometry and selected sections for two-bay 2T-CBFs with: a) uniform 7-7 configuration; b) non-uniform 6-8 configuration; and c) non-uniform 7-8 configuration.....54

Figure 6.2 Geometry and selected sections for two-bay 3T-CBFs with: a) uniform 7-7 configuration; b) non-uniform 6-8 configuration; and c) non-uniform 7-8 configuration.....55

Figure 6.3 Brace probable resistances for the initial column selection in a two-bay MT-CBF....56

Figure 6.4 Brace design forces for the first critical tier scenario: a) inelastic roof displacement; b) yielding of the upper right tier under the critical tier forces; c) final critical tier scenario 57

Figure 6.5 Frame deformed shape and brace probable resistances for the second critical tier scenario: a) deformed shape at roof inelastic displacement; b) yielding of tension brace in the lower right tier; and c) final brace forces for the second critical scenario 58

Figure 6.6 Selected initial out-of-plane geometric imperfections orientation for the columns of two-bay MT-CBFs 59

Figure 6.7 Deformed shape of a uniform two-bay 2T-CBF (elevation and side views): a) at brace buckling; and b) at maximum roof displacement (P-Delta column not shown) 61

Figure 6.8 Tier drifts against storey drift under the 1989 Loma Prieta - Hollister Differential Array earthquake: a) two-bay uniform 2T-CBF; and b) single bay 2T-CBF 62

Figure 6.9 Normalized brace forces against tier drifts for the uniform two-bay 2T-CBF under the 1989 Loma Prieta 1989 - Hollister Differential Array earthquake: a) discontinuous braces in left bay; b) discontinuous braces in right bay; c) continuous braces in left bay; and d) continuous braces in right bay.....63

Figure 6.10 Normalized column in-plane moments for the two-bay 2T-CBF uniform configuration using the same column sections under the 1989 Loma Prieta – Hollister Differential Array earthquake 64

Figure 6.11 History of drifts for the uniform 2T-CBF using 85% of R_yF_y in the top tiers under the 1989 Loma Prieta – Hollister Differential Array earthquake.....67

Figure 6.12 Normalized brace forces against tier drifts for the uniform two-bay 2T-CBF under the 1989 Loma Prieta earthquake, Hollister Differential Array with 85% R_yF_y in the tiers: a) discontinuous braces in left bay; b) continuous braces in the left bay; c) discontinuous braces in the right bay; and d) continuous braces in the right bay 68

Figure 6.13 Two-bay 2T-CBF non-uniform 6- and 8-meter bays configuration response under the 1989 Loma Prieta earthquake, Hollister Differential Array: a) drifts; and b) normalized in-plane moments in the columns 70

Figure 6.14 Normalized brace forces relative to tier drift in the left bay under the 1989 Loma Prieta earthquake, Hollister Differential Array record 71

Figure 6.15 Demand evolution on the two-bay 2T-CBF non-uniform 6- and 8-m bays configuration: a) drifts; b) in-plane bending moments in the columns 72

Figure 6.16 Deformed shape of the OpenSees numerical model of the 7- and 8-m bays 2T-CBF at yielding of the upper tiers 73

Figure 6.17 Response history of drifts for the two-bay 2T-CBF non-uniform 7- and 8-m bays under the 1989 Loma Prieta earthquake, Hollister Differential Array record 73

Figure 6.18 Elevation and side views of the deformed shape of the OpenSees numerical model for the uniform 7-meter bays 3T-CBF: a) at brace buckling; and b) at yielding of tier 3 75

Figure 6.19 Peak cumulative drifts of studied two-bay 3T-CBFs 76

Figure 6.20 Peak in-plane bending moments for exterior and interior columns of studied two-bay 3T-CBFs ("Ext." and "Int." stand for the exterior column and interior column respectively) 77

Figure 6.21 NLRH results for the two-bay 3T-CBF non-uniform 6- and 8-meter bays configuration under the 1989 Loma Prieta earthquake: a) tier drifts against storey drift; and b) normalized continuous brace forces against tier drifts in the left bay 78

Figure 7.1 Example of two-bay X-CBFs: a) without intermediate strut; and b) with intermediate strut 81

Figure 7.2 Building geometry of the studied two-bay X-CBFs 82

Figure 7.3 Geometry and sections of the studied two-bay X-CBFs: a) without strut; and b) with strut 84

Figure 7.4 Deformed shape of the OpenSees numerical model at tension brace yielding of a two-bay X-CBF without strut (leaning column not shown) 85

Figure 7.5 Two-bay X-CBF without strut response under 1983 Coalinga earthquake, Cantua Creek School record: a) storey drift; b) brace normalized forces; and c) in-plane column normalized moments 87

Figure 7.6 Deformed shape of the OpenSees numerical model of a two-bay X-CBF with strut: a) at first brace buckling; and b) at maximum roof displacement 88

Figure 7.7 Two-bay X-CBF with strut response under 1983 Coalinga earthquake, Cantua Creek School record: a) storey drift; b) brace normalized forces; and c) column in-plane normalized moments 90

Figure 7.8 Two-bay X-CBF with strut response under Coalinga 1983 earthquake, Cantua Creek School record: brace axial elongation 91

Figure 8.1 Geometry and sections of the studied split-X CBF 95

Figure 8.2 Deformed shape of the OpenSees numerical model of a split-X CBF under the Loma Prieta 1989 earthquake, Hollister Differential Array: a) at first discontinuous brace buckling, b) at first discontinuous brace buckling; c) at maximum roof displacement 96

Figure 8.3 Split-X response under the 1989 Loma Prieta earthquake, Hollister Differential Array: a) drifts; b) braces normalized forces; and c) column in-plane normalized moments 97

Figure 8.4 Split-X response under the 1989 Loma Prieta earthquake: a) in-plane and out-of-plane displacement of the brace intersection node; and b) brace elongation 99

Figure B.9.1 Spectral accelerations of the critical ground motions: a) Loma Prieta 1989 earthquake, Hollister Differential Array record; and b) Coalinga 1983 earthquake, Cantua Creek School record 115

Figure B.9.2 Ground accelerations of the critical ground motions: a) Loma Prieta 1989 earthquake, Hollister Differential Array record; and b) Coalinga 1983 earthquake, Cantua Creek School record 116

LIST OF SYMBOLS AND ABBREVIATIONS

Symbols

A	Section area
a_0	Rayleigh damping factor proportional to mass
a_1	Rayleigh damping factor proportional to stiffness
b	Section width
b (Abaqus model)	Second cyclic hardening parameter
C'_{prob}	Probable post-buckling compressive resistance of bracing members
C_1	First material kinematic component
C_{prob}	Probable compressive resistance at first buckling of bracing members
d	Section depth
E	Modulus of elasticity
E_t	Tangent modulus of elasticity
F_y	Yield strength
h	Storey height
h_i	Tier height
M_{cx}	Moment about the strong axis of the column
$M_{cx,\ design}$	Column moment around its strong axis coming from design
$M_{cx,\ NLRH}$	Column moment around its strong axis coming from nonlinear response history analysis
M_{cy}	Moment about the weak axis of the column
$M_{cy,\ design}$	Column moment around its weak axis coming from design
$M_{cy,\ NLRH}$	Column moment around its weak axis coming from nonlinear response history analysis

P_b	Axial force in a brace
Q_∞	First cyclic hardening parameter
R_d	Ductility-related force modification factor reflecting the capability of a structure to dissipate energy through reserved cyclic inelastic behaviour. (NBCC, 2015)
R_o	Overstrength-related force modification factor accounting for the dependable portion of reserve strength in a structure designed according to these provisions. (NBCC, 2015)
R_y	Modification factor on F_y used to calculate the probable yield stress
t	Section flange thickness
T_{prob}	Probable tensile resistance of bracing members
V'_{prob}	Probable post-buckling tier shear resistance
V_{prob}	Probable tier shear resistance at brace buckling
w	Section web thickness
Z_x	Plastic section modulus about the x-axis
Z_y	Plastic section modulus about the y-axis
δ_e	Elastic roof displacement from design
$\delta_{in\text{-}plane}$	In-plane displacement of the brace intersection node
$\delta_{relative,\ in\text{-}plane}$	Relative in-plane displacement of the brace intersection node
$\delta_{roof,NLRH}$	Inelastic roof displacement from nonlinear response history analysis
ω	Natural frequency
ξ	Damping rate
γ	Second material kinematic component

Abbreviations

2T-CBF	Two-tiered concentrically braced frame
3T-CBF	Three-tiered concentrically braced frame
AISC	American Institute of Steel Construction
CBF	Concentrically braced frame
CSA	Canadian Standards Association
DOF	Degree-of-freedom
MT-CBF	Multi-tiered concentrically braced frame
NBCC	National Building Code of Canada
NLRH	Nonlinear response history
NLRHA	Nonlinear response history analysis
NRCC	National Research Council of Canada
X-CBF	X-shaped concentrically braced frame

LIST OF APPENDICES

Appendix A LIST OF THE GROUND MOTION RECORDS USED IN NLRH ANALYSES 113

Appendix B CRITICAL GROUND MOTIONS STUDIED IN THIS THESIS 115

CHAPTER 1 INTRODUCTION

1.1 Background

The consideration of seismic hazard in the design of buildings was introduced in Canada and multiple other countries over the course of the 20th century. With design engineers always looking for more cost-efficient and resilient structural systems, multi-tiered concentrically braced frames (MT-CBFs) have become commonly used in North America for seismic force-resisting system of tall single-storey buildings over the past years. Such system is common in North America, and can be found in industrial facilities, airplane hangars, warehouses and sport centers. Figure 1.1 shows examples of buildings using two-tired CBFs (2T-CBFs) as part of the lateral force resisting system. MT-CBFs consist of multiple braced tiers stacked along the height of the storey. Horizontal intermediate struts are placed between each tier to redistribute unbalanced brace loads and prevent unsatisfactory K-brace response. Multi-tiered configurations are typically used when it is impractical to brace the entire storey height. Using shorter braces in multiple tiers allows for more effective members in compression and easier compliance with the stringent slenderness and width-to-thickness limits. In addition, the adoption of capacity-based design for seismic applications in North American standards means that reduced demand on columns, struts and connections is induced when smaller braces are used.

a) b)

Figure 1.1 Examples of MT-CBFs: a) construction of an industrial building using two-tiered concentrically braced frames in Varennes, QC; and b) example of a multi-storey MT-CBF

In MT-CBFs, columns are often laterally braced by struts at every tier level, while out-of-plane buckling can occur over the full frame height. Therefore, wide-flange sections are usually selected for the columns and oriented such that strong axis flexure is developed under out-of-plane bending. This is also suitable when columns are subject to wind loads or crane loads that generate out-of-plane flexure.

In Canada, the CSA S16-19 standard (Canadian Standards Association, 2019) and the National Building Code of Canada (National Research Council Canada, 2015) categorize MT-CBFs in three categories for seismic design: moderately ductile (Type MD), limited-ductility (Type LD) and conventional construction (Type CC). The MT-CBFs studied in this research project are in the moderately ductile category and are limited to a maximum of three tiers with no lateral support provided by a floor structure.

MT-CBFs exhibit a different behaviour compared to traditional multi-storey CBFs. First, because of the lack of out-of-plane support provided to the columns at tier levels that is otherwise provided by beams or floor decks at storey levels. Second, MT-CBFs essentially represent single-degree-of-freedom systems as the majority of structural mass is concentrated at the roof level. Therefore, they do not develop inertial forces at tier levels, unlike multi-storey CBFs. Past studies have demonstrated that under seismic loads, non-uniform yielding of the tiers develops, and inelastic deformations tend to concentrate in the weakest (critical) tier as brace tensile yielding occurs first in this tier that leads to large longitudinal plastic deformations, which in turn produces in-plane flexural demand on the columns (Imanpour & Tremblay, 2016). Furthermore, out-of-plane brace buckling produces out-of-plane flexural demands on the column. Therefore, the design of the columns must account for the axial demand, as well as both in-plane and out-of-plane flexural demands. Drift concentration in the critical tier can also lead to excessive ductility demand and provoke brace fracture due to low-cycle fatigue.

In some cases, either practical or aesthetic reasons might favour the use of two adjacent braced bays on a building wall. Although the seismic behaviour of MT-CBFs has been extensively studied, little to no attention has been given to the response of two MT-CBFs bays placed side by side. The current Canadian steel design standard (CSA S16-19) only allows two-bay MT-CBFs when the geometry and members are the same for the two bays. Thus, there is a need for a more thorough

understanding of the seismic behaviour of two-bay MT-CBF bracing configurations, including ones where uneven bays are used as depicted in Figure 1.2.

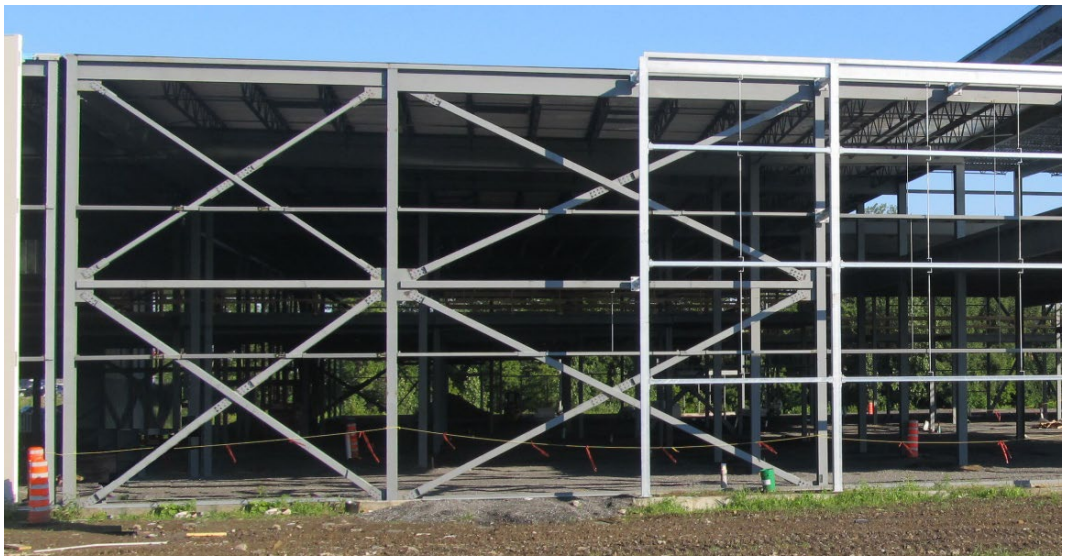

Figure 1.2 Example of a two-bay two-tiered CBF

Other commonly used bracing configurations in tall single-storey buildings are two-bay X-CBFs and split-X CBFs. Examples of such configurations can be seen in Figure 1.3. Two-bay X-CBFs consist of X-bracing placed between two column bays. One benefit of this bracing system compared to using two braced bays side by side is the less acute angle created between braces and columns, which effectively reduces the design axial load on the columns. Two-bay X-CBFs can also include a strut placed at mid-height providing lateral bracing to the side columns. With inherent variability in material strength, as well as erection and manufacturing defects, brace tensile yielding and compressive buckling may not necessarily occur simultaneously at the top and bottom bracing members which similar to MT-CBFs can lead to non-uniform plastic deformations and in-plane flexural demand on the middle or exterior columns.

A split-X braced frame is a traditional CBF, with the difference that a strut is placed at mid-height of the frame to provide horizontal in-plane bracing the columns and allow for a smaller column section to be selected. The strut is usually continuous, with braces welded or bolted to gussets plates on either side. It is anticipated that, similar to MT-CBFs, unbalanced brace loads are

transferred to the strut due to non-uniform yielding of braces, which then result in in-plane flexure on the columns.

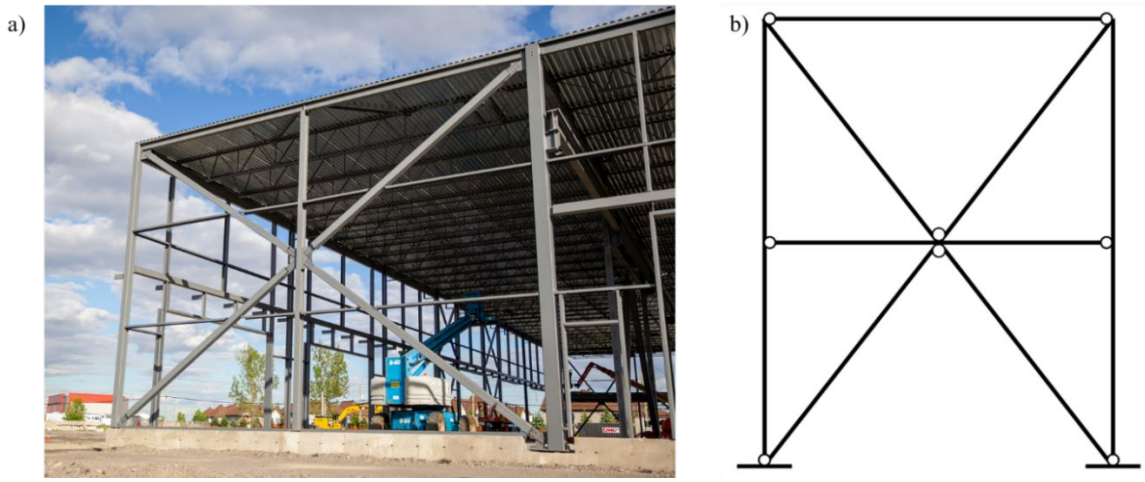

Figure 1.3 Other special concentrically braced frames studied in this project: a) two-bay X-CBF on an industrial building; and b) geometric representation of a split-X CBF

According to CSA S16-19, two-bay X-CBFs and split-X bracing systems do not require any additional special design considerations compared to standard MD concentrically braced frames. In depth design and analysis of these configurations is therefore required to determine if non-uniform yielding and in-plane bending of the column can occur, and if these phenomena can be predicted in design.

1.2 Objectives

The main objective of this research project is to assess the seismic behaviour of special bracing systems for which no requirements exist in the current Canadian design standards: two-bay MT-CBFs, two-bay X-CBFs, and split-X CBFs. Specifically, the project aims to:

- Design a two-tiered braced frame according to the Canadian steel design standard and the U.S. Seismic Provisions for Structural Steel Buildings and assess the main differences in the two methods.

- Assess the seismic behaviour of different two-bay MT-CBFs with variable bay widths and number of tiers by elaborating a design procedure following existing Canadian seismic provisions and by conducting nonlinear response history analyses.
- Assess the seismic behaviour of two-bay X-CBFs designed according to the Canadian seismic provisions by conducting nonlinear time history analyses that include and by evaluating the influence of the inclusion of a strut at mid-height of the frame.
- Assess the seismic behaviour of a split-X CBF designed following the Canadian seismic provisions by conducting nonlinear time history analyses.

1.3 Research methodology

The objectives of this research were accomplished through the following phases:

- An exhaustive review of the existing literature was performed at the start and throughout the whole duration of the project to understand the behaviour of concentrically braced frames, with a focus on multi-tiered configurations. This literature review also focused on the available numerical studies that have been carried out to examine the seismic response of braced frames.
- The design of MT-CBFs according to the Canadian and American design standards, as well as two-bay X-CBFs and split-X CBFs under the Canadian standards.
- The development of an *OpenSees* numerical model capable of simulating nonlinear response of bracing and column members.
- The evaluation of the seismic behaviour of the aforementioned bracing systems using nonlinear response history analyses.

1.4 Thesis organization

This master's thesis is divided in nine chapters. After the introduction provided in chapter 1, chapter 2 presents the literature review. Chapter 3 describes the design of a two-tiered CBF according to Canadian and American standards and provides a comparison between the two methods. Chapter 4 details the *OpenSees* numerical model and its validation against an *Abaqus* model. In chapter 5, the seismic behaviour of a typical 2T-CBF is studied. Chapter 6 outlines the

seismic response of two-bay MT-CBFs using nonlinear response history analyses. Chapter 7 discusses the seismic behaviour of two-bay X-CBFs, while chapter 8 is focused on the seismic behaviour of a split-X CBF. Finally, a summary of the work is presented in chapter 9, along with recommendations for future research.

CHAPTER 2 LITERATURE REVIEW

This chapter presents a literature review of the subjects of interest for this research project. A review of the seismic behaviour of steel CBFs is first detailed, followed by the seismic behaviour of MT-CBFs. Seismic design requirements for MT-CBFs are explained according to both CSA S16-19 and AISC 341-16. Finally, current available numerical studies of MT-CBFs are presented.

2.1 Seismic behaviour of steel CBFs

Steel concentrically braced frames are commonly used in low-rise steel buildings as a lateral force resisting system. CBFs make use of bracing members, often placed diagonally between columns and beams, which resist lateral loads by truss action. Typical lateral loads include seismic loading, wind loading and crane loading. Following the assumption of truss action, braces are typically considered pinned at their extremities. Various geometric configurations can be used for bracing members, such as X-bracing, chevron bracing, and split-x bracing amongst others. Figure 2.1 shows an example of a split-X CBF over two storeys in Varennes, Qc, Canada.

Figure 2.1 Example of an inverted-V steel CBF in Varennes, Qc

As part of the seismic force resisting system, the main role of steel CBFs is to maintain structural integrity of the capacity protected elements and prevent collapse under a seismic event. Capacity protected elements include columns, roof diaphragms, connections, and foundations amongst others. These braced frames are labelled as *concentric* because axial loads in the created truss are distributed through concentric points between columns, beams and bracing members. As such, no eccentricity is created, preventing the transfer of bending moments between members.

As capacity seismic design has been adopted by a multitude of standards, including the Canadian CSA S16-19, elements of the seismic force resisting system are designed as *fuses*. These fuses act as energy dissipating elements. In a steel CBF, braces are designed to yield and buckle under earthquake loads and dissipate seismic energy (Filiatrault, 2013). Capacity design allows engineers to safely select the energy dissipating elements, while ensuring the conservation of the structural integrity of gravity-load carrying members.

Both Canadian and American seismic design provisions categorize steel CBFs by their ductility. Ductility is the capacity to undergo plastic deformations, without failure. The ductility-related modification factor R_d in Canada and the response modification factor R in the U.S. are used to characterize the ductility of a bracing system. The Canadian standard categorizes steel CBFs in three ductility levels: limited-ductility (LD), moderately-ductile (MD), and conventional construction (CC) (Canadian Standards Association, 2019). The American standard specifies three ductility levels for braced frames: ordinary concentrically braced frames (OCBFs), special concentrically braced frames (SCBFs) and steel systems not specifically detailed for seismic resistance (American Institute of Steel Construction, 2016a). In this research project, braced frames designed following Canadian provisions are of type MD and those designed following American provisions belong to the SCBF category.

One advantage of CBFs is the facility with which the forces can be determined in each member, as it is designed as a truss. Under low lateral loading, all members remain elastic and the bracing members at a given storey participate in equal parts to resisting the lateral loads. When lateral loading is increased, the compression braces buckle, reaching their expected resistance at first buckling C_{prob}. At this point, the tension members remain elastic, as their tensile resistance is higher than their compressive resistance. After further increasing lateral loads, the compression braces reach their post-buckling compressive resistance, C'_{prob}. Tension braces remain elastic, but now

resist most of the lateral load as the compression brace resistance is heavily reduced. The next increment of lateral force produces yielding of the tension braces. When this condition is reached, other members in the structure, such as connections and columns in bending, start participating in the lateral integrity of the structure. Since this is not a satisfactory behaviour and because the mentioned elements are capacity protected, their design include the condition where bracing members reach their probable resistances.

Finally, in the objective of permitting satisfactory brace cyclic response, brace end connections must be designed to allow sufficient rotation in the direction of brace buckling. This is achieved by introducing a fold line on the gusset plate created in a space equal to two times the plate thickness. This requirement is explicitly stated in both CSA S16-19 (2019) and AISC 341-16 (2016a).

2.2 Seismic behaviour of steel MT-CBFs

The seismic behaviour of steel MT-CBFs has been extensively studied in the past (Imanpour & Tremblay, 2016; Imanpour, Tremblay, Davaran, Stoakes, & Fahnestock, 2016; Imanpour, Tremblay, Fahnestock, & Stoakes, 2016). These studies highlighted the non-uniform yielding response between tiers of MT-CBFs under seismic loading. Figure 2.2 illustrates different configurations of multi-tiered bracing systems. As shown, MT-CBFs can vary in their geometry and their use. They differ from conventional CBFs in two aspects. First, no floor diaphragms are present between tiers, which makes MT-CBFs effectively single degree of freedom systems. Second, the columns of MT-CBFs are not laterally restrained in the out-of-plane direction, as would be the case in a conventional CBF. This can lead to instability problems when out-of-plane bending moments are developed.

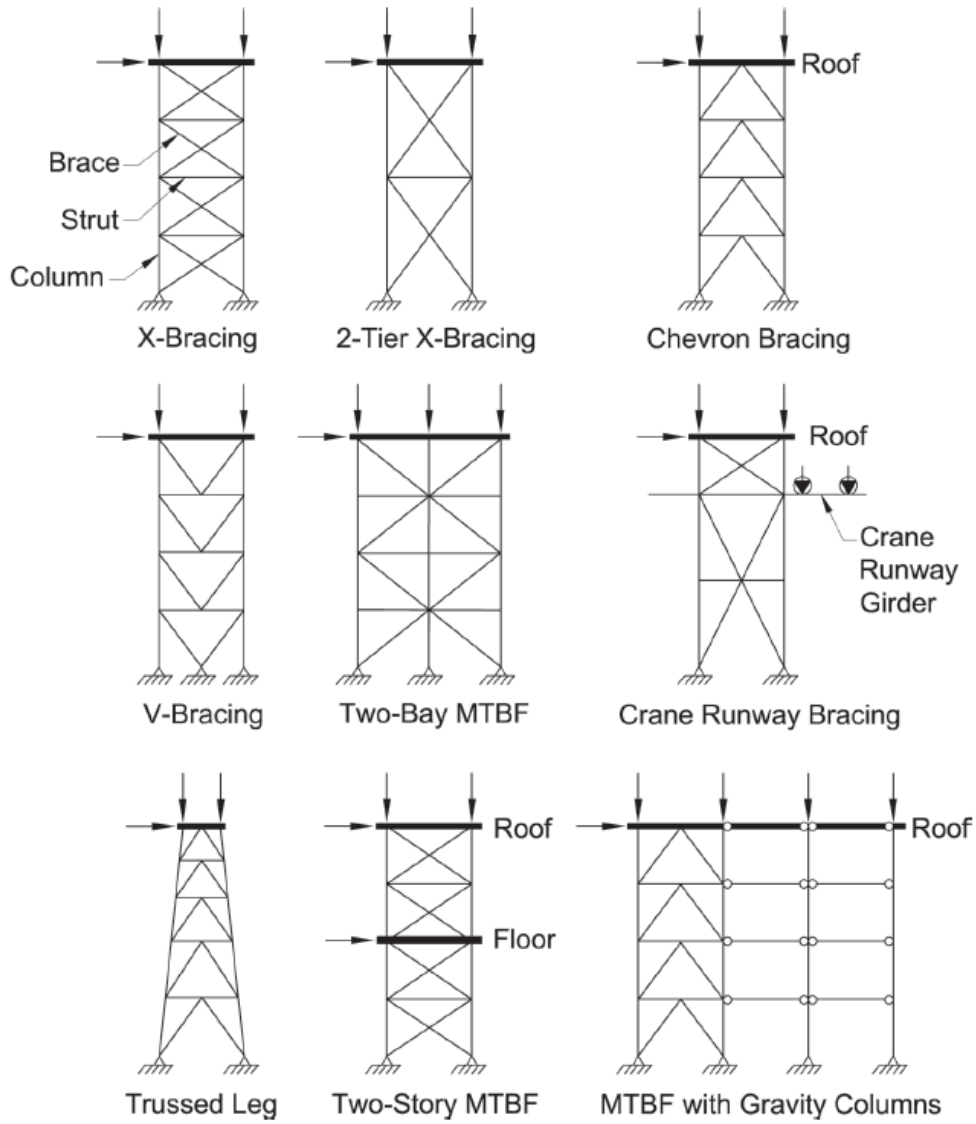

Figure 2.2 Typical MT-CBF configurations (American Institute of Steel Construction, 2016a)

Progressive yielding between tiers was studied by Imanpour and Tremblay (2012) and Figure 2.3 illustrates the behaviour of a two-tiered CBF using incremental nonlinear pushover analysis. The roof displacement is increased throughout the analysis, and the progression of brace buckling and yielding is clearly observed. At 0.3% storey drift, compression braces buckle. They reach their probable compression resistance C_{prob}, while the tension braces remain elastic. Past this point, the axial force in the compression braces is reduced towards C'_{prob}, until yielding is reached for the

tension brace in tier 2. This produces inelastic drift concentration in the second tier (the critical tier), while in-plane flexure is developed in the columns.

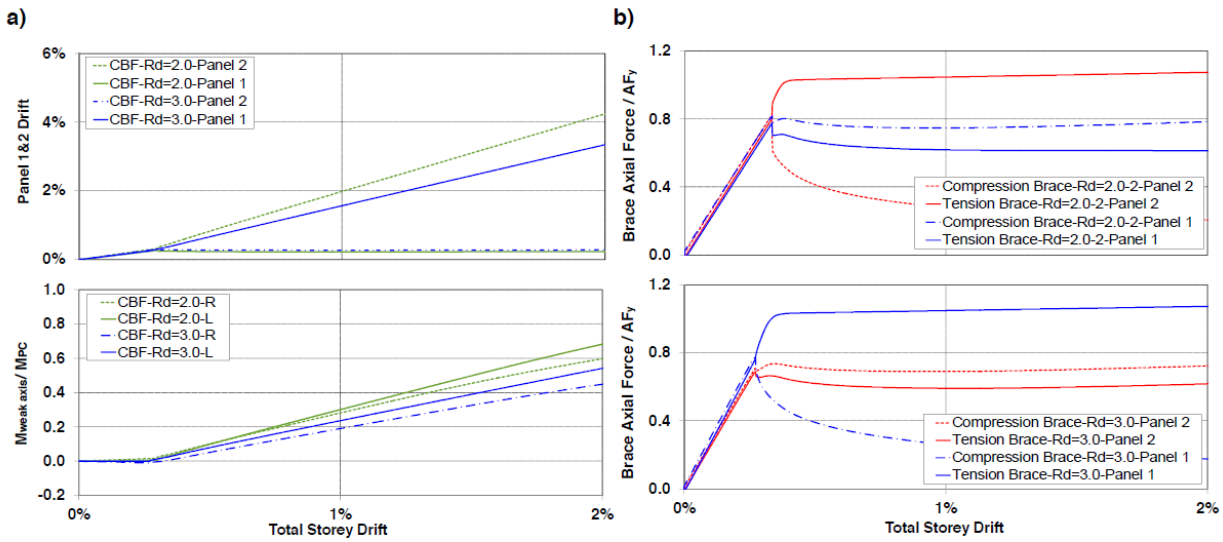

Figure 2.3 Pushover analysis of a 2T-CBF: a) drift in braced panels and column in-plane bending moments; and b) brace axial forces (tension and compression forces are positive to ease comparison) (Imanpour & Tremblay, 2012)

In a recent study, Imanpour and Tremblay (2016) presented design requirements to improve the seismic response of MT-CBFs and to prevent column instability after tier yielding. Their results showed that in-plane flexure in the columns can be considered by realizing a progressive yielding analysis of the different tiers. The critical tier can be identified as the tier with the lowest probable shear resistance (V_{prob}). The resulting loading condition considers post-buckling resistances in the compression brace and probable tensile resistance in the tension brace of the critical tiers. In the remaining tiers, the tension braces remain elastic, while the compression braces are assumed to have reached their probable buckling resistances. This study also recommended that tier drifts be limited to 2%, to prevent brace fracture due to low-cycle inelastic fatigue. Sufficient column stiffness can allow this requirement to be met.

2.3 Seismic design requirements for steel MT-CBFs

This section presents the current design requirements for MT-CBFs according to the Canadian design standard CSA S16-19 (Canadian Standards Association, 2019) and the American seismic provisions (American Institute of Steel Construction, 2016a) which refers to the specification for structural steel buildings (American Institute of Steel Construction, 2016b). In Chapter 3, the design of a two-tiered CBF is presented according to both methods. In later chapters, where NLRH analyses of different frames are conducted, design methods are based on the Canadian provisions.

2.3.1 CSA S16-19

As mentioned previously, MT-CBFs are designed for seismic loads using capacity-based design. In Canada, for MD type frames, the ductility and overstrength modification factors are respectively R_d = 3.0 and R_o = 1.3. It must be noted that the design lateral seismic load should be limited to its value calculated with R_dR_o = 1.3. During a seismic event, capacity protected elements must be able to withstand forces generated when the braces reach their probable resistances. These are calculated as follows:

$$T_{prob} = AR_yF_y \quad \text{(Eq. 2-1)}$$

$$C_{prob} = \min\left(T_{prob}; \frac{1.2C_r}{\phi}\right) \quad \text{(Eq. 2-2)}$$

$$C'_{prob} = \min\left(0.2T_{prob}; \frac{C_r}{\phi}\right) \quad \text{(Eq. 2-3)}$$

In these equations, A is the area of the section and R_y is the modification for F_y used to obtain the probable yield stress. The factored compression resistance C_r is detailed later. R_y is taken equal to 1.1, but the probable yield stress of HSS bracing members must be taken as 460 MPa minimally. In the equations above, C_r is calculated with R_yF_y.

The elements that are not part of the energy dissipation system must be designed for the two following loading conditions:

- The compression braces reach C_{prob}
- The compression braces reach C'_{prob}

For both loading conditions, the axial force in the tension braces is taken as T_{prob}.

The first step in the design of a braced frame is the selection of the bracing members, as the other capacity protected elements are based on the probable brace resistances. After the design storey shear from seismic loading has been calculated including the U_2 factor and horizontal notional loads, static analysis can be used to compute the axial force transferred to each brace. The contribution of gravity loads on the columns must be included in this analysis. The braces must provide a factored resistance C_r higher than the factored load C_f, as well as respect the limits on width-to-thickness and slenderness ratios of KL/r ≤ 200.

A first selection for the column section can be made using the two loading conditions above. In addition, columns must resist the combined action of the following loads:

- Gravity loads
- The axial loads, shear loads, and bending moments produced by yielding and buckling of the braces at the anticipated inelastic storey drift ($R_d R_o \Delta_e / I_e$) obtained from progressive yielding analysis.
- An out-of-plane notional load at each tier level equal to 2% of the factored axial load in the column segment under that tier level.

The forces arising from the second point above can be determined by analysis of the different critical tier scenarios. Figure 2.4 shows the critical tier scenarios to be considered in the design of a three-tiered CBF. The first critical tier is taken as the one with the lowest probable shear resistance, V_{prob}. For the following critical tier scenarios, brace probable resistances are reduced by increments of 5% until their tier becomes critical.

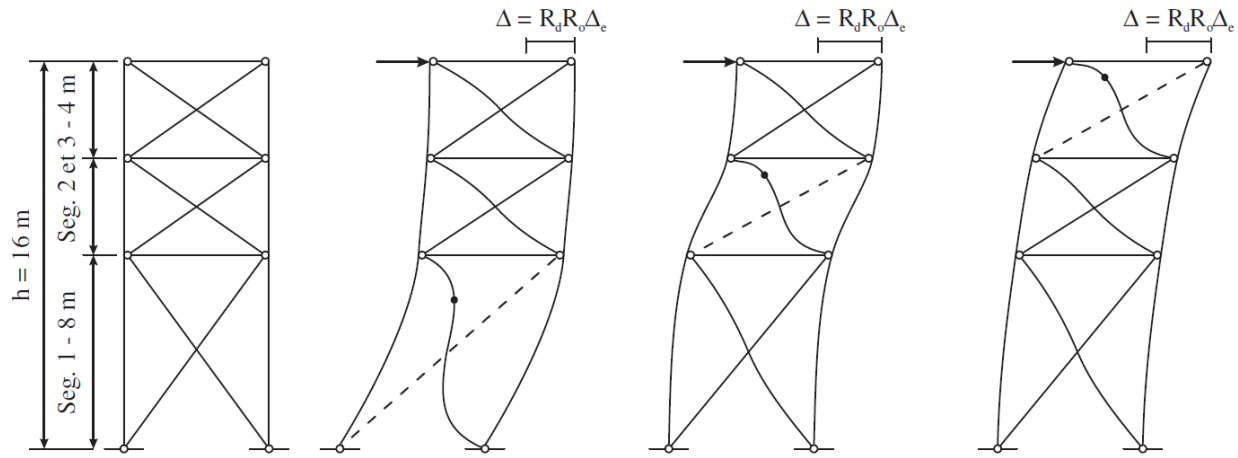

Figure 2.4 Critical tier scenarios for a three-tiered CBF (Auger, 2017)

Finally, struts must be placed between each tier. CSA S16-19 specifies the axial load in the strut as the maximum of the two following conditions:

- The axial forces arising when the braces in the tier below the strut reach T_{prob} and C_{prob} and the braces in the tier above the strut reach T_{prob} and C'_{prob}.
- The axial forces arising when the braces in the tier below the strut reach T_{prob} and C'_{prob} and the braces in the tier above the strut reach T_{prob} and C_{prob}.

In addition to these axial loads, struts must be designed to resist out-of-plane bending moments coming from brace buckling. Lastly, they must provide appropriate lateral and torsional restraint of the columns as described in the following subsections.

2.3.1.1 Lateral restraint of columns

The struts are used to provide lateral in-plane restraints to the columns at tier levels. As such, tier heights are considered for the calculation of in-plane buckling of the columns. For this, the strut must provide sufficient resistance and stiffness. The following equations from Yura (2001) detail the design for this condition.

$$\beta^*_{L,i} = \frac{2N\left(\frac{M_{fx,i}}{h}\right)C_L C_d / h_{s,i}}{0.75}; N = 4 - \frac{2}{n} \qquad \text{(Eq. 2-4)}$$

In (Eq. 2-4, n is the coefficient accounting for the number of braces on the member. M_{fx} is the maximum bending moment in tier i, h is the depth of the column, C_L is the coefficient accounting for the loading position, C_d is the column curvature coefficient and h_s is the height of the column. In this calculation, M_{fx} can be taken equal to the factored bending resistance M_{rx} calculated for a height $L_s = h_s$. Because the loading is applied to the compressed flange, C_L is taken equal to 1 + 1.2/n. This factor is applied because this loading condition is critical for lateral-torsional buckling. C_d is taken as 1, as the out-of-plane notional loads applied to the frame produce a single curvature for the column. The resulting brace stiffness must be greater than $\beta^*_{L,i}$ for each tier.

The brace resistance is calculated as follows:

$$F_{br,i} = 0.01 C_L C_d M_{fx,i}/h \qquad \text{(Eq. 2-5)}$$

As for the previous equation, M_{fx} can be taken as M_{rx}. The obtained axial force in the brace F_{br} must be lower than its factor resistance C_r.

2.3.1.2 Torsional restraint of columns

In addition to the lateral restraint provided to the columns, struts must provide torsional restraint at tier heights. According to Helwig and Yura (Helwig & Yura, 1999), this is calculated as follows:

$$\beta_{T,req} = A \frac{\left\{C_f r^2 - C_{ey}\left[\frac{d^2}{4} + a^2\right]\right\}^2}{(4nEI_y/L)\left[\frac{d^2}{4} + a^2\right]}; A = 4 - \frac{2a}{4} \qquad \text{(Eq. 2-6)}$$

Where A considers the loading eccentricity a relative to the center of gravity of the column. C_f is the maximum axial force in the column, r is the polar gyration radius of the column, C_{ey} is the Euler buckling load about the weak axis ($\pi^2 EI_y/L$), d is the section depth, n is the number of braces, I_y is the column's weak axis moment of inertia and L is the total height of the column. For I-shaped column members, a can be taken equal to zero.

To achieve efficient torsional stiffness, struts are typically oriented such that the web is in the horizontal plane. This allows for the connection to be made between the flanges of the column and the flanges of the strut. Under lateral loads, one column is in compression and the torsional stiffness provided by the strut is taken as $3EI_x/L_b$, and the required strong axis moment of inertia for the strut is equal to:

$$I_{x,req} = \frac{\beta_{T,req} L_b}{0.75\text{x}3E} \qquad \text{(Eq. 2-7)}$$

When the required stiffness has been determined, the required strut rotational strength can be calculated. For this step, the bending moment induced in the strut is calculated using the initial rotational deformation θ_0 in the column as the rotation value.

$$M_{br} = \beta_{T,req}\theta_0;\ \theta_0 = \frac{s}{500d}\ rad \qquad \text{(Eq. 2-8)}$$

In this equation, *s* is the maximum tier height and *d* is the column depth. The resulting moment M_{br} in the strut is thereafter added to the strong axis bending demand produced by out-of-plane brace buckling, as explained previously. The total rotation at the strut extremity must not exceed θ_0.

2.3.2 AISC 341-16

Design requirements in the 2016 revision of the American seismic provisions are detailed in this section. MT-CBFs must be designed for three loading conditions specified in Chapter F of the 2016 AISC seismic provisions (American Institute of Steel Construction, 2016a). The first two loading conditions correspond to those described for CSA S16-19. The third one corresponds to progressive yielding analysis, where brace yielding first occurs in the critical tier.

Brace selection is realized by determining the axial forces with static analysis. It is not required for gravity loads to be considered for brace selection. When brace sections are determined, a column section can be designed. Figure 2.5 shows the progression of brace buckling and yielding under lateral loads, which is used for column design.

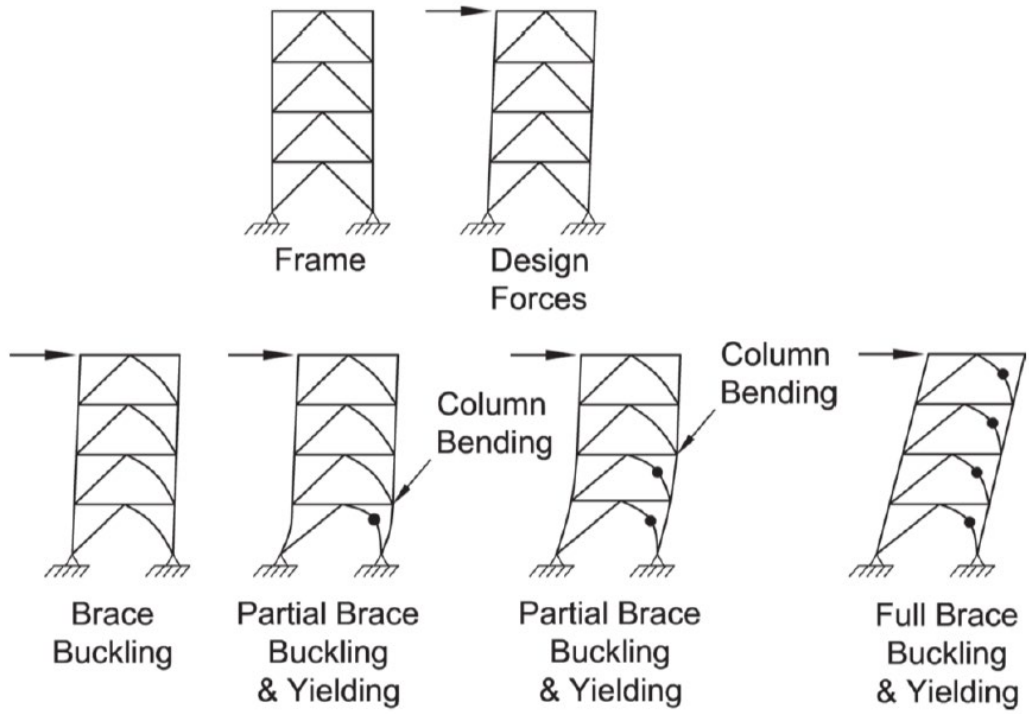

Figure 2.5 Progressive brace buckling and yielding in MT-SCBFs (American Institute of Steel Construction, 2016a)

This loading condition is similar to what is detailed in the Canadian design method. However, in-plane moments in the columns are obtained by calculating the unbalanced storey shear force when tier yielding occurs. For a two-tiered frame, this moment is obtained from the following equation:

$$M_{cy} = \frac{\Delta V_{br}}{2}\frac{h_1 h_2}{h_s} \qquad \text{(Eq. 2-9)}$$

Where M_{cy} is the resulting bending moment in the column, h_1 and h_2 are the tier heights and h_s is the storey height. ΔV_{br} is the difference in tier shear when the braces in the critical tear reach C'_{prob} and T_{prob} and when the compression brace in the non-critical tier reach C_{prob} while the tension brace remains elastic.

The design of the struts follows the same process as CSA S16-19, where the axial load in a strut corresponds to ΔV_{br} detailed above. Additionally, lateral and torsional bracing must be provided to the columns at tier levels. This can be checked following the procedure detailed in Section 2.3.1.1 and Section 2.3.1.2. Figure 2.6 shows the considered bending moments arising from brace

buckling. As a result of the moment being transferred to the column, an out-of-plane notional load is applied at tier height and taken equal to 0.006 times the vertical component of the compression brace that meets the column at the tier level. Finally, the provisions require that maximum tier drifts be limited to 2% to prevent brace fracture.

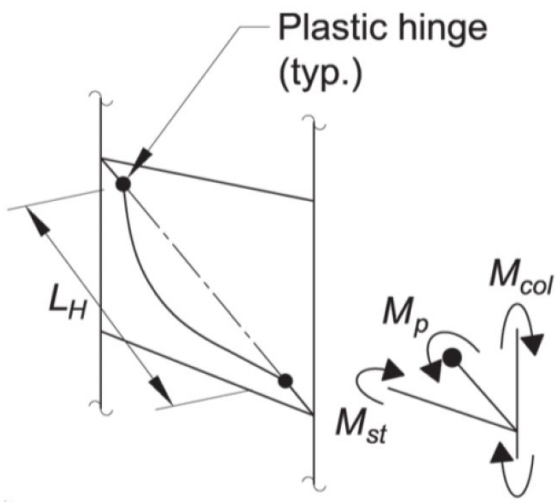

Figure 2.6 Bending moments in column and strut coming from brace buckling (American Institute of Steel Construction, 2016a)

2.4 Available numerical studies on MT-CBFs

Numerous numerical studies have been conducted on MT-CBFs using the *OpenSees* program (McKenna & Fenves, 2016). Recent works by Imanpour (2015) and Auger (2017) showed that such a numerical model is able to adequately simulate seismic behaviour of MT-CBFs, including brace inelastic response at yielding and buckling, as well as column inelastic response. The numerical model detailed in Chapter 4 is based on these studies.

The aforementioned studies used the *Steel02* material, part of the *OpenSees* library, to model in a fiber-based discretization element of braces and columns. It was also used for elastic members, such as struts and roof beams. Figure 2.7 illustrates the geometry of the numerical model, as well as the considered initial imperfections and residual stresses.

Continuous and discontinuous bracing members were modeled with a rotational spring at their ends, simulating the gusset plate connection. Rigid elements were also considered at the

intersection of braces with columns and strut, to simulate the added stiffness of the gusset plate. Full specifications of the rigid element properties are given in Auger (2017). It was shown that these connections correlated well with previously observed braced frame behaviour, from numerical analysis and experimental results.

Initial geometric imperfections were implemented using a *corotational* formulation. Brace imperfections were taken as 1/500th of the brace length and applied in the out-of-plane direction, matching the typical orientation of gusset plates in braced frames. Column out-of-plane and in-plane geometrical imperfections were specified as shown in Figure 2.7 b, using half-sine waves.

Residual stresses were added to the column members, based on the formulation by Galambos and Ketter (1961). Figure 2.7 c illustrates how the fiber discretization of columns and braces was realized and the amplitude of residual stresses in columns.

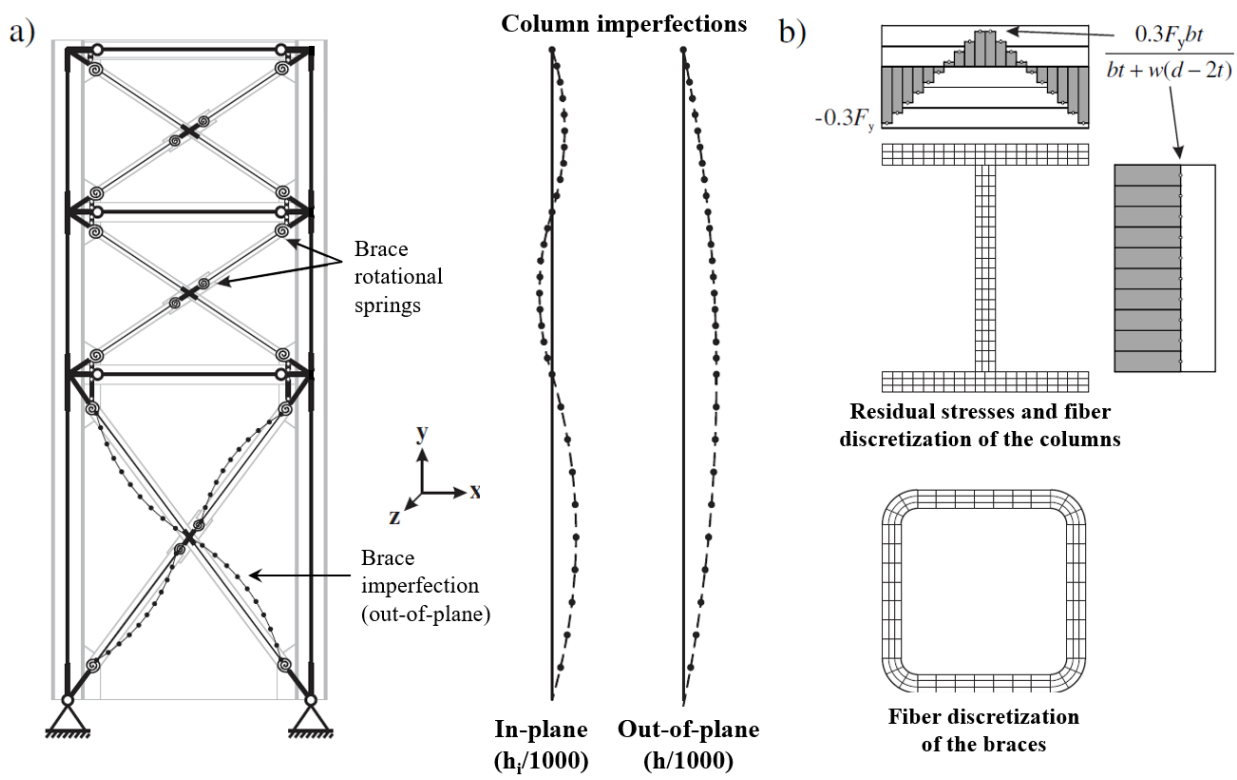

Figure 2.7 Numerical model of a three-tiered CBF: a) initial geometric imperfections; b) residual stresses and fiber discretization (Auger, 2017)

A leaning column was added to the frame and constrained in the horizontal direction to the top node of the right-hand side column. This leaning column simulates P-Δ effects, which occur when the frame is displaced laterally. This leaning column was modelled using an elastic material formulation and a near-rigid section. It was considered pinned at its base.

Restraints were applied at the base and top of the frame. At their base, the columns are restrained for all three displacements axes, while depending on the analysis rotation restraint can be applied. At the top, columns were considered braced in the out-of-plane direction and torsionally restrained, to simulate the effect of the building girders.

Gravity loading was applied to the top of both frame columns, as well as the leaning column using a static analysis pattern. These loads were applied before conducting NLRH analysis.

CHAPTER 3 DESIGN OF TWO-TIERED CBFS ACCORDING TO CSA S16-19 AND AISC 341-16

This chapter focuses on the design of a typical two-tiered CBF according to the Canadian and American standards. The Canadian design is first presented, detailing the geometry and location of the building under study and the section selection for the braced frame. This process is then repeated for the American design, before presenting a comparison between the results obtained by the two approaches. For both cases, braces are of the ASTM A1085 grade, while columns and beams are I-shaped members made of ASTM A992 steel (ASTM, 2015, 2020).

3.1 Design according to CSA S16-19

In this section, a two-tiered type MD concentrically braced frame is designed. The relevant seismic provisions for this type of frame are stated in section 27.5 of CSA S16-19 (Canadian Standards Association, 2019).

3.1.1 Building selected

A prototype building is selected for the design of the braced frame. It represents a typical industrial building, where no interior columns are used to maximize the usable floor space. It is located in Vancouver, BC, a high seismic region in Western Canada. The building site is assumed to be of soil Class E. Figure 3.1 shows the building geometry, along with the orientation of the columns. It is typical for columns to be placed as shown, to provide sufficient resistance and exterior wall stiffness under wind loading. Two braced bays are present on each exterior wall. The braced bays designed in this section are situated on the long 84 m side of the building. These were selected because column members will sustain higher axial loads, as the girders spanning across the 35 m side are connected to the top of the columns.

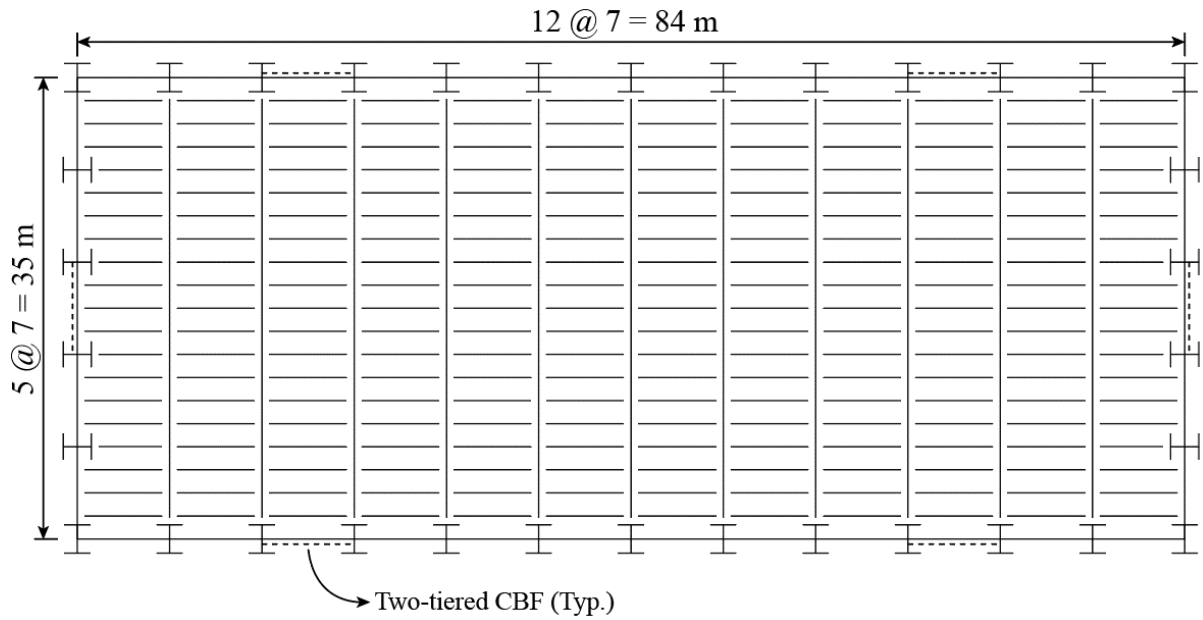

Figure 3.1 Building geometry of the designed 2T-CBF

The building height is 9 m, and bays are 7 m wide. For the braced frame, the bottom tier height is equal to h_1 = 5 m and the upper tier height is equal to h_2 = 4 m. For Vancouver, the specified snow load in NBCC (2015) is S_L = 1.64 kPa. At roof level, the dead load is equal to D_L = 1.35 kPa while the live load is equal to L_L = 1 kPa. Because the roof is not used for outdoor occupancy, snow loads and live loads must not be considered simultaneously.

The seismic load combination 1.0D + 1.0E + 0.5L + 0.25S results in a gravity loading of 228 kN on the frame's columns.

3.1.2 Seismic loading

The design base shear is determined using the equivalent static force method. For a type MD CBF, R_d = 3.0, R_o = 1.3 and for the industrial building under study I_e = 1. The total building seismic weight is 6245 kN, considering an exterior wall weight of 1 kPa. With the final selected sections, the fundamental period calculated manually of the building is equal to T = 0.44 s. It is obtained with following equation:

$$T = 2\pi\sqrt{\frac{m}{k}} \qquad \text{(Eq. 3-1)}$$

where m is the frame seismic mass, obtained by dividing the building seismic mass by the number of frames in one direction and k is the frame lateral stiffness. This results in a total design base shear for the building of V = 1633 kN. When accounting for 5% of accidental torsion, the braced frame design base shear is V_{frame} = 449 kN.

3.1.3 Braced frame design

The braces, columns and strut sections are determined in this section. It must be noted that they are only verified for the load combination including seismic effects.

3.1.3.1 Brace design

Braces are made from the steel grade ASTM A1085 with F_y = 345 MPa and R_yF_y = 460 MPa. Braces are designed to resist the lateral seismic load of 449 kN. They also have to resist the contribution of gravity loading. For the bottom braces, gravity loads produce an axial loading of 20 kN, while they produce an axial force of 15 kN in the top braces. When in the elastic range, braces in the bottom tier must resist a factored axial load of 300 kN and braces in the top tier must resist a factored load of 277 kN. An effective length of 0.45 times the total length of the braces is used to account for the lateral bracing provided by the tension brace, as well as the length of the end connections. The most economical brace section was determined to be the one that presented the lowest area. HSS 102x102x6.4 are selected for both tiers, as they satisfied resistance requirements, as well as slenderness and width-to-thickness ratios. For this building, the seismic force calculated with R_dR_o = 1.3 did not govern the design. Table 3.1 summarizes the braces characteristics.

Table 3.1 Braces characteristics for the Canadian 2T-CBF

Tier	Section (HSS)	A (mm^2)	KL/r	b/t (limit)	C_r (kN)	C_{prob} (kN)	C'_{prob} (kN)	T_{prob} (kN)	V_{prob} (kN)	V'_{prob} (kN)
2	102x102x6.4	2316	95	12.0 (17.6)	322	484	213	1065	1345	1110
1	102x102x6.4	2316	101	12.0 (17.6)	304	439	213	1065	1224	1040

3.1.3.2 Column design

For the design of columns, CSA S16-19 requires a progressive yielding analysis of the frame to be conducted. With the selected braces, Tier 1 is critical as it presents the lowest probable shear resistance V_{prob}. It is expected that the tension brace in tier 1 will yield first and experience large inelastic axial deformations. However, the difference in probable shear resistance with Tier 2 is only of 9.8% and the scenario where tier 2 is critical must be considered. For this scenario, expected brace resistances in tier 2 will be reduced by 10%.

A first column selection is made from the loading condition where braces in both tiers reach T_{prob} and C_{prob}. The loading conditions where braces reach T_{prob} and C'_{prob} is not presented as it is not critical for the columns. For this loading conditions, roof displacement is relatively low, and no bending moments are developed in the columns. The resulting axial compression load, including gravity, is 1615 kN in the first tier. For the calculation of factored compressive resistance, a strong-axis buckling length L_x = 9000 mm and a weak-axis buckling length L_x = 5000 mm are considered. A W310x79 section is first selected, with a factored compressive resistance C_r of 1779 kN. The final column selection is a W310x86 section, for which the resistance is also satisfactory.

Columns are made from steel of grade ASTM A992, with F_y = 345 MPa. The columns satisfying the requirements below and providing the lowest section area are selected. To realize the progressive yielding analysis, a *SAP2000* model of the frame is created (CSI, 2019). This numerical frame is specified with the selected sections and pinned base conditions, and in-plane bending moments and axial loads in the columns can be readily obtained.

This *SAP2000* model is first used to obtain the inelastic storey drift, $R_d R_o \delta_e$. The design seismic base shear is applied at the top of the frame, including notional forces accounting for stability effects in the form of the U_2 factor and gravity loads. The obtained inelastic roof displacement is 52.9 mm.

The first critical tier scenario is defined as being the one where the tension brace in tier 1 yields. Figure 3.2 shows the deformed shape obtained from the *SAP2000* model for both critical tier scenarios. In the first critical tier scenario, braces in the bottom tier are replaced with their respective probable tensile resistance (T_{prob}) and post-buckling compressive resistance (C'_{prob}). The tension brace in tier 2 is kept elastic, while the compression brace in tier 2 is replaced by forces equivalent to its probable compressive resistance at buckling (C_{prob}). In the second critical tier

scenario, probable brace resistances in tier 2 are reduced by 10% so that it becomes critical. The same process is realized by replacing members by their probable resistances.

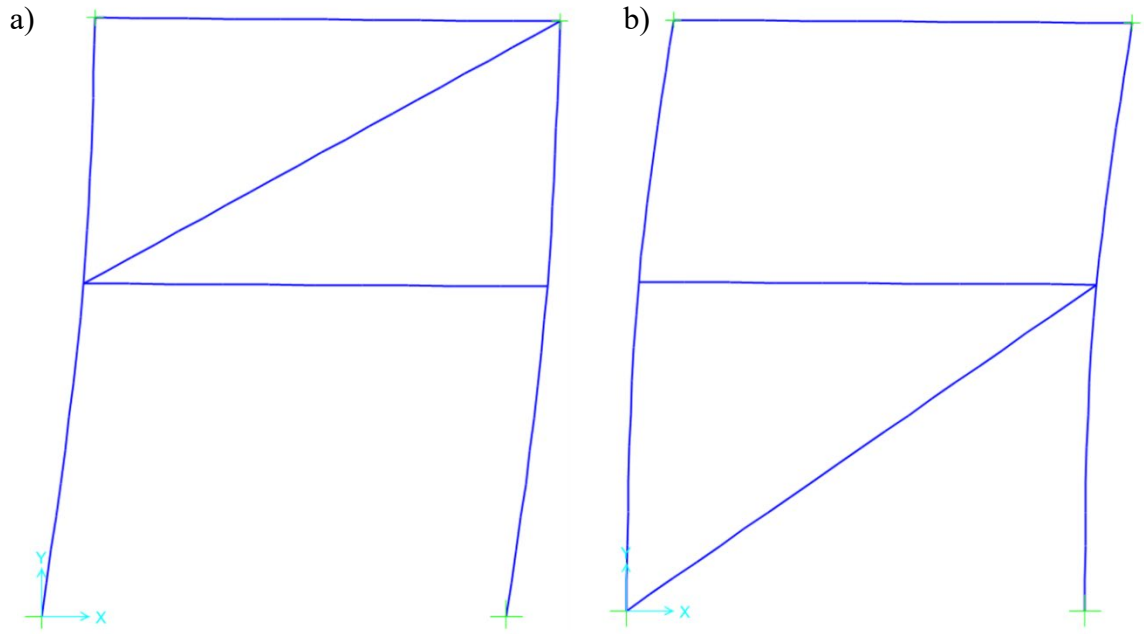

Figure 3.2 Deformed shape of the SAP2000 model for: a) tier 1 critical; and b) tier 2 critical

From the two loading conditions described above, the design compression axial load (C_{fy}) and the design in-plane bending moment (M_{fy}) are obtained for the column in compression. This column governs the section selection as it is critical for member instability. Out-of-plane bending moment is calculated by applying an out-of-plane notional load at tier level equal to 2% of the compressive force in the column below tier level. The interaction equation for axial compression and bending of Clause 13.8.2 in CSA S16-19 is used to determine if a selected section is sufficiently resistant and a W310x86 section is selected. It is also verified that the column section satisfies requirements for width-to-thickness ratios for class 1 or class 2 members loaded in axial compression and bending. Table 3.2 summarizes the column design.

Table 3.2 Design parameters for the braced frame columns according to CSA S16-19

Critical tier	M_{fy} (kN-m)	C_{fy} (kN)	Not. Load (kN)	M_{fx} (kN-m)	ω_{1x}	ω_{1y}	ω_2	Section	Max. Interaction
1	5.18	1440	28.8	64.0	0.85	0.60	1.75	W310x86	0.91
2	9.84	1282	25.6	57.0	0.85	0.60	1.75	W310x86	0.94

The first critical tier scenario produces a higher axial load in the column than the second critical tier scenario. However, this is reversed when looking at the in-plane flexural demand. Thus, it is paramount to consider all possible critical tier scenarios to ensure that the most demanding conditions are captured in design.

3.1.3.3 Strut design

The design of the strut located between braced tiers is presented here. The strut is selected such that its section depth is similar to the column depth as it allows for a torsionally braced connection between the columns and the strut by connecting the flanges of each member. From both possible loading conditions described in Section 2.3.1, the condition where the compression brace in tier 1 reaches C_{prob} and the compression brace in tier 2 reaches C'_{prob} is critical as it produces an axial load of 625 kN in the strut. This includes the axial load from lateral bracing of the columns, as described in Section 2.3.1. The weak-axis bending moment due to the strut self-weight is equal to 4.7 kN-m at the mid-length of the strut. The final strut section is a W310x79. At the strut extremity, strong axis bending moment is produced by the buckling of the brace in compression. The proportion of this moment transferred to the strut is 30.5 kN-m. In addition, a strong axis moment of 1.2 kN-m due to the torsional bracing of the column is considered. The selected W310x79 section is found acceptable. Under the applied demands, the axial force-bending moment interaction ratio is 0.66. Although this member possesses extra strength capacity, it is still the most economical because of the depth constraint described above.

3.2 Design according to AISC 341-16

In this section, an MT-SCBF is designed using the 2016 AISC Seismic Provisions (American Institute of Steel Construction, 2016a). The same steps as in the Canadian design are followed, where braces are first selected, then columns and strut sections are determined.

3.2.1 Building selected

An industrial single-storey building located in Seattle, Washington was selected for the design. The building dimensions were specified such that the column gravity loading, and the resulting brace selection becomes the same that of the Canadian design. This was decided to provide a point of comparison for column design. As a result, the building dimensions are 70 m by 168 m. The braced frame placed on the long direction of the building is designed here. Interior columns are present, to cut in half the 70 m span of the building. The design loads were determined in accordance with ASCE 7-16 (ASCE, 2016). The building if of Risk Category II and located on a site class C with a seismic design category D. The roof dead load is equal to 1.0 kPa, while the roof live load is taken as 0.96 kPa and the exterior walls as 0.5 kPa. The resulting axial gravity loading on columns, including vertical seismic effects, is 228 kN. The total seismic weight of the building is 12 831 kN, with 3208 kN tributary of the selected braced frame.

3.2.1.1 Seismic loading

For this SCBF, the response modification factor is R = 6.0. The overstrength and deflection amplification factors are respectively Ω_o = 2 and C_d = 5.0. The parameters in Table 3.3 were used to obtain the design base shear.

Table 3.3 Seismic design parameters according to ASCE 7-16

Parameter	Value
S_S (g)	1.362
S_1 (g)	0.528
S_{DS} (g)	0.908
S_{D1} (g)	0.458
C_S	0.151

With the final selected shapes, the calculated fundamental period of the frame is equal to 0.61 s, which results in a total design base shear of 1942 kN. The design base shear per braced frame including accidental torsion is equal to 534 kN.

3.2.2 Braced frame design

3.2.2.1 Brace design

The selection of braces is similar to what was presented for the Canadian design. Braces must resist the effects of lateral seismic loading in their elastic range. However, AISC 341-16 does not require braces to include the contribution of gravity loads. As a result, the factored axial force in tier 1 braces is 328 kN and the factored axial forces in tier 2 braces is 308 kN. For the calculation of compressive resistance, an effective length factor of 0.45 was used. The identical brace section HSS 102x102x6.4 is achieved for both tiers. Table 3.4 shows the design values for the selected braces.

Table 3.4 Braces characteristics for the American 2T-CBF

Tier	Section (HSS)	A (mm^2)	KL/r	b/t (limit)	C_r (kN)	C_{prob} (kN)	C'_{prob} (kN)	T_{prob} (kN)	V_{prob} (kN)	V'_{prob} (kN)
2	102x102x6.4	2316	95	12.0 (14.0)	374	502	151	999	1303	998
1	102x102x6.4	2316	101	12.0 (14.0)	341	449	135	999	1178	922

3.2.2.2 Columns

The first loading conditions for the column design correspond to what was specified for the Canadian frame. An initial column selection can be made when probable resistances are reached in both tiers at low storey displacement, which results in negligible in-plane flexural demand.

AISC 341-16 specifies a third loading condition, which accounts for non-uniform yielding between braces. The column in-plane bending moment M_{fy} is calculated using unbalanced brace storey shear force ΔV_{br} using the following equations:

$$\Delta V_{br} = \left(T_{prob,tier\ 2} + C_{prob,tier\ 2}\right)\cos\theta_2 - \left(T_{prob,tier\ 1} + C'_{prob,tier\ 1}\right)\cos\theta_1 \qquad \text{(Eq. 3-2)}$$

$$M_{fy} = \frac{\Delta V_{br}}{2}\frac{h_1 h_2}{h_s} \qquad \text{(Eq. 3-3)}$$

The unbalanced tier shear ΔV_{br} must be evaluated considering the loading condition where the compression brace in tier 1 reaches its post-buckling resistance, as well as the condition where the compression brace in tier 2 reaches that same value. For the frame studied, the critical loading condition is given by Eq. 3-2, where θ_1 and θ_2 are brace angle with respect to the horizontal plane in Tiers 1 and 2 respectively.

For the frame studied, the resulting shear force and bending moment values are ΔV_{br} = 388 kN and M_{fy} = 428 kN-m. In addition, and out-of-plane notional load at strut level equal to 0.006 times the vertical load contributed by the compression brace and the moment caused by the buckling of braces in the out-of-plane direction are considered. The moment induced by brace buckling is equal to $1.1R_yM_{pb}/\alpha_s$, where M_{pb} is the plastic bending moment of the minimum between the compression brace and the brace connection, and α_s is the LRFD force adjustment factor taken as 1.0. The resulting strong axis bending moment on the column is 7.95 kN-m. The interaction equation from the Specification for Structural Steel Buildings for members loaded in axial compression and bi-axial bending is applied and a W310x196 is selected, with an interaction ratio of 0.92 (American Institute of Steel Construction, 2016b). It is also verified that this member satisfies requirements for a moderately ductile member by evaluating its web and flange width-to-thickness ratios.

3.2.2.3 Strut design

For the strut design, two loading conditions must be considered:

- In both tiers, the tension braces reach T_{prob} and the compression braces reach C_{prob}.
- In both tiers, the tension braces reach T_{prob} and the compression braces reach C'_{prob}.
- The MT-CBF specific loading condition where the tension braces reach T_{prob} and the compression braces above and below the strut reach their respective C'_{prob} and C_{prob} values.

The second condition produces a higher axial load in the strut, equal to 721 kN. With this axial load, the same procedure as the Canadian design is followed to obtain the most economical section. The strut depth must match the column depth, and strong axis bending moments coming from brace buckling and torsional restraint of the column are considered. As a result, a W360x79 is selected, with a design ratio value of 0.98.

3.3 Comparison between the braced frame designs

A two-tiered CBF was designed according to CSA S16-19 and AISC 341-16. The building geometry was adjusted to provide both designs with the same bracing members in both tiers: HSS102x102x6.4. The resulting column section for the Canadian frame was a W310x86, while a W360x196 was selected for the American frame.

To achieve the same selection of bracing members, a higher seismic weight was considered in the American design. This is due to the response modification factor in AISC 341-16 R = 6.0 that is higher than its Canadian equivalent R_dR_o = 3.9. Furthermore, to reach similar design ratios for bracing members, the design base shear is slightly higher for the American frame, as the factored compressive resistance equation produces higher values than its Canadian counterpart for the relevant KL/r range. As a reminder, the braces slenderness ratios were 95 and 101 in tier 1 and tier 2 respectively. The design base shear for the American frame can also be larger because the contribution of gravity load in the braces axial force is neglected, whereas CSA 16-19 requires that it is considered.

Column design is significantly different for both frames. As columns are designed as capacity-protected elements, they are influenced by probable brace resistances. Both American and Canadian provisions specify different values for the expected yield stress (R_yF_y), as well as slightly different equations for the calculation of probable brace resistances. Table 3.5 shows the obtained values for braces in tier 1.

Table 3.5 Tier 1 braces (HSS 102x102x6.4) parameters for the Canadian and American frame

Design standard	C_r (kN)	R_yF_y (MPa)	C_{prob} (kN)	C'_{prob} (kN)	T_{prob} (kN)	V_{prob} (kN)	V'_{prob} (kN)
CSA S16-19	304	460	439	213	1065	1224	1040
AISC 341-16	341	431	449	135	999	1178	922

Furthermore, CSA S16-19 and AISC 341-16 use different approaches to evaluate the column axial and flexural demands when brace yielding is reached. The Canadian frame is designed using progressive yielding analysis, which is used to determine brace forces when one tier becomes critical. Under this approach, not all tension braces must reach their probable tensile resistance. On the contrary, the American frame is designed to achieve a full plastic mechanism, where the tension braces in all tier will reach T_{prob}. This results in a significantly higher in-plane flexural demand and a heavier section in the U.S. However, it must be noted that the American method has the benefit of being straightforward and only requiring traditional static equations.

Although both design standards include out-of-plane notional loads, AISC 341-16 explicitly requires considering the out-of-plane moment due to brace out-of-plane buckling. CSA S16-19 specifies a notional load equal to 2% of the factored axial load in the column below the tier level, which results in a higher strong axis bending demand on the column. Despite this last point, the difference in in-plane bending demand is significantly large so that the American frame requires a heavier column section.

CHAPTER 4 NUMERICAL MODEL

This chapter presents the numerical model of the braced frame developed in the *OpenSees* program. The model was used to conduct the nonlinear response history analyses described in Chapter 5 through Chapter 8. This model is based on previous works detailed in the literature review, and the chapter details the different inputs and assumptions that were used. Subsequently, the selection and scaling of the ground motion records applied to the different studied braced frames is presented. Finally, a detailed finite element model developed in *Abaqus* (Simulia, 2011) is used to compare and validate the NLRH analysis results obtained from *OpenSees* for a typical two-tiered CBF located in Seattle, Washington.

4.1 *OpenSees* numerical model

The *OpenSees* model used in this research project was created using the modelling technique described in Imanpour (2015) and Auger (2017) that have been described in section 2.4. Different bracing systems are studied in this project: two-tiered CBFs, two-tiered and three-tiered two-bay CBFs, split-X CBFs, and two-bay X-CBFs. For all bracing systems, the same base model is used with the same following characteristics.

Members are each divided in 10 elements, with columns and braces defined using the *force-based nonlinear beam-column* element. The roof beam and struts were simulated using *elastic beam-column* elements, because they are expected to remain elastic throughout a seismic event. Rigid elements used to represent the connections between columns, struts and braces are also modeled using *elasticBeamColumn* elements. A leaning column is added to the model to represent the P-Δ effects and its top node is constrained to one of the top column nodes for horizontal translation in-plane.

Figure 4.1 shows the undeformed shape of a typical two-tiered concentrically braced frame. On this figure, the shorter rigid elements representing the gusset connections can be seen at each member end. Truss elements are also present between the brace ends and the corresponding strut or roof beam node, to simulate the in-plane flexural stiffness provided by the gusset plates. Auger (2017) demonstrated that truss elements between the brace ends and the columns don't contribute significantly to the flexural response of the columns and were not included. The length of these truss elements varies depending on their location of the frame, as the roof beam and strut don't

have the same depth. The roof beam is bent around its strong axis when in-plane flexure is applied, whereas the strut is bent around its weak axis under the same loading. As such, the truss element linking the roof beam to the braces in the second tier is longer. Rotational springs are modelled at each brace end to reproduce the out-of-plane flexural stiffness as well as the torsional stiffness of the gusset plates.

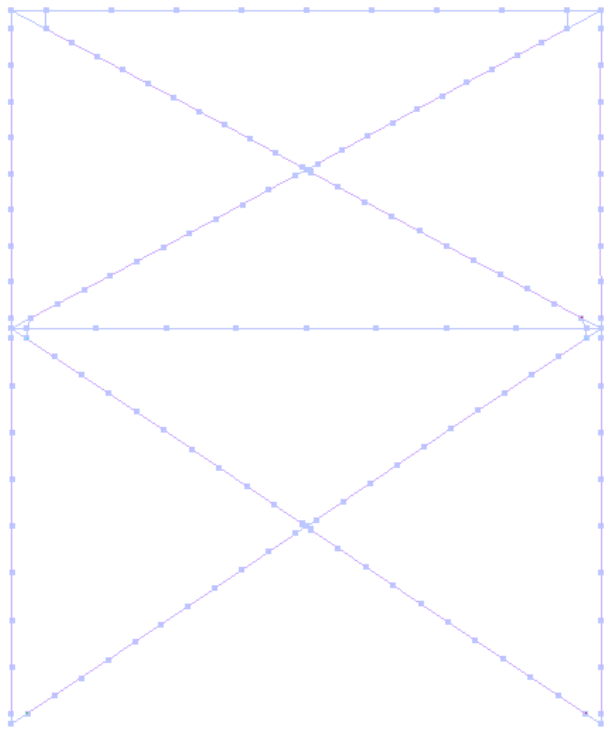

Figure 4.1 Undeformed shape of a typical 2T-CBF modeled with OpenSees (leaning column not shown)

Geometric initial imperfections are specified to the brace and column members as shown by Figure 2.7. In the plane of the frame, out-of-straightness of the column is equal to $h_i/1000$, where h_i is the tier height. For the out-of-plane imperfections, the same ratio is used but for the entire storey height, h_s. The initial imperfections of the braces are assigned out-of-plane in a sinusoidal shape and correspond to a 1/1000 of the bracing member's length. Geometric nonlinearity is considered using the *corotational* formulation. Column and brace sections are discretized in fibers as represented in Figure 2.7.

The building seismic weight tributary to the braced frame is applied in the horizontal direction to the top of the frame's columns.

For columns and braces, the *Steel02* material is used. This material is capable of reproducing kinematic and isotropic hardening as well as the *Bauschinger* effect. The parameters for this material are calibrated following what is presented in section 2.4 from results by Imanpour (2015) and Auger (2017).. Table 4.1 shows the resulting parameters used in the numerical model.

Table 4.1 Steel02 calibration parameters used in the OpenSees model

Parameter	Value
E (MPa)	200 000
$E_{t,\ columns}$ (MPa)	$\frac{0.075F_y}{0.02E}$
$E_{t,\ braces}$ (MPa)	$\frac{0.1F_y}{0.04E}$
R_0	24.0237
cR_1	0.8887
cR_2	0.0701
a_1	0.3411
a_2	12.2044
a_3	0.3158
a_4	12.2044

Rayleigh mass proportional damping was added to the model and was set to 2 % of the critical damping in the first mode of vibration, because single-storey buildings only have one dynamic degree-of-freedom corresponding to the roof horizontal displacement.

4.1.1 End conditions

At the roof level, the translational DOF in out-of-plane and rotational DOF about the longitudinal axis of the columns are constrained. This is to represent the restraints that are provided by the

building beams and the roof steel deck respectively. The roof beam nodes are constrained in the out-of-plane direction, to represent the roof steel deck punctually welded to that beam.

In the selected building, the base plate, anchors and concrete footing can all contribute to restraining the rotation of the column at their base, resulting in a semi-rigid condition. A pinned base condition, however, can represent the case where yielding and buckling of the column can take place earlier (i.e., in a lower storey drift demand). Thus, a pinned base condition was assumed for the columns.

4.1.2 Model limitations

The numerical model described above has some limitations attributable to the different assumptions and the software itself.

- *OpenSees* is unable to reproduce lateral-torsional buckling of the column members. This can be checked by manual calculation using the equations provided in CSA S16-19 and is also unlikely to occur because of the torsional restraint provided by the strut.
- Fibre elements used in *OpenSees* cannot reproduce local buckling of the members.
- As mentioned previously, the base conditions of the columns are taken as pinned, but the fixity to the concrete foundation provides some rotational stiffness.
- The connections do not consider the fact that the strut is connected to web of the column, which has a lower flexural stiffness than the whole column section.
- Material assumptions and calibration can cause a lot of variability in the behaviour of the structure, especially regarding the braces. Material calibration was realised using experimental results by Imanpour (2015) and Auger (2017).

4.1.3 Calculation of response parameters

For all analyses, when average values are presented in lieu of values from a specific ground motion, the presented result is taken as the average of the five biggest values, as recommended in the NBC User's Guide (NRCC, 2017). For example, the first five ground motions might cause the largest roof displacement, whereas the maximum in-plane bending demand in the columns might come from another five ground motions.

It is also important to indicate from which nodes the force and displacement values are taken. Roof and tier level displacements are taken as the average of different column nodes at the required level. The column axial force, in-plane moment, and out-of-plane moment are taken from the element right below the tier level. This is to prevent extracting results from the rigid elements used to model the connection between column, strut and braces as they can be artificially higher because of the stiffness of the element. Furthermore, the maximum average bending moment value for a given column is computed only when the column is loaded in compression. As detailed in design, this is the critical scenario for the column because its stiffness is reduced, and it can be prone to instability. Lastly, brace forces are taken at the middle of the bracing members. For each tier, values are plotted for the continuous and the discontinuous brace.

4.2 Ground motions

The selection and scaling of the ground motions to be used in NLRH analyses can significantly affect the results (Heo, Kunnath, & Abrahamson, 2011). A set of ground motions was selected and scaled in accordance with Method A of the NBC User's Guide (NRCC, 2017). All studied buildings are located in Vancouver, British Columbia. As such, three suites of five ground motion records are selected for a total of fifteen records. Each suite corresponds to one of the three earthquake sources that can occur in southwest British Columbia: shallow crustal earthquakes, in-slab subduction earthquakes and interface subduction earthquakes. Since the studied buildings are all located on a Type E soil and their fundamental period remains similar regardless of the configuration or bracing system, one ensemble of fifteen ground motions was selected and scaled.

The selected period range (T_R) was 0.09 s to 1.5 s, with each suite of records being scaled for a scenario-specific period range within that period range. The selected period range was determined using following Figure 4.2, in accordance with Method A of the NBC User's Guide (NRCC, 2017). The frames studied in this thesis can be represented as single degree of freedom systems. Therefore, their first mode period (T_1) is taken equal to the period of the mode that is necessary to achieve 90% mass participation (T_{90}). The scenario-specific period ranges were determined for each tectonic source contributing to the seismic hazard in British Columbia: crustal earthquakes, in-slab subduction earthquakes and interface subduction earthquakes.

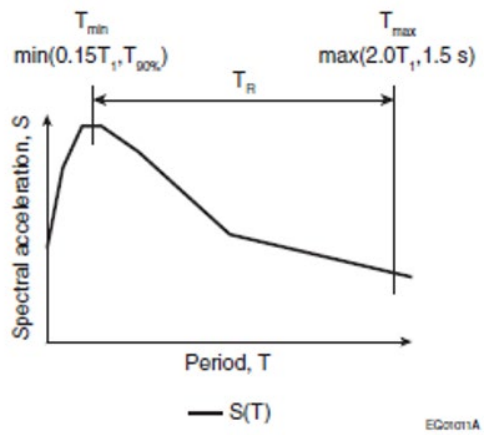

Figure 4.2 Determination of the period range for ground motion scaling (NRCC, 2017)

Figure 4.3 shows the target spectrum and the scaled ground motion spectrum for each suite. Table A.9.1 details the characteristics for the selected records.

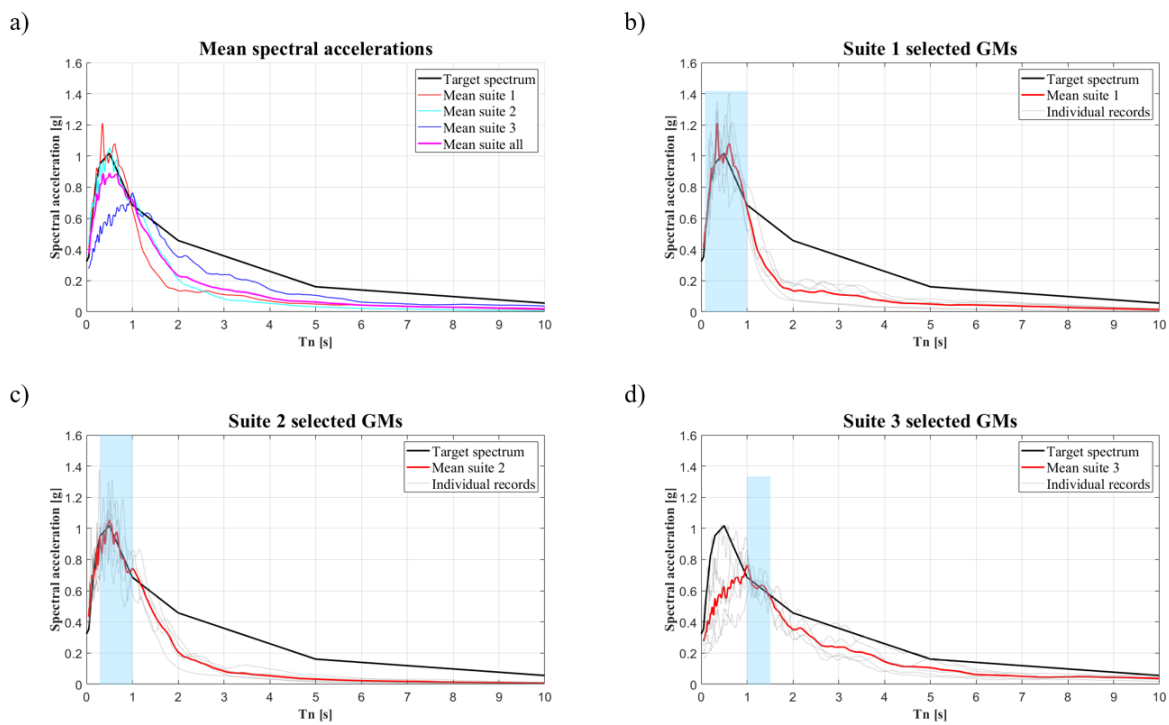

Figure 4.3 Scaled spectral acceleration of the selected ground motions in Vancouver, soil type E: a) mean spectral accelerations; b) crustal earthquakes; c) in-slab subduction earthquakes; and d) interface subduction earthquakes

4.3 Validation of the *OpenSees* numerical model

This section presents the *Abaqus* numerical model and the two-tiered CBF that were used to validate the results obtained from the *OpenSees* NLRH analyses with the model described above. The frame geometry and loading are first detailed, followed by the *Abaqus* numerical model. Results are then compared for a selected ground motion for two base fixity conditions.

4.3.1 Frame geometry used for the validation

The building used for this comparison is located on a soil of Class C in Seattle, Washington and is laterally braced by two two-tiered CBFs on each exterior wall. The braced bays on the long sides of the building are studied and their geometry and sections are shown in Figure 4.4. This frame was designed according to AISC 341-10 (American Institute of Steel Construction, 2010a) and AISC 360-10 (American Institute of Steel Construction, 2010b).

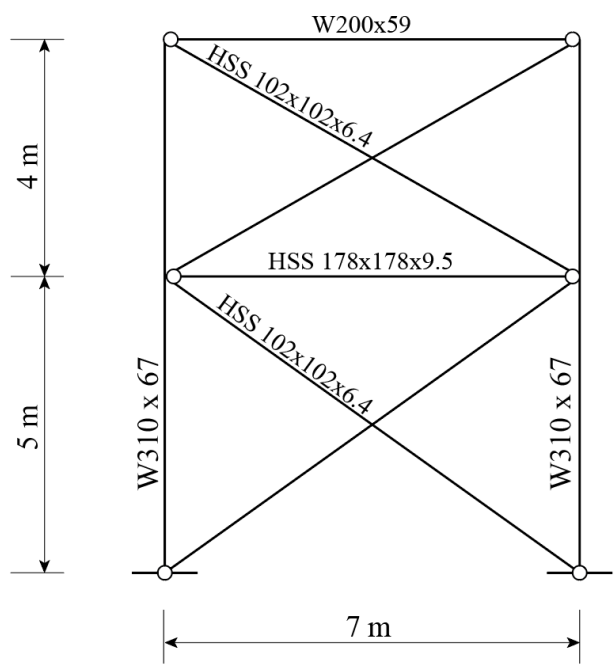

Figure 4.4 Two-tiered CBF geometry and sections used for OpenSees and Abaqus comparison

The total seismic weight of the building is 12 832 kN, which gives 1604 kN of seismic weight per braced frame column. The gravity load applied on each frame column is 229 kN and the leaning column gravity loading is 5031 kN. The fundamental period of the frame, by hand calculation, is

equal to 0.64 s. For both numerical models, columns yield stress is equal to 397 MPa and braces yield stress is equal to 431 MPa.

The frame was designed assuming pinned conditions at the base of the columns, but two analyses were completed: one with a pinned base and one with a fixed base along the three axes of rotation. It was deemed pertinent to validate the *OpenSees* model for both these conditions to ensure that the response can be adequately captured.

4.3.2 *Abaqus* numerical model

The prototype frame illustrated above was modelled and analysed using the *Abaqus* finite element program (Simulia, 2011). The *Abaqus* model can reproduce local buckling and lateral-torsional buckling of members. This chapter presents the modelling steps and assumptions that were followed.

The numerical model is based on the information gathered during the literature review and was developed with the contribution of Pablo Cano, a collaborator of this project. All members were modelled using 4-node stress/displacement shell elements. The kinematic/isotropic plastic material model from the *Abaqus* library was selected, as it can simulate the cyclic inelastic behaviour of steel. The calibration values used for this material are shown in Table 4.2.

Table 4.2 Material model assumption of the the Abaqus model

Parameter	Value
E (MPa)	200 000
C_1	3370
γ	20
Q_∞ (MPa)	90
b	12
$F_{y,\ columns}$ (MPa)	397
$F_{y,\ braces}$ (MPa)	431
$F_{y,\ gussets}$ (MPa)	350

Connections were modelled using welded gusset plates based on initial design calculations. The geometry of the frame using *Abaqus* is shown in Figure 4.5. Mesh density was finer around the connection areas, as well as the center of the braces and was set to approximately 25 mm. The rest of the frame used shell elements varying between 30 to 40 mm in size. Boundary conditions were specified in the same manner as in the *OpenSees* model, using reference points where needed. P-Δ effects were considered by including a leaning column constrained to the top node of the right-hand side column. Geometrical imperfections were included by applying initial loading to the frame corresponding to the desired initial deformed shape, and thereafter extracting the nodes positions to input them in the NLRH model. Finally, residual stresses in the columns were specified in the same manner as in the *OpenSees* model, discretizing columns in *slices* for the flanges and the web.

The gravity loads, masses and ground motion were the same as described above, for both numerical models.

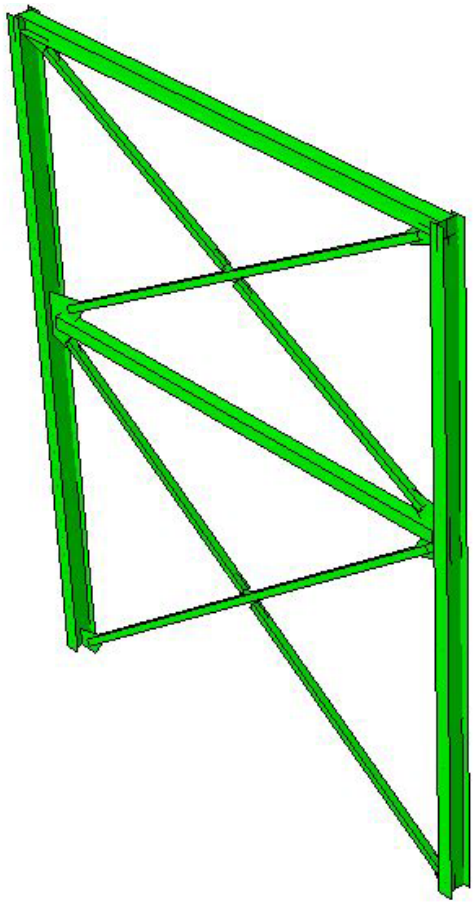

Figure 4.5 Geometry of the two-tiered CBF in *Abaqus*

4.3.3 Comparison of the *OpenSees* numerical model with the *Abaqus* numerical model

The ground motion record selected for this comparison was taken from an ensemble of records selected and scaled for a site class C in Seattle, Washington by Professor Robert Tremblay, the supervisor of this research project, in June of 2020. This record corresponds to a pulse ground motion from the Loma Prieta earthquake of 1989, recorded at the station *Gilroy Array #2*.

4.3.3.1 Pinned base condition

The results from the frame with a pinned base condition are first presented. The fundamental period of the frame obtained from *OpenSees* is 0.63 s while the fundamental period obtained from the *Abaqus* model is 0.62 s. These make for a difference of respectively 0.02 % and 0.03 % with the hand calculation. The slightly higher value from the hand calculation is due to the axial deformation of the brace members, which is calculated using their center-to-center lengths, whereas the lengths in the models are shorter because of the gusset plates. As the seismic weight applied to the frame is the same in both models, these close values demonstrate that the initial stiffness is well represented and that the frame geometry and section shapes are modelled accurately. The same fundamental period values are obtained for the fixed base condition. Figure 4.6 shows the drifts and normalized brace forces in both tiers from NLRHA of the two models under pinned base conditions. Figure 4.7 shows the deformed shape from both numerical models at column buckling. In this figure, data coming from *OpenSees* and *Abaqus* are labeled as “OS” and “AB” respectively. Also, each tier is composed of a continuous and a discontinuous brace, where the latter is typically connected to a plate going through the continuous brace ad mid-length. The continuous brace is abbreviated as “cont.” and the discontinuous brace as “disc.”.

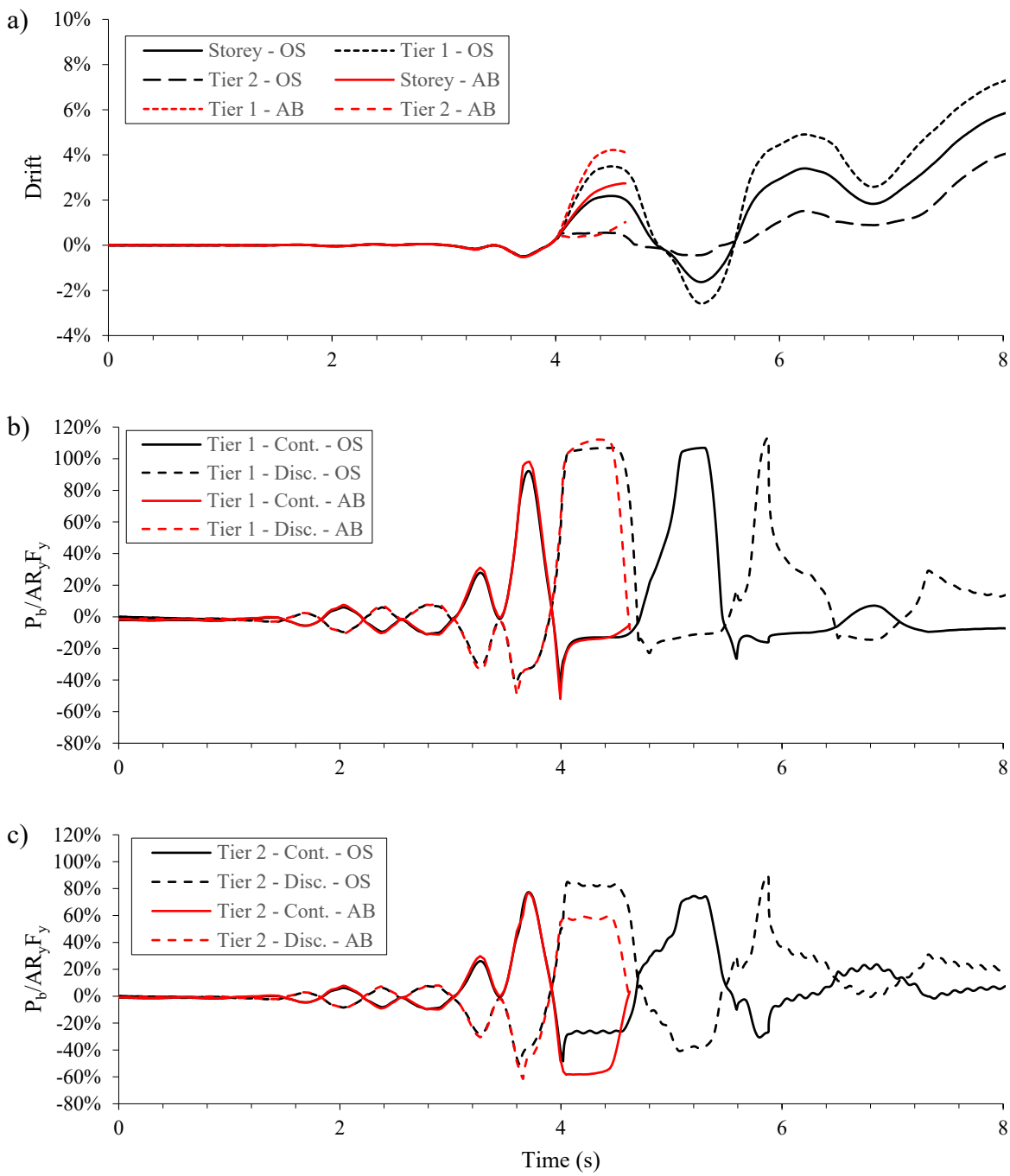

Figure 4.6 Comparison of OpenSees and Abaqus models for pinned conditions under the 1989 Loma Prieta earthquake, Gilroy array #2: a) drifts; b) brace forces in tier 1; and c) brace forces in tier 2

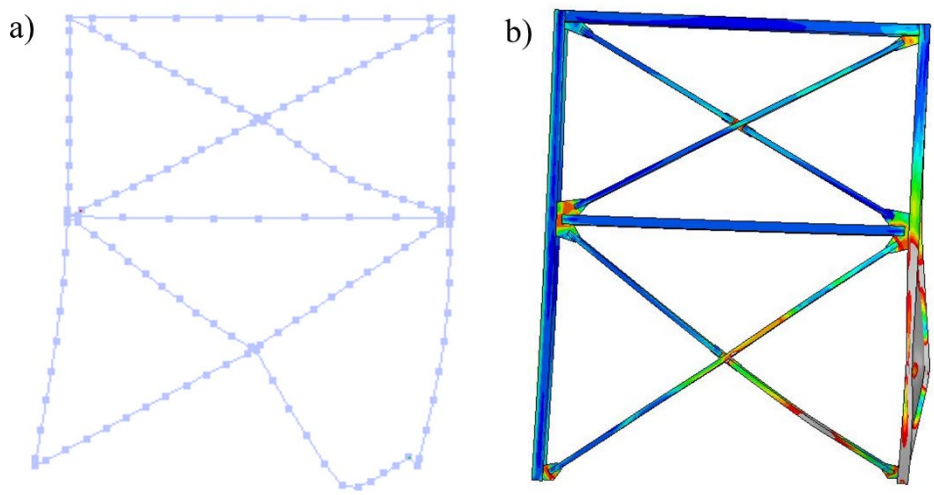

Figure 4.7 Comparison of *OpenSees* and *Abaqus* models for pinned conditions under the 1989 Loma Prieta earthquake Gilroy array #2: a) *OpenSees* deformed shape at column buckling; and b) *Abaqus* deformed shape at column buckling

When a pinned base is used, column buckling occurs. The buckling shape of the column from both numerical models is similar, with high deformations in the in-plane direction. *Abaqus*, however, is able to simulate local buckling of one flange of the column, which starts to induce torsion in the member at the end of the analysis. In general, both models can simulate closely the seismic response of the selected frame with a pinned base condition.

4.3.3.2 Fixed base condition

The same numerical models and ground motion were analysed using fully fixed column bases. All three axes of rotation were fixed in theses analyses. Figure 4.8 presents the drifts, normalized brace forces and normalized in-plane bending moments from both models, while Figure 4.9 shows the deformed shapes at tier yielding.

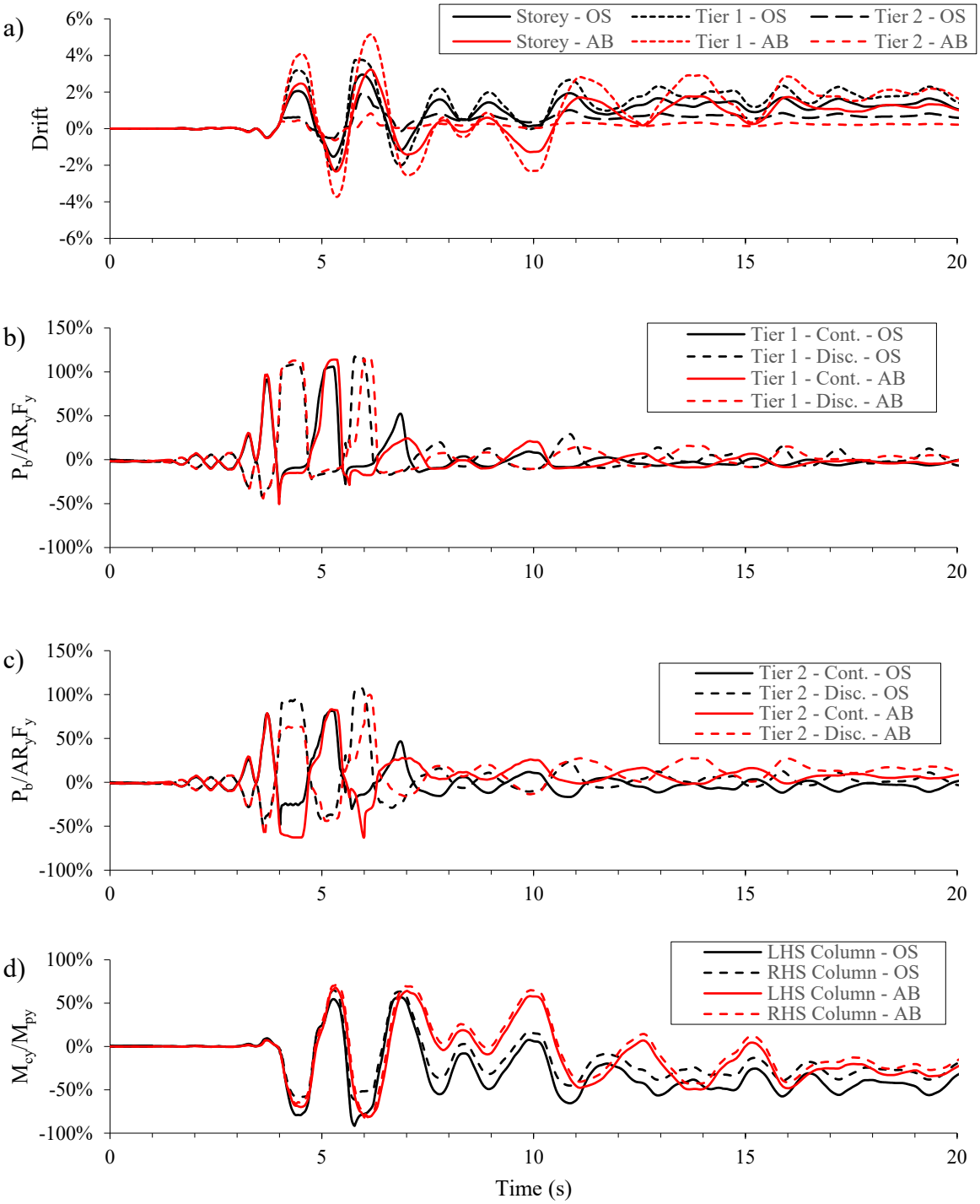

Figure 4.8 Comparison of OpenSees and Abaqus models for fixed conditions under the 1989 Loma Prieta earthquake Gilroy array #2: a) drifts; b) brace forces in tier 1; c) brace forces in tier 2; and d) in-plane bending moment in columns

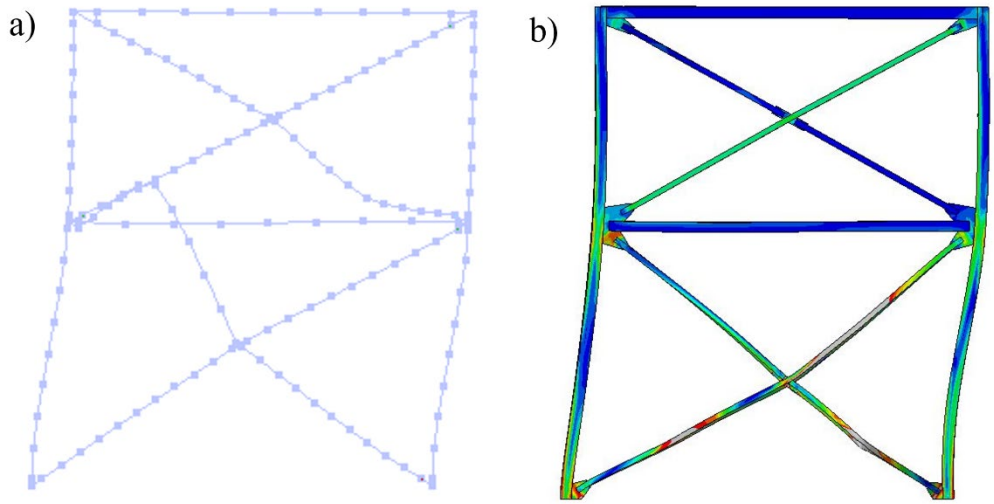

Figure 4.9 Comparison of OpenSees and Abaqus models for fixed conditions under the 1989 Loma Prieta earthquake Gilroy array #2: a) *OpenSees* deformed shape at yielding of tier 1; and b) *Abaqus* deformed shape at yielding of tier 1

In both numerical models, no failure of the columns is observed. This allows a yielding mechanism to develop in the first tier. Both models predict similar drift cycles, with variable amplitude, and retain residual deformations in the first tier at the end of the ground motion. *Abaqus* and *OpenSees* are both in agreement for the axial forces in the braces at tier 1, as they remain close throughout the earthquake. In tier 2, however, peak brace forces differ between the two programs. This explains the variation in peak drift amplitudes observed in Figure 4.8 a. Despite this, in-plane bending demand in the columns correlates well between the two models. This is a key factor, as the in-plane flexure of the columns is essential for predicting column failure and comparing design methods.

Finally, the disparity observed in brace behaviour can be attributed to the differences in material modelling and calibration. The material models used in *OpenSees* and *Abaqus* do not rely on the same equations and were not calibrated from the same sources, as detailed in Chapter 2. An upcoming experimental program held at Polytechnique Montréal in collaboration with the University of Alberta aims to study the cyclic behaviour of bracing members commonly used in MT-CBFs. This program, lead by collaborators of this project, will allow for a more thorough calibration of the material properties for both *OpenSees* and *Abaqus*. Comparing the *OpenSees*

numerical model to the *Abaqus* numerical model permits the validation of the former, as the global behaviour of the studied 2T-CBF is similar in both. Predictions until tier yielding agree very well from both models, while residual drifts and brace axial demands differ because of material definition.

CHAPTER 5 SEISMIC BEHAVIOUR OF A TWO-TIERED CBF

This chapter presents the results of nonlinear response history analyses conducted to examine the seismic response of the two-tiered concentrically braced frame designed in Chapter 3.

The same prototype building as described in Chapter 3, located in Vancouver, BC on a soil type E, is used. The columns base nodes are considered free to rotate in all three main axes (pinned). Each frame column is loaded axially to the extent of 228 kN from gravity and a seismic mass of 781 kN is applied to the frame. As they are capacity protected elements, columns are specified with a yield stress of 345 MPa. The yield stress for the bracing members is specified as their expected strength R_yF_y = 460 MPa. Figure 5.1 shows the geometry and sections of the studied frame.

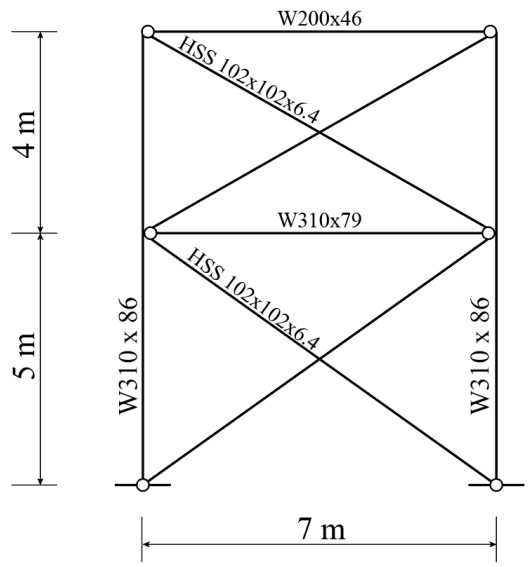

Figure 5.1 Geometry and selected members for the studied two-tiered CBF

5.1 Nonlinear response history analysis

NLRH analysis was conducted on the 2T-CBF using the set of ground motions described in Chapter 4. This same ensemble of ground motions is used throughout the following chapters. The time histories and acceleration spectra of two critical ground motions, identified because they generate the largest lateral displacement and bending demands in the columns, are shown in Figure B.9.1 and Figure B.9.2.

In this section and in the subsequent chapters, the following response parameters are identified and discussed:

- Storey drifts and tier drifts, as a percentage of the relevant height (storey height h_s or tier height h_i).
- Normalized axial forces of bracing members, P_b/AR_yF_y. The axial forces are divided by AR_yF_y of the respective brace, which represents the probable tensile resistance. Braces forces for continuous or discontinuous members are shown for both tiers. These are identified as "cont." and "disc" respectively.
- Normalized bending moments M_{cx}/M_{px} and M_{cy}/M_{py} in the columns. They are normalized by the strong axis plastic moment or by the weak axis plastic moment, respectively: Z_xF_y and Z_yF_y. Left-hand side and right-hand side columns are identified as "LHS" and "RHS" respectively. When applicable, the middle (or interior) column is identified as "Mid".
- Peak roof drift obtained from NLRH analyses, $\delta_{roof,NLRH}$.

Figure 5.2 shows the deformed shape from the *OpenSees* numerical model of the 2T-CBF at brace tensile yielding in Tier 1. Brace buckling occurs before that point, between 0.3% and 0.4% tier drift. Brace buckled shape is oriented out-of-plane, following the initial geometric imperfections. Inelastic deformations are then concentrated in the tier where the brace yielding took place first, which produces in-plane bending moments on the columns.

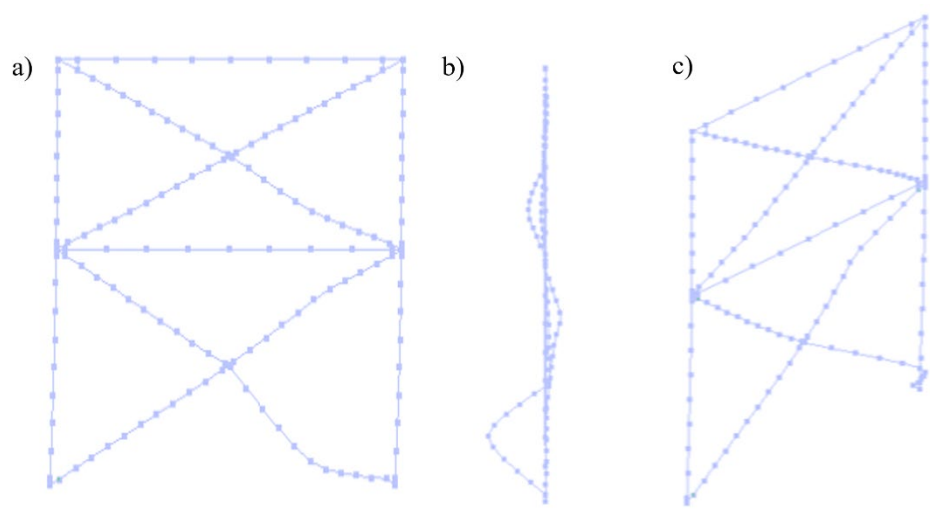

Figure 5.2 2T-CBF deformed shape of the OpenSees numerical model at the verge of brace yielding in Tier 1: a) elevation view; b) side view; and c) isometric view

Figure 5.3 presents the storey and tier drifts in the 2T-CBF during the Loma Prieta 1989 earthquake. Before yielding of the brace in tier 1 at 8.7 s, tier drifts and storey drifts are of the same amplitude, as no inelastic deformation has yet occurred. After yielding of tier 1, inelastic deformations can be observed as the storey and tier 1 drifts oscillate around 0.2%.

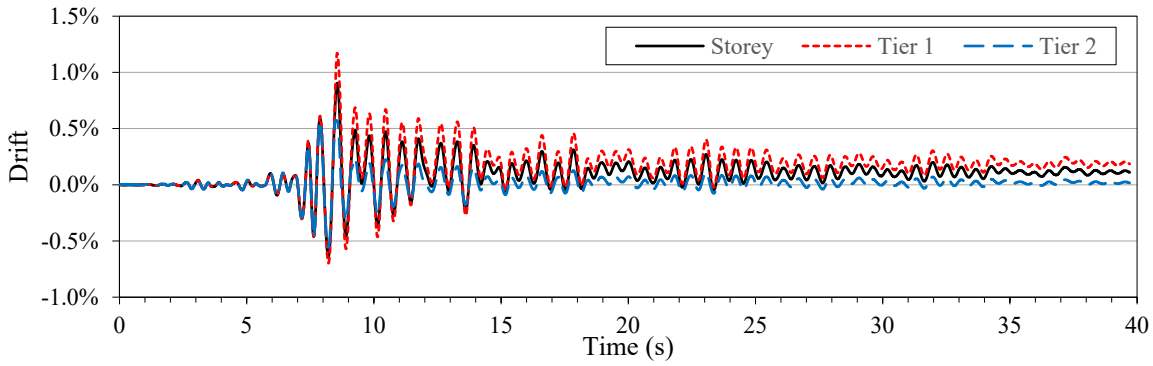

Figure 5.3 Frame drifts for the 2T-CBF under Loma Prieta 1989 earthquake, Hollister Differential Array

Figure 5.4 shows the drifts, normalized brace forces and normalized bending moments in the columns under the 1989 Loma Prieta record. A vertical line is traced at the point where maximum in-plane flexural demand occurs in the columns.

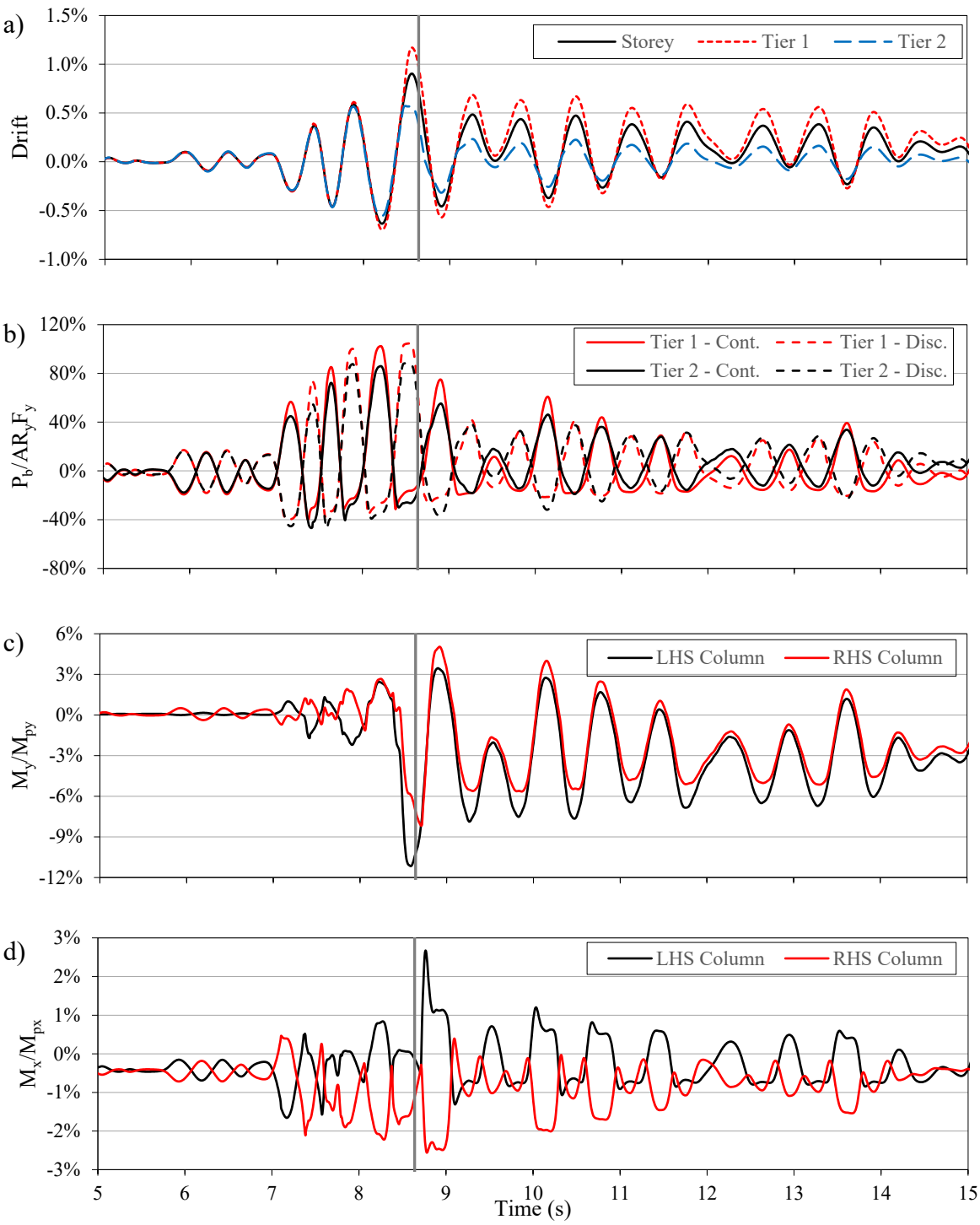

Figure 5.4 2T-CBF response under 1989 Loma Prieta, Hollister Differential Array record: a) drifts; b) normalized brace forces; c) normalized in-plane column moment; and d) normalized out-of-plane column moment

Brace axial forces correspond well to the design prediction. At tier yielding, the tension brace of tier 1 reaches AR_yF_y before attaining slightly higher values because of material strain hardening. Compression values correspond well to the probable resistances at buckling (C_{prob}) and at post-buckling (C'_{prob}), with differences varying between 1.5% and 4.5% with respect to the design values.

At large storey drifts, the tension brace in the critical tier attain their tensile strength and during this same cycle drift is concentrated in the critical tier. This moment is illustrated by the vertical line in Figure 5.4. This coincides well with the maximum in-plane flexural demand on the columns. The RHS column, axially loaded in compression, reaches 8.2% of its plastic moment about its weak axis.

Peak out-of-plane bending moments in the columns occur simultaneously with brace buckling. When the brace gusset plates yield in flexure, they transfer part of that bending moment to the columns. Indeed, the moment in the gusset plate produces torsional moments in the columns and out-of-plane moments in the struts. The axial force in the brace deformed ot-of-plane may induce strong axis moment in the column. It can also be observed that out-of-plane flexure is influenced by the side to which the frame is pushed, as well as the point were directions are reversed. This is due to the buckling of the braces connecting to the columns occurring towards two opposite directions. Table 5.1 shows peak frame response from NLRH analyses compared to anticipated design values. Values are presented for the case where $R_yF_y = 460$ MPa was specified for the braces, as well as the case where 85% of that value was specified for the braces in tier 2.

Table 5.1 Peak frame response for 2T-CBF

Parameter	$1.0R_yF_y$ in both tiers	$0.85R_yF_y$ in tier 2
$\delta_{roof,NLRH}$ (% h_s)	0.73	0.74
$\delta_{roof,NLRH}/R_dR_o\delta_e$	1.24	1.26
Tier 1 drift (% h_1)	0.85	0.51
Tier 2 drift (% h_2)	0.67	1.06
$M_{cy,\ NLRH}$ / M_{py}	0.05	0.10
$M_{cy,\ NLRH}$ / $M_{cy,\ design}$	1.73	1.80
$M_{cx,\ NLRH}$ / M_{px}	0.02	0.03
$M_{cx,\ NLRH}$ / $M_{cx,\ design}$	0.18	0.18

Peak drift demands remain under the NBCC limit of 2.5%. However, they exceed the inelastic design roof drift by a ratio of about 1.25. Despite this, frame response remains satisfactory, since no exceedingly large force demands are observed in the braces or columns.

In design, the maximum in-plane bending demand for the columns was taken from the scenario where tier 2 was critical, when the braces probable yield stress was reduced by 15%. Table 5.1 confirms this design expectation, as flexural demand is increased for that scenario. This demand is underestimated by the design method, because of the underestimation of the inelastic storey drift in design. When using the inelastic roof displacement from NLRHA in the design procedure, in-plane bending moments match well with differences ranging between 2% and 7.4%.

Out-of-plane bending moments in the columns are largely overestimated by CSA S16-19. As stated in Chapter 3, a notional load equal to 2% of the compression force in the column below the tier level is applied to create out-of-plane flexure. In the model, this flexure is mainly produced by the flexural buckling of the gusset plates produced by out-of-plane compression buckling of the braces. The plastic moment of these gusset plates is approximately 4 kN-m for the selected brace sizes, and the transferred flexure to the column is far inferior to the design predicted values.

CHAPTER 6 SEISMIC BEHAVIOUR OF TWO-BAY MT-CBFS

The focus of this chapter is on the seismic response of MT-CBFs placed in two adjacent bays. The current Canadian steel design standard prohibits the use of two-bay MT-CBFs, unless both bays use the same geometry and members. However, for various practical or economical reasons, architects and engineers might favour a two-bay configuration. As such, it is pertinent to evaluate if the behaviour of these frames can be accurately predicted in design, and if their response is satisfactory. The different frame geometries studied here are first presented. Both uniform and non-uniform bay widths are then analysed. Further, the design procedure used for a non-uniform two-bay 2T-CBF is detailed. Finally, NLRH analyses results for the frames are presented.

6.1 Studied geometries

Six two-bay frames based on the same building geometry detailed in Chapter 3 are studied here. Three consist of two-tiered frames, while the others consist of three-tiered frames. It should be noted that CSA S16-19 prohibits the use of MT-CBFs having more than three tiers as well as those using different geometries or members in adjacent bays. Three different bay width configurations are examined: a uniform configuration with two 7-meter bays, a non-uniform configuration with 6- and 8-meter bays, and a non-uniform configuration with 7- and 8-meter bays. Figure 6.1 and Figure 6.2 show the different frame geometries and selected sections for the two-tiered and three-tiered frames studied here.

For a given frame, the selected column section for all three columns was the largest required to resist the force demands in the three columns. The first reason for this assumption is to allow for the use of the same connections for torsion transfer between the columns and the struts for the exterior and interior columns. To achieve this, the flanges of the strut are connected to those of the column, which requires that the two sections be of a similar depth. The second reason being that engineers would probably favour using the same column section as this results in easier detailing of the connections, and a more streamlined fabrication and erection process. However, the two-tiered uniform configuration was also studied with different column sections, to examine if the design procedure can accurately predict the frame response in this scenario. For the same reasons, the same strut section is used at both tiers in three-tiered frames.

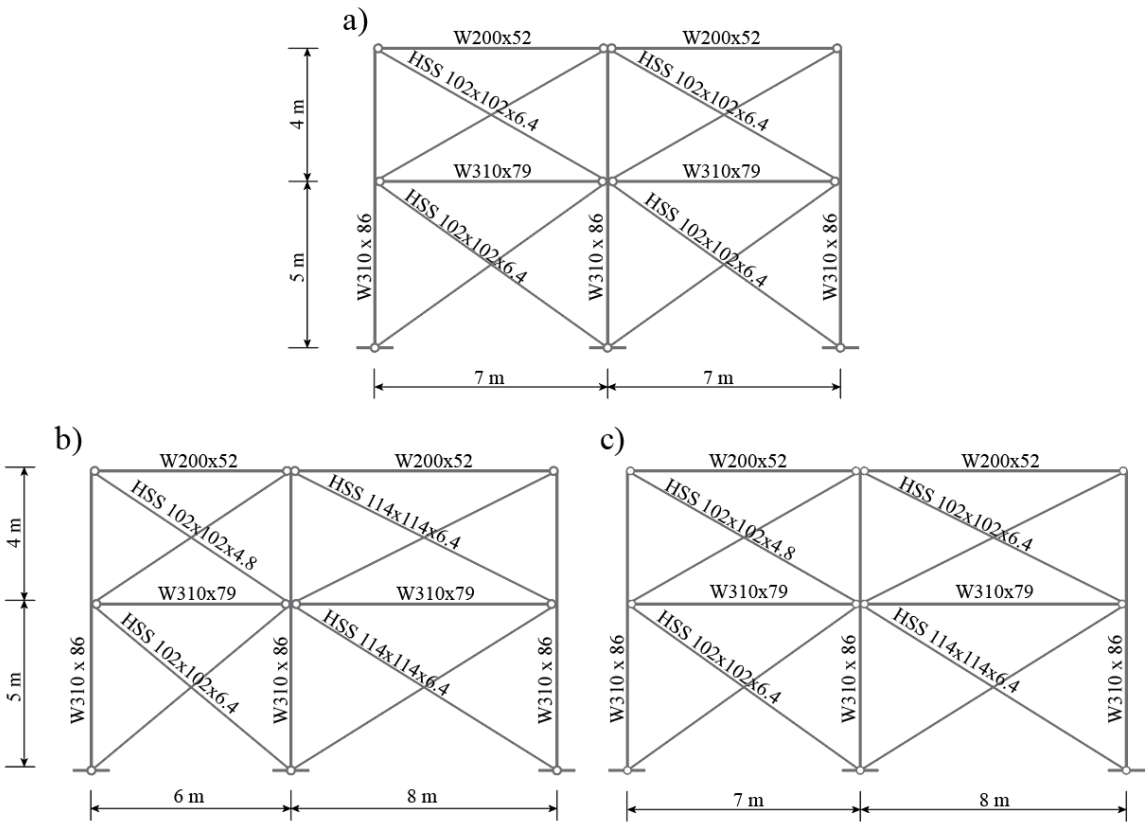

Figure 6.1 Geometry and selected sections for two-bay 2T-CBFs with: a) uniform 7-7 configuration; b) non-uniform 6-8 configuration; and c) non-uniform 7-8 configuration

The uniform two-tiered configuration was selected to match the frame designed and modelled in the previous chapters. The other configurations were selected so that the variation in bay widths would influence the slenderness ratios of the braces and lead to different brace selection between tiers and bays. This also leads to different probable shear resistances (V_{prob}) in adjacent tiers and larger flexural demand is anticipated in the middle column.

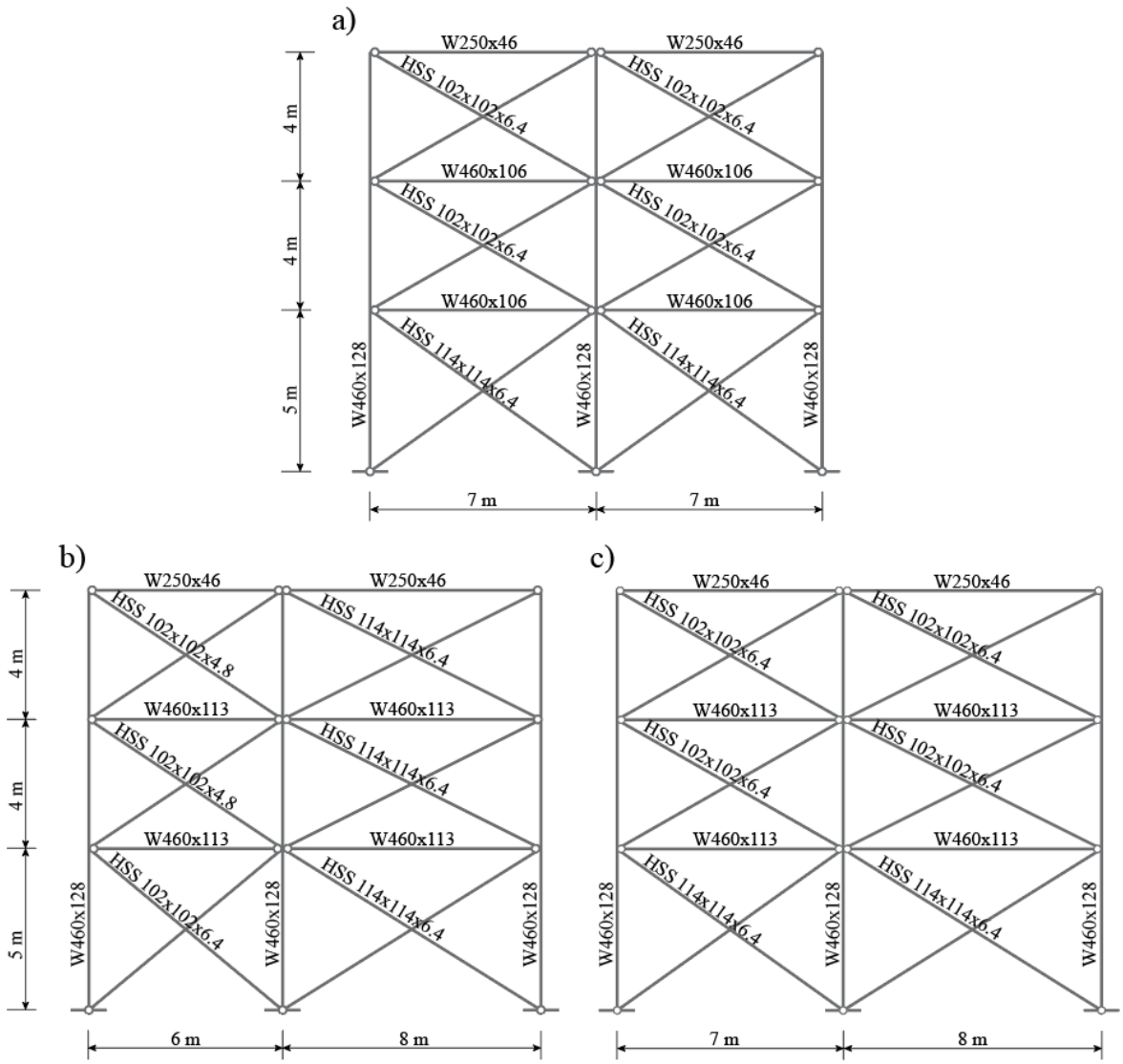

Figure 6.2 Geometry and selected sections for two-bay 3T-CBFs with: a) uniform 7-7 configuration; b) non-uniform 6-8 configuration; and c) non-uniform 7-8 configuration

6.2 Design of the braced frames

This section details the design steps that were followed for the design of the two-tiered braced frame with 6- and 8-meter wide bays. The same procedure was applied for all other frames in this chapter. The building height is the only difference between the two-tiered and three-tiered frames, allowing for a close comparison between the different selected geometries.

The geometry of the building is shown in Figure 3.1. It is located in Vancouver, BC, on soil of Class E. The total seismic weight for the building using two-tiered frames is 6275 kN, while it is

6751 kN for the building using three-tiered frames. This design example is focused on the non-uniform two-tiered 6-m and 8-m configuration and with the final selected sections the fundamental period of the building is 0.43 s. Two adjacent multi-tiered braced bays are placed on each exterior wall of the building. As such, the corresponding design base shear for the two bays is 1640 kN. Brace selection is similar to the procedure described in Chapter 3, with the exception that the design base shear is applied to each bay in proportion of their lateral stiffness. This iterative process allows for the selection of the braces shown in Figure 6.1 b. The design base shear is 419 kN in the left bay and 483 kN in the right bay.

Because the bay widths are non-uniform, the axial gravity loads on each column differ slightly. The left, middle and right columns must sustain 212 kN, 228 kN, and 244 kN respectively. As in the single bay two-tiered CBF, an initial column selection is realized using the loading condition where all tension braces have yielded (T_{prob}), and all compression braces have attainted their buckling strength (C_{prob}) as shown in Figure 6.3 for a roof displacement applied towards the right. However, as the braced frame is not symmetrical, the condition where the displacement is applied towards the left must also be considered.

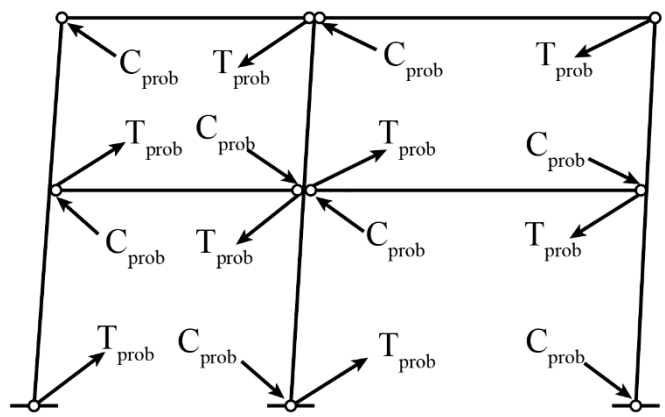

Figure 6.3 Brace probable resistances for the initial column selection in a two-bay MT-CBF

Under the aforementioned loading condition, a W310x79 is selected for the exterior columns and a W310x60 is found adequate for the interior column, as the axial load due to probable resistance of the braces is lower due to each bay opposing the forces in the other.

The inelastic roof displacement is obtained under the design base shear using *SAP2000* and is equal to $R_d R_o \delta_e$ = 50.35 mm. Progressive yielding is considered as it was for single-bay MT-CBF. The

tier with the lowest probable shear resistance (V_{prob}) is identified as the critical tier. For this frame, the critical tier is the upper tier in the left bay, where the HSS102x102x4.8 provide a V_{prob} = 1060 kN. Figure 6.4 illustrates the frame forces assigned to the *SAP2000* model to obtain axial loads and in-plane moments in the columns when the frame is pushed towards the right.

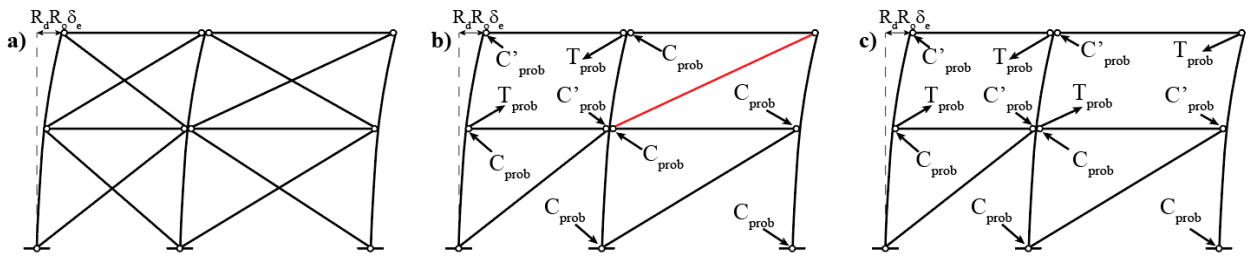

Figure 6.4 Brace design forces for the first critical tier scenario: a) inelastic roof displacement; b) yielding of the upper right tier under the critical tier forces; c) final critical tier scenario

When the tension and compression braces in the upper left tier reach T_{prob} and C'_{prob} respectively at the anticipated inelastic roof displacement, the tension brace in the upper right tier also yields (Figure 6.4 b). The two upper tiers are then identified as critical and it is assumed that both compression braces reach C'_{prob}. It is verified that the tension braces in the other tiers do not yield ($T < T_{prob}$). Axial forces and in-plane moments are extracted from the program and the strength and stability of columns are verified for this scenario. Concomitant out-of-plane bending resulting from a notional load applied at tier height equal to 2% of the column axial load under that point is also considered. As mentioned previously, when using non-uniform bays, both directions of loading must be considered as the frame is not symmetrical. This process is repeated with the inelastic roof displacement applied towards the left of the frame. Under this loading condition, only the tension brace in the upper left tier yields, and the design forces for the columns are extracted.

Furthermore, other critical tier scenarios must also be evaluated. After the first critical tier has been examined, the next closest V_{prob} is identified and reduced until it becomes critical. The reduction was limited to 15%. For this design example, the next critical tier is the lower left one, when its probable brace resistances are reduced by 15%. Figure 6.5 shows the considered design forces, in the same manner than what was realized for the first critical scenario.

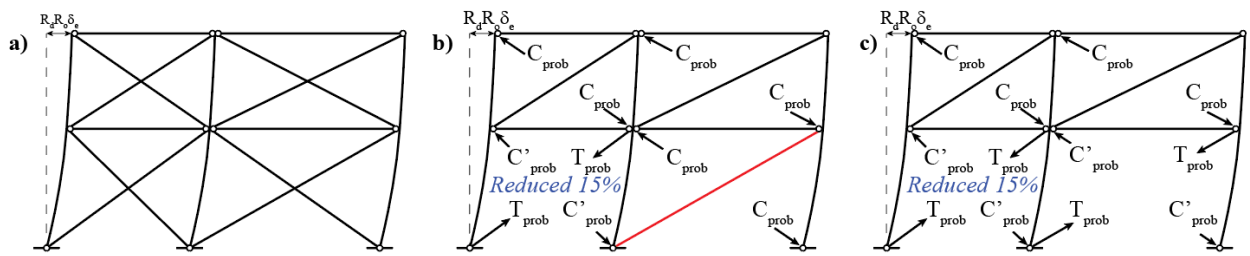

Figure 6.5 Frame deformed shape and brace probable resistances for the second critical tier scenario: a) deformed shape at roof inelastic displacement; b) yielding of tension brace in the lower right tier; and c) final brace forces for the second critical scenario

When pushed towards the right to the inelastic roof displacement, the tension brace in the lower left tier is replaced by its probable tensile resistance. At this storey drift, it is observed that the tension brace in the lower right tier also yields. This tier is then also considered critical, but its probable resistances are not reduced, contrary to the lower left tier. This produces greater bending demand in the columns. This critical tier scenario is the one governing the column selection. Under these design forces, the RHS column section must be increased to a larger W310x86 section. As discussed earlier, the same section is selected for all three columns, despite a W310x79 and W310x60 being adequate for the left-hand side and middle column respectively.

This process is repeated until all critical tier scenarios are verified. For the designed configurations, the process was very similar to the design of two distinct MT-CBFs, although precaution must be exercised to ensure that all possible scenarios are investigated so that the critical frame response can be identified.

6.3 Initial geometric imperfections

As described in Chapter 4, out-of-plane imperfections were oriented in the positive *Z*-axis for a single-bay MT-CBF. For the two-bay 2T-CBFs, different orientations were studied evaluate the influence of each one on the seismic stability of the columns. The imperfection orientations are as follows:

- All out-of-plane imperfections in the positive *Z* direction.
- All out-of-plane imperfections in the negative *Z* direction.

- Exterior columns out-of-plane imperfections in the positive *Z* direction and interior column out-of-plane imperfections in the negative *Z* direction.
- Exterior columns out-of-plane imperfections in the negative *Z* direction and interior column out-of-plane imperfections in the positive *Z* direction.

The fourth orientation for out-of-plane geometric imperfections is illustrated in Figure 6.6. This orientation produced in-plane moments up to 42% larger in the exterior columns than the first configuration, and up to 12% larger in the interior column, depending on the ground motion. Out-of-plane bending moments and drifts remained largely unaffected by the selected orientation.

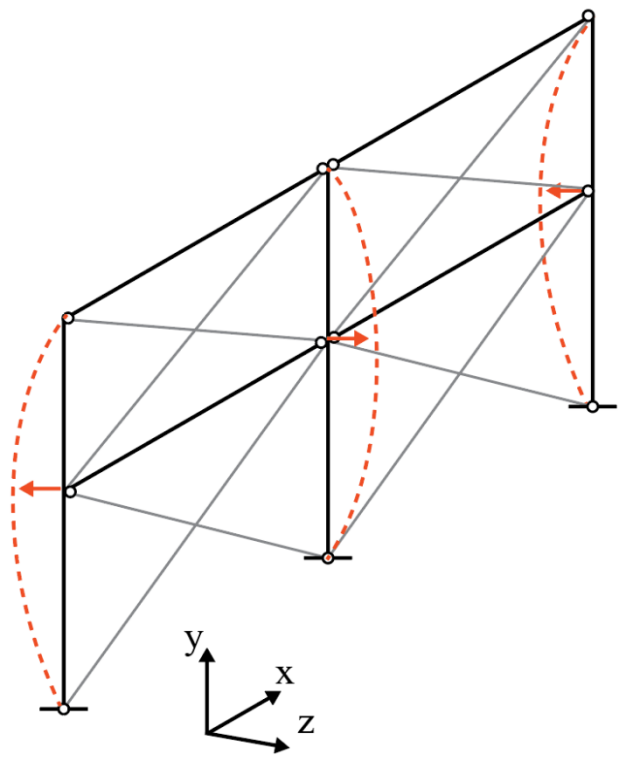

Figure 6.6 Selected initial out-of-plane geometric imperfections orientation for the columns of two-bay MT-CBFs

6.4 Nonlinear response history analysis of two-bay two-tiered CBFs

The results for the uniform 7-meter bays configuration are first presented. The case for which all column sections are the same is compared the one where different column sections are specified. Next, the non-uniform 6- and 8-meter bays configuration as well as the 7- and 8-meter bay configuration are detailed.

The columns are considered pinned at their base for both in-plane and out-of-plane bending and restrained at their top for torsion and out-of-plane displacement. Because they are capacity protected elements, the yield stress for the columns is specified as 345 MPa, while the yield stress for the braces is set to R_yF_y = 460 MPa. Peak values presented in this section are obtained from the mean of the five most demanding ground motions for each parameter.

6.4.1 Uniform configuration: 7-meter bays

This two-bay 2T-CBF configuration uses two 7-meter bays and tier heights of 5 and 4 meters, for a total storey height of 9 meters. This configuration is representative of two of the 2T-CBF designed in Chapter 3 put side by side in adjacent bays.

6.4.1.1 Frame designed using identical column sections

The uniform two-bay 2T-CBF was first modeled and analysed using a W310x86 for all three columns. The fundamental period obtained at the design phase was equal to 0.422 s, while the fundamental period obtained from the OpenSees model is equal to 0.416 s. The period calculated manually uses brace lengths calculated from the working points, whereas *OpenSees* takes gusset plates lengths into consideration, thus reducing the effective brace lengths. This leads to a slightly more rigid frame, as is observed by the periods. Figure 6.7 illustrates the deformed shape of the studied frame at brace buckling and at maximum storey drift. At the latter point, non-uniform deformation of the tiers can be observed, as most of the drift demand is concentrated in the lower tiers. Because of the depth of the roof beam, the top braces exhibit smaller out-of-plane displacements after buckling. This is very similar to what was shown for the single-bay two-tiered CBF, where tier 1 was critical and experienced the majority of the frame inelastic deformations.

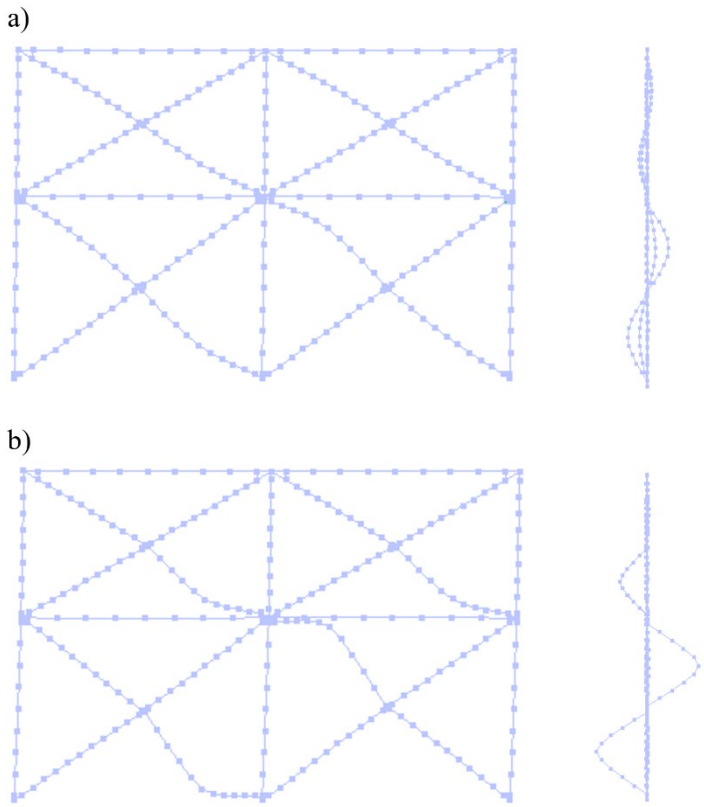

Figure 6.7 Deformed shape of a uniform two-bay 2T-CBF (elevation and side views): a) at brace buckling; and b) at maximum roof displacement (P-Delta column not shown)

To further compare the two-bay response to its single-bay counterpart, Figure 6.8 shows the tier drifts relative to the storey drifts for both braced frames under the 1989 Loma Prieta earthquake, Hollister Differential Array record. For the two-bay frame, drifts were computed as the average of the three columns displacement, whether at mid-height or at storey height. In both frames, brace tensile yielding was observed in the lower tiers only. This is expected due to their lower probable shear resistance (V_{prob}). However, the two-bay frame exhibits less drift demands at both tier and storey levels. Even though the initial stiffness is the same for both frames, and that the total applied mass is two times higher than the single-bay frame, the two-bay system results in more uniform drift demands in both tiers. In the two-bay frame, the middle column is able to compensate for the unbalanced shear force developed between the braces of two tiers.

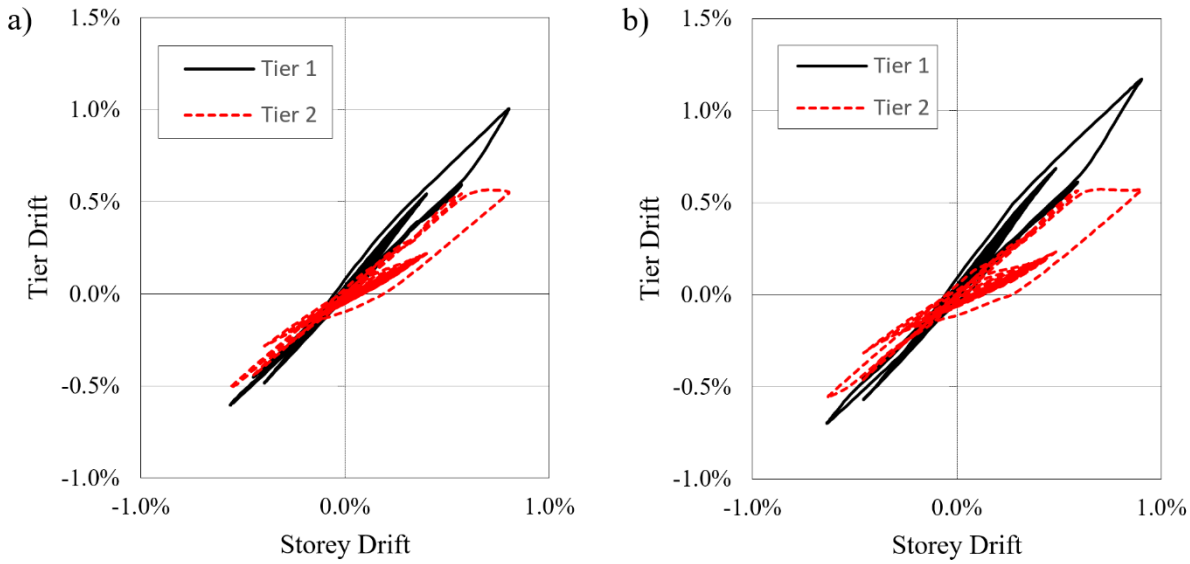

Figure 6.8 Tier drifts against storey drift under the 1989 Loma Prieta - Hollister Differential Array earthquake: a) two-bay uniform 2T-CBF; and b) single bay 2T-CBF

Figure 6.9 shows the normalized brace forces relative to the tier drifts in all four tiers under the 1989 Loma Prieta earthquake. This record was selected because it produced the largest peak drift response on the frame. As seen for the single-bay 2T-CBF, probable brace resistances agree well with the design predictions, both for tension yielding and compression buckling. On average, the observed brace resistance at first buckling and post-buckling brace resistance differ by 1.8% and 4.8% respectively from the design prediction by CSA S16-19. During the largest of two yielding cycles in the tension braces of the lower tiers brace axial forces surpass AR_yF_y because of material strain hardening. As these braces yield, their counterparts in the upper tiers only reach 90%-95% of AR_yF_y, which leads to non-uniform drift demands as illustrated in Figure 6.8.

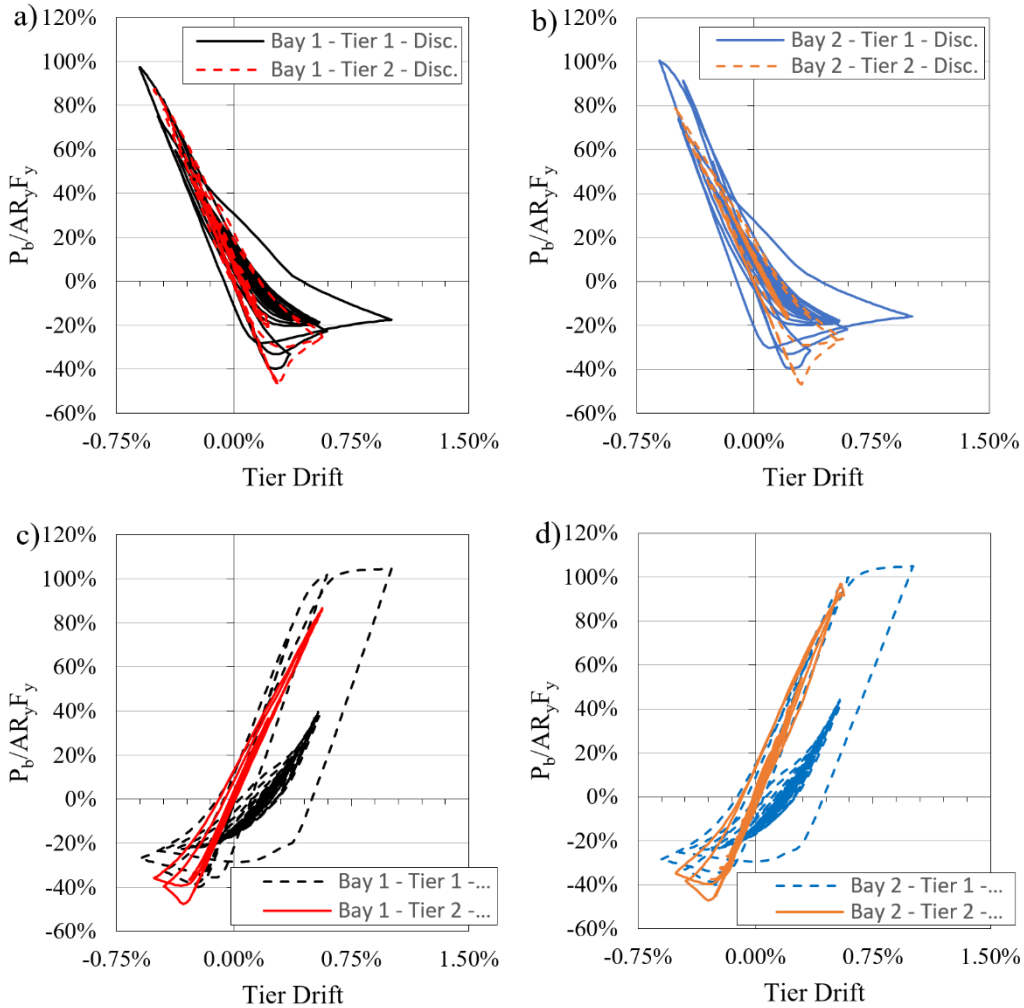

Figure 6.9 Normalized brace forces against tier drifts for the uniform two-bay 2T-CBF under the 1989 Loma Prieta 1989 - Hollister Differential Array earthquake: a) discontinuous braces in left bay; b) discontinuous braces in right bay; c) continuous braces in left bay; and d) continuous braces in right bay

Table 6.1 presents the peak frame response parameters, including tier and storey drifts as well as column flexural demand for the two-bay 2T-CBF.

Table 6.1 Peak frame response from NLRHA for the two-bay 2T-CBF uniform configuration with the same column sections

Parameter	Value	
	Exterior columns	Interior column
$\delta_{roof,NLRH}$ (% h_s)	0.71	0.69
$\delta_{roof,NLRH}/R_dR_o\delta_e$	1.29	1.26
Tier 1 drift (% h_1)	0.83	0.85
Tier 2 drift (% h_2)	0.57	0.58
$M_{cy,\ NLRH}$ / M_{py}	0.042	0.051
$M_{cy,\ NLRH}$ / $M_{cy,\ design}$	1.79	1.46
$M_{cx,\ NLRH}$ / M_{px}	0.026	0.023
$M_{cx,\ NLRH}$ / $M_{cx,\ design}$	0.20	0.38

NLRH analyses produce a peak roof displacement that exceeds the design value by about 30%. However, drift demands remain well under the NBCC limit of 2.5%. Out-of-plane flexural demand is overestimated by the design method, and it appears that brace buckling is not adequately represented by the design notional loads at tier height. Figure 6.10 shows the response history of the in-plane flexural demand on the columns under the 1989 Loma Prieta earthquake.

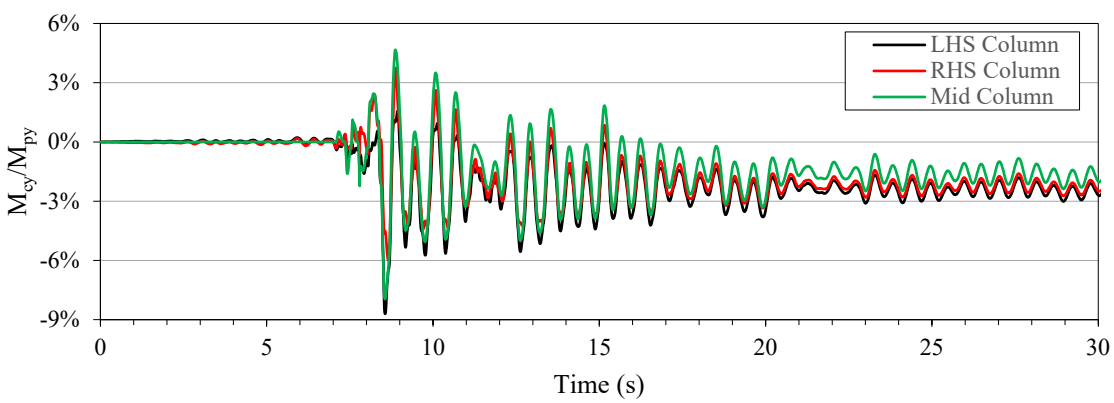

Figure 6.10 Normalized column in-plane moments for the two-bay 2T-CBF uniform configuration using the same column sections under the 1989 Loma Prieta – Hollister Differential Array earthquake

In-plane bending moments are similar for all three columns throughout the seismic event, although the interior column shows peak values 18% higher than the exterior column when the latter is subjected to compression. At tier height, the interior column undergoes slightly larger in-plane displacements than the exterior columns, due to inelastic brace behaviour and because of axial deformations of the struts. Also, the axial compression loading in the interior column is lower than the one of the exterior columns. This makes the interior column stiffer in flexure than the exterior column loaded in compression. For these two reasons, even though all columns have the same in-plane moment of inertia, the interior column therefore attracts higher bending moments. Along with residual displacements at the end of the ground motion, residual in-plane flexure is observed in the columns. After the braces experience inelastic cycles in tension, elongation of the members occurs. This reduces the frame stiffness compared to its initial value and leads to residual deformations in braces and columns.

Table 6.1 also shows that in-plane bending moments in the columns are underestimated in design. This is largely due to the underestimation of the inelastic roof displacement. When using the maximum inelastic roof displacement from NLRH analysis of the 1989 Loma Prieta – Hollister Differential Array earthquake in design, the ratio between the moments NLRHA and design is reduced to 0.76 and 0.79 for the exterior column loaded in compression and the interior column respectively. These ratios are closer to 1.0 compared to the previous ones, but most importantly they show that the design method *overestimates* the in-plane flexural demand if a more representative design storey drift was used in design. As discussed in Chapter 5, the overestimation is attributed to the compression brace forces at maximum storey displacement. The design assumes that the compression braces in non-critical tiers will attain a value of C_{prob}, whereas NLRH analyses show that compression braces in all tiers attain values close to C'_{prob} at maximum storey displacement. This behaviour is observed for all two-bay MT-CBFs. In design, specifying precise values from NLRH analyses can prove to be difficult and time-consuming. The assumption of C'_{prob} in the critical tiers and C_{prob} in the non-critical tiers is deemed to provide a more realistic and yet conservative estimation of the in-plane flexural demand in the columns, given the challenges involved with a more accurate brace resistances estimation corresponding to the design storey drift (e.g., ones obtained from NRLHA).

6.4.1.2 Frame designed using dissimilar column sections

The same uniform two-bay 2T-CBF is analyzed, this time using the most economical column sections selected in design. The exterior columns remain W310x86, while the interior column is reduced to a W310x60. The overall response of the frame is close to previous observations. Table 6.2 presents peak frame response for the parameters of interest.

Table 6.2 Peak frame response from NLRHA for the two-bay 2T-CBF uniform configuration using different column sections

Parameter	Value	
	Exterior columns	Interior column
$\delta_{roof,NLRH}$ (% h_s)	0.71	0.69
$\delta_{roof,NLRH}/R_dR_o\delta_e$	1.29	1.26
Tier 1 drift (% h_1)	0.82	0.84
Tier 2 drift (% h_2)	0.57	0.58
$M_{cy,\ NLRH}$ / M_{py}	0.041	0.033
$M_{cy,\ NLRH}$ / $M_{cy,\ design}$	1.74	1.24
$M_{cx,\ NLRH}$ / M_{px}	0.026	0.026
$M_{cx,\ NLRH}$ / $M_{cx,\ design}$	0.20	0.29

Similar drift is observed, as brace stiffness is the principal contributor to this parameter. Tier drifts also remain similar, with most of the non-uniform deformations concentrated in the lower tiers. As expected, using a smaller section for the interior column leads to reduced in-plane flexure. This is because the exterior columns have a relatively larger moment of inertia and attract higher bending moments. The ratio between NLRH results and design expectations for the exterior column in compression remains similar, while the design method can predict in-plane bending more accurately for the interior column than the frame where the same sections were used.

When using the maximum roof displacement of 70.2 mm obtained from the Loma Prieta 1989 earthquake in the *SAP2000* design method, in-plane moments of 6.81 kN-m and 11.5 kN-m are obtained for the interior and exterior column respectively. The corresponding ratios between

NLRH analysis results and the design values are 0.81 and 0.85. This shows a good agreement between the design method and the observed frame response, as the remaining difference can be explained by lower axial force values in the compression braces in the non-yielded tiers compared to what is considered in design.

It must be noted that for the rest of the studied designs, whether they are two-tiered or three-tiered, the same column sections was used for interior and exterior columns.

6.4.1.3 Influence of the brace yield stress

In different tiers or bays, the brace yield stress can be different because of material variability. This was explicitly considered in design, in order to cover all possible critical tier scenarios and selecting the columns for the most demanding possible loading case. The brace yield stress in the upper tiers was reduced by 15% and a yield stress of 391 MPa was used. This scenario produced a higher flexural demand in the columns. Figure 6.11 plots storey and tier drifts for the 1989 Loma Prieta earthquake.

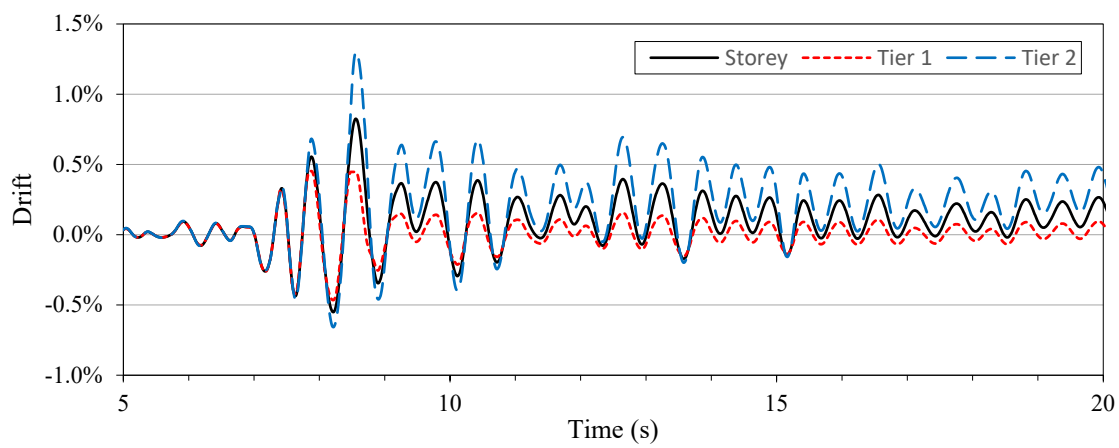

Figure 6.11 History of drifts for the uniform 2T-CBF using 85% of R_yF_y in the top tiers under the 1989 Loma Prieta – Hollister Differential Array earthquake

As predicted, the lower yield stress in the upper braces shifts the frame response. Instead of yielding being observed in the first tier, the inelastic drift demand of the frame is concentrated in the second tier. The total storey drift, however, remains close the first critical scenario of section 6.4.1.1. Figure 6.12 shows brace response under the 1989 Loma Prieta earthquake.

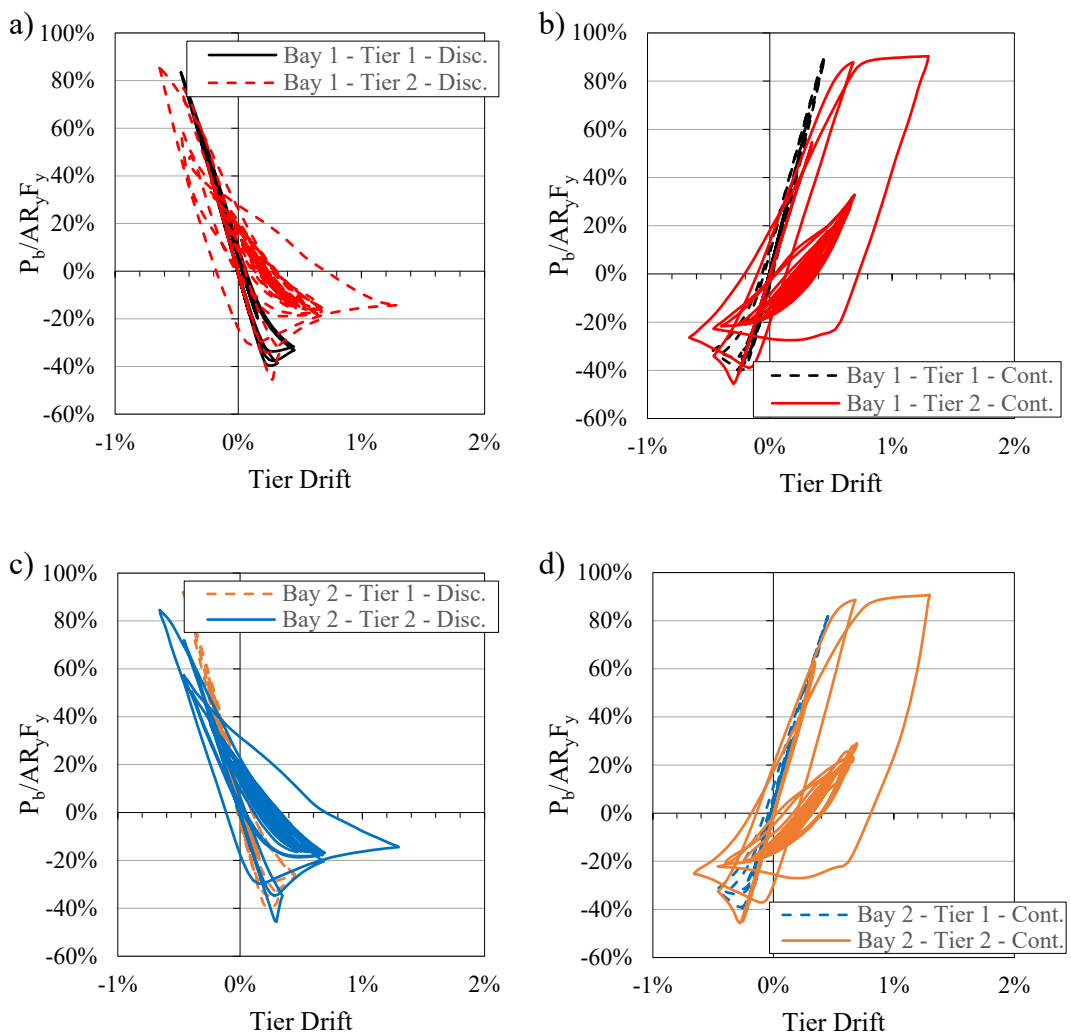

Figure 6.12 Normalized brace forces against tier drifts for the uniform two-bay 2T-CBF under the 1989 Loma Prieta earthquake, Hollister Differential Array with 85% R_yF_y in the tiers: a) discontinuous braces in left bay; b) continuous braces in the left bay; c) discontinuous braces in the right bay; and d) continuous braces in the right bay

As shown in Figure 6.12, the tension braces in the lower tiers yield at 85% of AR_yF_y. The tension brace yielding patterns closely match the first critical scenario with the obvious difference that this time tension braces in the second tiers yield, producing most of the inelastic deformations. From the average of the five most critical ground motions, the peak in-plane bending moment is equal to 8.7% of the member's plastic moment for the exterior columns and equal to 8.2% of the plastic moment for the interior column. When using the maximum storey displacement from *OpenSees* in

the design procedure, these values are well captured and the ratio between NLRHA and design is 0.77 and 0.78 for the exterior columns and interior column respectively. This confirms that the design method can accurately predict the frame seismic behaviour. As confirmed here, it is imperative to consider all possible critical scenarios in order to obtain a realistic estimation of the force demand on the columns.

6.4.2 Non-uniform configuration: 6-m and 8-m bays

This section details the results obtained for the 6-m and 8-m bays configuration. All columns are W310x86, and tier heights are 5 m and 4 m for the bottom and top tiers. Table 6.3 shows the peak frame response as obtained from the set of 15 selected ground motions.

Table 6.3 Peak frame response from NLRHA for the two-bay 2T-CBF non-uniform 6- and 8-meter bays

Parameter	Value	
	Exterior columns	Interior column
$\delta_{roof,NLRH}$ (% h_s)	0.65	0.64
$\delta_{roof,NLRH}/R_dR_o\delta_e$	1.17	1.17
Tier 1 drift (% h_1)	0.54	0.55
Tier 2 drift (% h_2)	0.80	0.80
$M_{cy,\ NLRH}$ / M_{py}	0.049	0.041
$M_{cy,\ NLRH}$ / $M_{cy,\ design}$	0.92	1.02
$M_{cx,\ NLRH}$ / M_{px}	0.036	0.012
$M_{cx,\ NLRH}$ / $M_{cx,\ design}$	0.31	0.11

Peak storey drifts are about 10% lower than for the uniform configuration of the previous section. The tier offering the lowest probable shear resistance (V_{prob}) is the upper left tier. As predicted in design, the two upper tiers are critical and experience most of the inelastic deformations. Figure 6.13 shows the histories of drifts and column in-plane moments for the 1989 Loma Prieta earthquake.

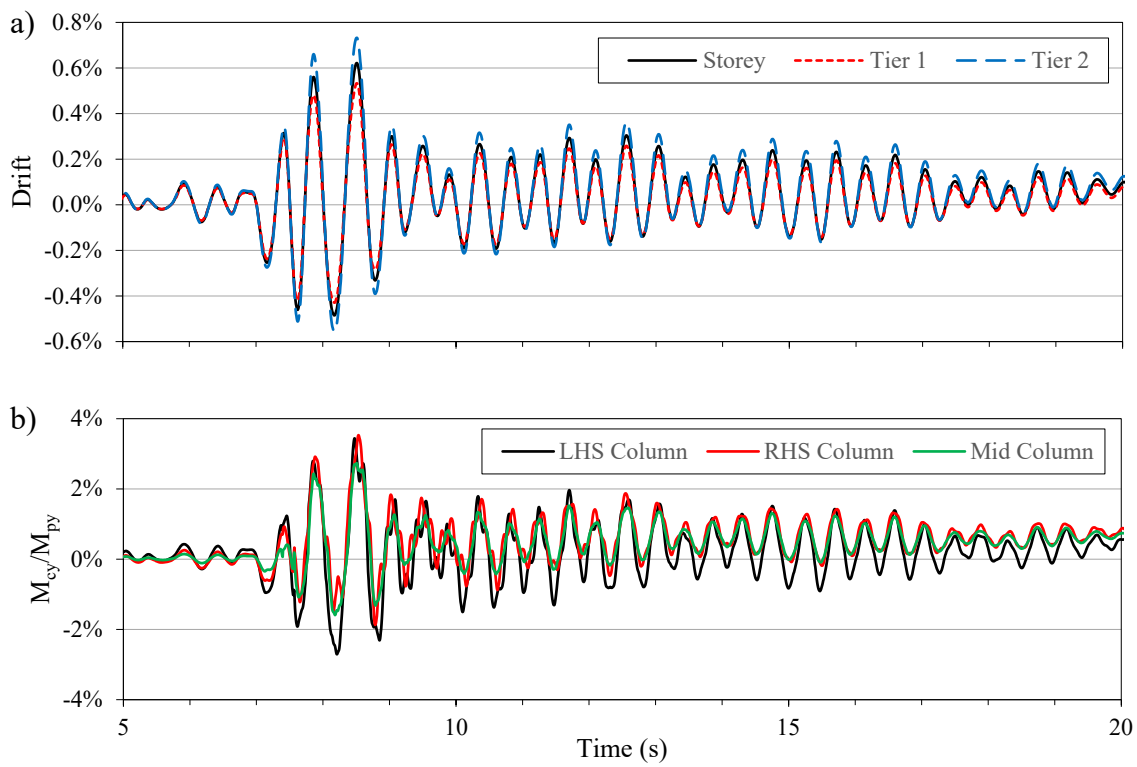

Figure 6.13 Two-bay 2T-CBF non-uniform 6- and 8-meter bays configuration response under the 1989 Loma Prieta earthquake, Hollister Differential Array: a) drifts; and b) normalized in-plane moments in the columns

Figure 6.13 shows that very little yielding of the second tier occurs, as all three curves are close. This is in contrast of the previous frame where yielding was more clearly defined the lower or upper tiers. This leads to reduced in-plane moments in the exterior and interior columns. In this frame, the probable shear resistances (V_{prob}) of the four tiers are nearly identical, whereas in the uniform frame a more significant deviation was present between V_{prob} in the two.

For the 6- and 8-meter bay configurations, the critical tier is the upper left one, with V_{prob} = 1060 kN. The upper right tier has a probable shear resistance of V_{prob} = 1479 kN. In design, it was observed that the deformation caused upon yielding of the upper left tier causes the upper right tier to also yield. Together, both upper tiers have a probable shear resistance of $V_{prob,\ tier\ 2}$ = 2658 kN. This is very close to the combined probable shear resistance of the lower tiers, equal to $V_{prob,\ tier\ 1}$ = 2687 kN. This leads to a more uniform frame response between lower and upper tiers, which is illustrated in Figure 6.14 for the continuous braces in the left bay. Even

though tier drifts differ slightly, both braces reach similar values, reducing the flexural demands on the columns.

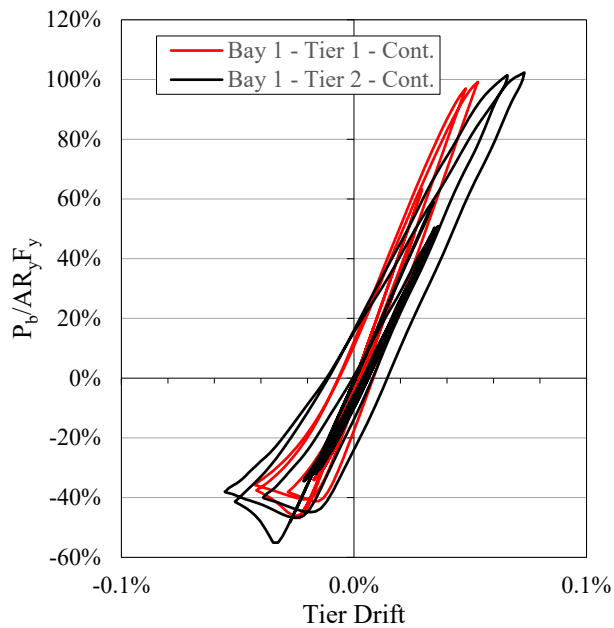

Figure 6.14 Normalized brace forces relative to tier drift in the left bay under the 1989 Loma Prieta earthquake, Hollister Differential Array record

The behaviour that was described is well captured in design. As given in Table 6.3, the ratios for in-plane moments are very close to 1.0. However, the scaling of the ground motions relies on multiple assumptions and the evaluation of seismic hazard is in constant evolution. To determine if the design procedure would be able to adequately predict flexural demand in the columns under a stronger earthquake, the most critical ground motion (1989 Loma Prieta) was scaled up three times by 10% increments to re-evaluate the frame response. Figure 6.15 illustrates the evolution of the drifts and in-plane moments in the columns as the ground motion amplitude is increased.

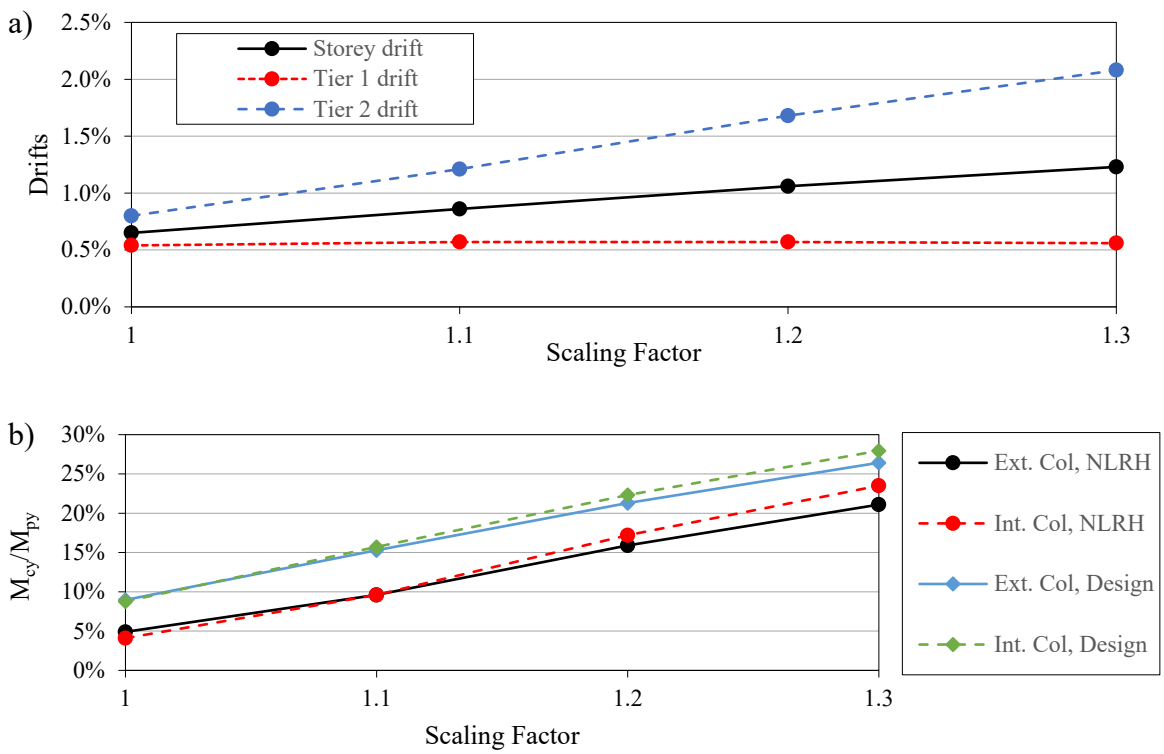

Figure 6.15 Demand evolution on the two-bay 2T-CBF non-uniform 6- and 8-m bays configuration: a) drifts; b) in-plane bending moments in the columns

As the scaling factor is increased, tier 2 and storey drifts increase gradually. Drift in tier 1, however, remains around 0.55%. This shows that inelastic deformations are concentrated in the upper tiers, as they present the lowest V_{prob}. The storey drift increases proportionally. Furthermore, the exterior and interior columns see a very similar increase in in-plane flexural demand for all three scaled-up scenarios because of brace tensile yielding in tier 2. Using the roof displacement from NLRHA, the in-plane bending values obtained by the design method correlate well with the numerical model. Design values consistently overestimate flexural demand by about 5% of the column's plastic moment. In summary, this highlights the influence of the target inelastic storey drift and the importance of a reliable seismic hazard estimation.

6.4.3 Non-uniform configuration: 7-meter and 8-meter bays

The last two-bay two-tiered CBF under study comprises uneven 7- and 8-m bays. The overall behaviour of the braced frame resembles what was observed for the uniform 7-m bay frame. As

illustrated in Figure 6.16, the upper tiers are critical the majority of the frame inelastic deformation takes place in these tiers. Figure 6.17 shows the response history of the tier and storey drifts under the Loma Prieta 1989 earthquake.

Figure 6.16 Deformed shape of the OpenSees numerical model of the 7- and 8-m bays 2T-CBF at yielding of the upper tiers

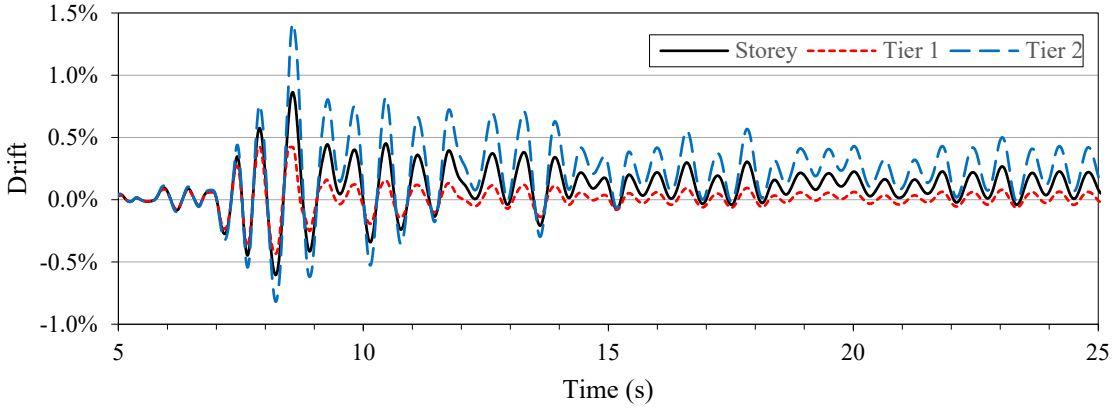

Figure 6.17 Response history of drifts for the two-bay 2T-CBF non-uniform 7- and 8-m bays under the 1989 Loma Prieta earthquake, Hollister Differential Array record

As shown in Figure 6.17, frame inelastic deformations are concentrated in the second tier, as it reaches peak drift values more than two times larger than the first tier, for which tension braces

remain elastic throughout the ground motion. This produces large in-plane bending moments on the columns, as shown in Table 6.4

Table 6.4 Peak frame response parameters for two-bay 2T-CBF non-uniform 7- and 8-m bays configuration

Parameter	Value	
	Exterior columns	Interior column
$\delta_{roof,NLRH}$ (% h_s)	0.73	0.71
$\delta_{roof,NLRH}/R_dR_o\delta_e$	1.28	1.27
Tier 1 drift (% h_1)	0.44	0.44
Tier 2 drift (% h_2)	1.11	1.11
$M_{cy,\ NLRH}$ / M_{py}	0.10	0.10
$M_{cy,\ NLRH}$ / $M_{cy,\ design}$	1.40	1.41
$M_{cx,\ NLRH}$ / M_{px}	0.031	0.011
$M_{cx,\ NLRH}$ / $M_{cx,\ design}$	0.23	0.20

The peak storey drift is again underestimated in design by about 30%. This also leads to an underestimation of the bending demand, as observed in the previous two-bay frames. Using the inelastic roof displacement as the design value leads to a closer match between NLRHA and design. Although the bays differ in geometry and brace sections, the in-plane moments in interior and exterior columns are similar, following design predictions. This uneven 7- and 8-m bays configuration shows that high in-plane flexural demand can be imposed to the columns. However, it shows that an appropriate design procedure can accurately capture the frame seismic response.

6.5 Nonlinear response history analysis of two-bay three-tiered CBFs

Three two-bay three-tiered frames were studied, where their bay widths and brace sections varied. Each frame is abbreviated below using its bay widths. The uniform 7-m bays configuration is referred below as the “7-7” configuration, the non-uniform 6- and 8-m bays configuration is referred to as “6-8”, and the non-uniform 7- and 8-m bays configuration as the “7-8” frame.

Like the numerical models for the two-tiered CBFs, the columns are considered pinned at their bases, and restrained for out-of-plane displacement and torsion at their tops. The column yield stress is specified as F_y = 345 MPa, while the braces are assigned with R_yF_y = 460 MPa. In depth analysis was conducted for the two-tiered frames, and non-uniform drift distribution between tiers as well as in-plane flexural demand on the columns were described. Figure 6.18 depicts the deformed shape from the *OpenSees* model for the *7-7* configuration.

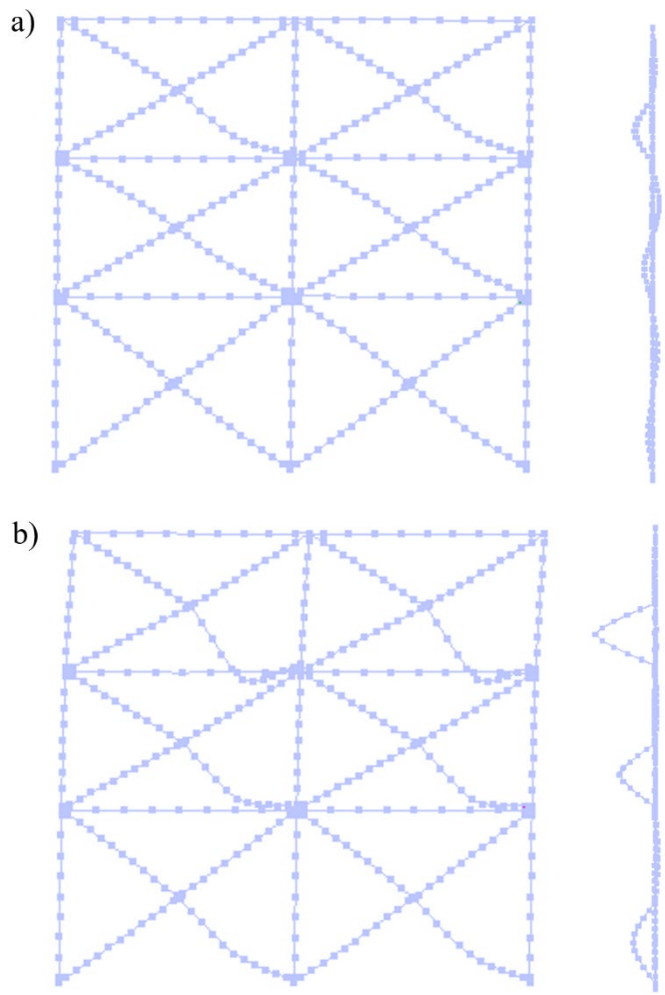

Figure 6.18 Elevation and side views of the deformed shape of the OpenSees numerical model for the uniform 7-meter bays 3T-CBF: a) at brace buckling; and b) at yielding of tier 3

As shown in Figure 6.18, brace buckling occurs almost simultaneously in all tiers, but the shorter braces exhibit larger out-of-plane displacements. Note that out-of-plane displacements are amplified on the figure. The uppermost tier is critical, as its tension brace yields first and develops the largest inelastic deformations. For all three frames, tier 3 was critical, which was predicted in design since it possesses the lowest probable shear resistance (V_{prob}). This produces large in-plane flexural demand on the columns at tier 2 strut level. Figure 6.19 presents the cumulative drifts along the frame height for the three studied frames. Figure 6.20 shows the peak in-plane bending moments in columns along the frame height.

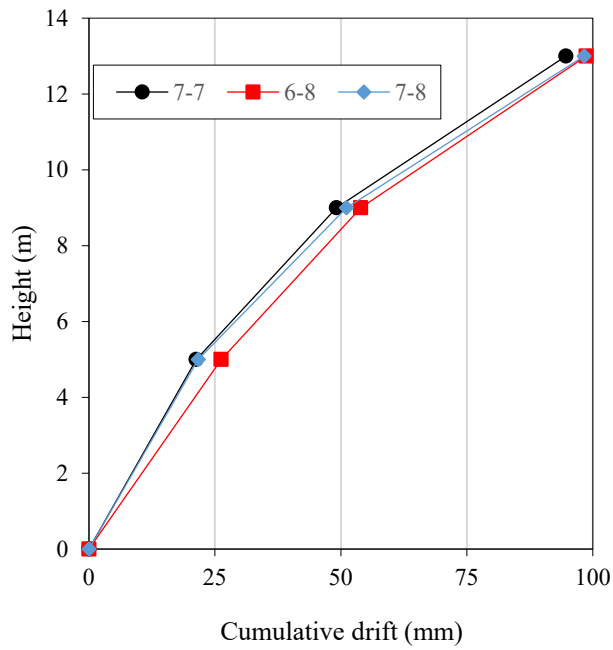

Figure 6.19 Peak cumulative drifts of studied two-bay 3T-CBFs

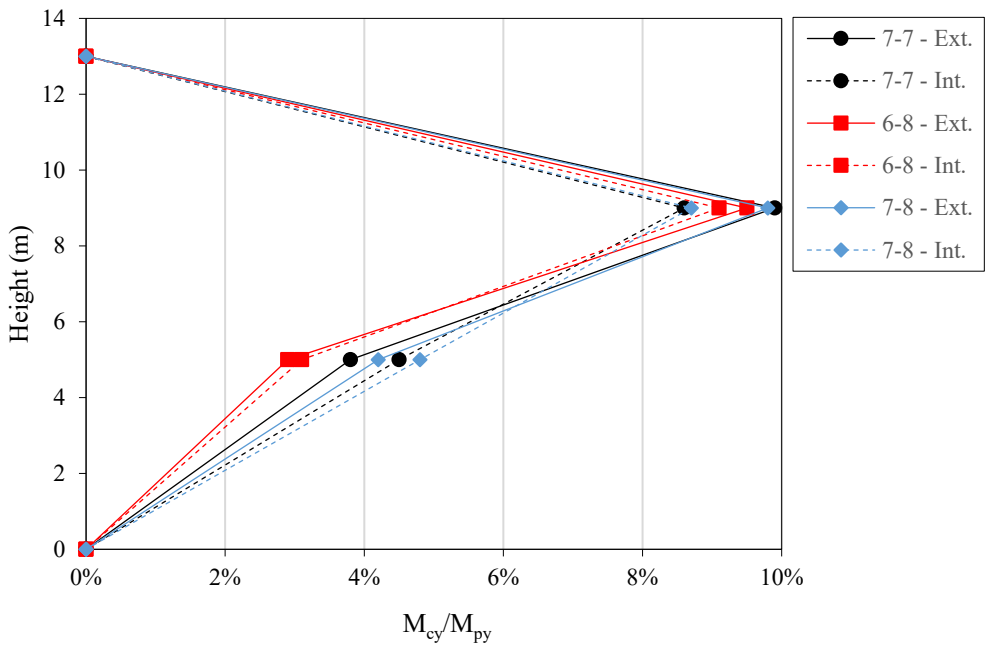

Figure 6.20 Peak in-plane bending moments for exterior and interior columns of studied two-bay 3T-CBFs ("Ext." and "Int." stand for the exterior column and interior column respectively)

For all three frames, brace inelastic deformations are more pronounced in the third tier. Braces in the second tier show some yielding, as the slopes of the curves in Figure 6.19 are slightly lower for this tier than in the first tier. The in-plane flexural demand in the columns matches this observation, as peak bending demands occurred at 9 m from the ground level. On average, in-plane moments at the tier 1 strut level are 45% lower than the moments observed at the tier 2 strut level. It was observed that all three frames exhibit similar in-plane flexure. Furthermore, moments in the interior columns are always higher than those included in the exterior columns at the tier 1 height, while this is reversed at the tier 2 height. By examining the deformed shape of the columns for the different frames, its was determined that this is mainly due to axial strut deformations being not uniform for different tiers. In fact, the strut between tier 2 and tier 3 undergoes higher axial loads than the strut between tier 1 and tier 2. This higher unbalanced load is due to the lower axial compression value in the braces of tier 3, which attain values close to C'_{prob}. The strut in compression effectively acts as a restraint against column lateral displacement and produces more bending in the exterior columns at tier 2. At tier 1, this effect is less pronounced, and the interior column sustains higher bending moments due to P-δ effects.

Figure 6.21 presents tier drifts and normalized brace forces for the *6-8* configuration under the Loma Prieta 1989 earthquake.

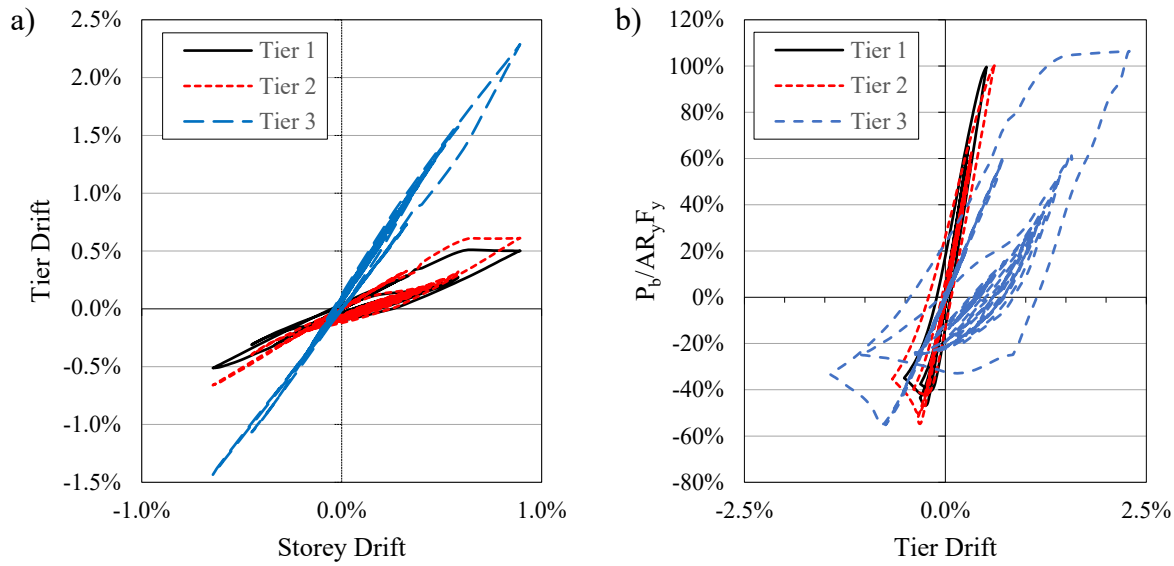

Figure 6.21 NLRH results for the two-bay 3T-CBF non-uniform 6- and 8-meter bays configuration under the 1989 Loma Prieta earthquake: a) tier drifts against storey drift; and b) normalized continuous brace forces against tier drifts in the left bay

The Loma Prieta earthquake is the critical ground motion for all two-bay three-tiered CBFs, as it produces the highest displacement column and in-plane bending demands. In Figure 6.21 b, the normalized forces for the continuous braces of the left bay are shown. The response in the right bay is largely similar, and the discontinuous braces do not present any significant inelastic cycle as the ground motion mainly pushes the frame towards the right-hand side. For the *6-8* configuration, inelastic deformations are concentrated in tier 3, while brace tensile yielding occurs in tier 2 only during one cycle, whereas the tension brace in tier 1 does not exceed 97% of its capacity. Incidentally, none of these two braces undergo large inelastic deformations, as opposed to the tier 3 brace.

6.5.1 Comparison of NLRH analyses of two-bay three-tiered CBFs with design predictions

The NLRH analyses conducted on two-bay 2T-CBFs showed that the design procedure was able to predict the frame response under seismic loading, when an realistic inelastic roof displacement was used in design. Similar results are obtained for the three-tiered frames, where the same design method was used.

For all three-tiered CBFs studied here, peak storey displacement was underestimated in design. On average, the ratio between the maximum storey displacement from NLRH analysis and that predicted in design was 1.27, following the trend observed for the two-tiered frames. When using the design inelastic storey displacement, in-plane bending moments for the columns were largely underestimated, as anticipated. However, when the maximum storey drift from NLRHA ($\delta_{roof,\ NLRHA}$) under the Loma Prieta earthquake was used to perform the design, the columns in-plane flexural demand was predicted with a higher accuracy. Table 6.5 shows the ratios for in-plane bending moments of the columns. The average values from all three frames are presented.

Table 6.5 Average ratios between in-plane bending moments from NLRHA and design in columns for all three studied two-bay 3T-CBFs

	$M_{cy,\ NLRH}$ / $M_{cy,\ design}$	
	Exterior column	Interior column
Tier 1	0.97	0.95
Tier 2	0.86	0.81

Overall, the design method used in 6.2 allows for a good prediction of the flexural demand in the columns. At tier 1, inelastic deformations are limited and the bending moment is properly estimated in design. At the critical tier, the design values overestimate in-plane bending moments. As described in Chapter 6.4.1, this is mainly due to the assumed brace compression forces when yielding takes place in the tensile brace. In design, axial forces in the compression braces of the non-critical tiers are taken as their respective C_{prob}, whereas the results of NLRHA indicate that they approach the lower value of C'_{prob}. This is explained by the number of loading cycles that led

to brace buckling before the maximum roof displacement is reached. This significantly affects the axial compression capacity of the brace, reducing the value to C'_{prob}.

CHAPTER 7 SEISMIC BEHAVIOUR OF TWO-BAY X-CBFS

In this chapter, the results obtained from the nonlinear response history analysis of two-bay X-CBFs are presented. Two-bay X-CBFs consist of bracing members forming an X-shape across two bays. In practice, this system is used for single-storey buildings such as those studied in this thesis when the columns are closely spaced together. This configuration can be more economical in terms of steel tonnage compared to having two full braced bays side by side, as well as requiring less assembly time because of the reduced number of members. Figure 7.1 a) shows a two-bay X-CBF used on the short side of a one storey building. An intermediate strut can be added at mid-height of the frame, which provides in-plane bracing of the exterior columns as shown in Figure 7.1 b). Typically, the middle column is continuous over the storey height, while the braces are connected to gusset plates welded or bolted on either side of the column.

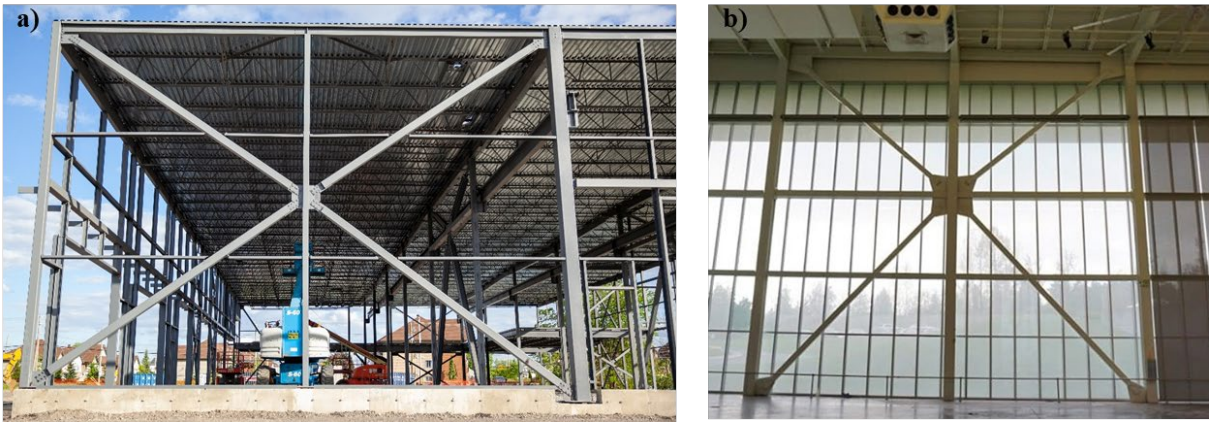

Figure 7.1 Example of two-bay X-CBFs: a) without intermediate strut; and b) with intermediate strut

7.1 Two-bay X-CBFs studied

Two braced frame configurations are studied in this chapter: X-CBF without a strut and X-CBF with a horizontal strut. The prototype building is located in Vancouver, British Columbia on a soil of Class E and illustrated in Figure 7.2. The building height is 9 m. Its overall dimensions are slightly different from the building studied in the previous chapters, in order to have a brace selection that is determined by the seismic loading, and not by the upper base shear limit imposed

by the capacity design principle with R_dR_o = 1.3. The two-bay X-CBF is placed on the long side of the buildings. This leads to larger axial gravity loads in the columns. The total seismic weight of the building is 9935 kN, the gravity loading on the frame columns for the load combination including seismic effects is 281 kN, and the leaning column axial force applied in the numerical model is 1403 kN. With the final sections, the fundamental period of the building is equal to 0.37 s by hand calculation and the corresponding design base shear is 714 kN for each braced frame, including 5% of accidental torsion.

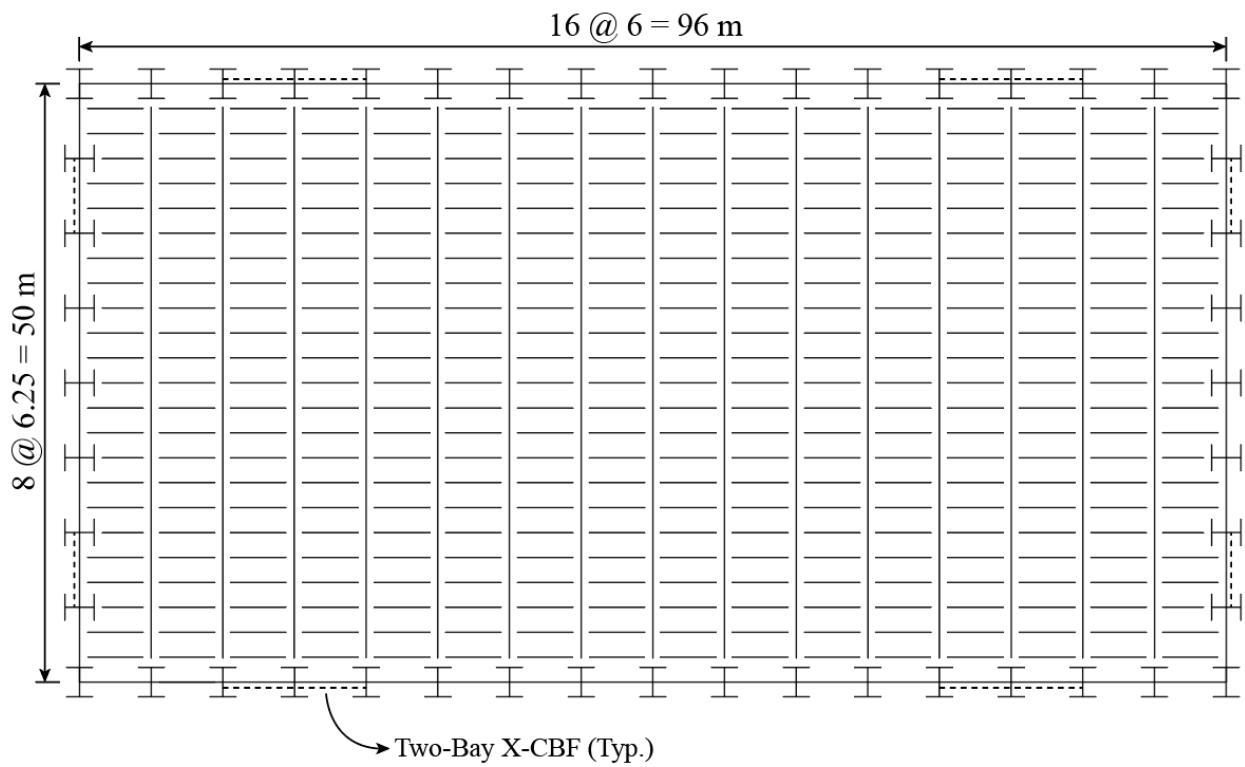

Figure 7.2 Building geometry of the studied two-bay X-CBFs

The selection of the braces is realized in a similar manner to what is presented in Chapter 3. With the conditions described above, the factored axial load in each brace is 478 kN, including 25 kN from gravity loading. With a member length of 15 m and a K factor of 0.45, HSS 152x152x7.9 are selected.

The axial load in the roof beam coming from the condition where braced have reached C'_{prob} and T_{prob} is equal to 652 kN. Gravity loading produces a strong axis bending moment of 12.6 kN-m and a W200x52 section is selected.

The interior column is designed under gravity loads only, as lateral loading does not induce any axial or flexural demand when using static analysis. Therefore, the factored compression load is determined under 1.25D + 1.5S. For in-plane buckling, it is considered that the tension brace provides an appropriate lateral restraint at all times at mid-height of the column. The effective lengths for in-plane buckling and out-of-plane buckling are respectively taken as 4.5 m and 9.0 m, regardless whether a strut is present or not. A W200x46.1 section is selected to resist the 640 kN axial compression load.

The exterior columns are designed for the seismic load combination: 1.0D + 1.0E + 0.5L + 0.25S. When a strut is used, the effective lengths are the same as the interior column. When no strut is used, both bucking lengths are taken equal to 9 m. The factored axial compression load is equal to 1504 kN. Furthermore, an in-plane bending moment equal to $0.2Z_yF_y$ is considered, similar to what is required for multi-storey CBFs. This was considered to account for the possibility of non-uniform brace yielding occurring in the top and bottom tiers, which would induce an axial load in the strut that would, in turn, induce in-plane bending in the exterior columns. As a result, a W310x158 section is selected for the configuration without a strut, and a W310x79 is selected for the configuration using a strut.

Finally, the strut is designed only to provide sufficient resistance and stiffness to laterally brace the exterior columns. No bracing is provided for torsion or out-of-plane buckling. As a result, an HSS 89x89x4.8 is selected. Figure 7.3 shows the final geometries and sections for the two frames.

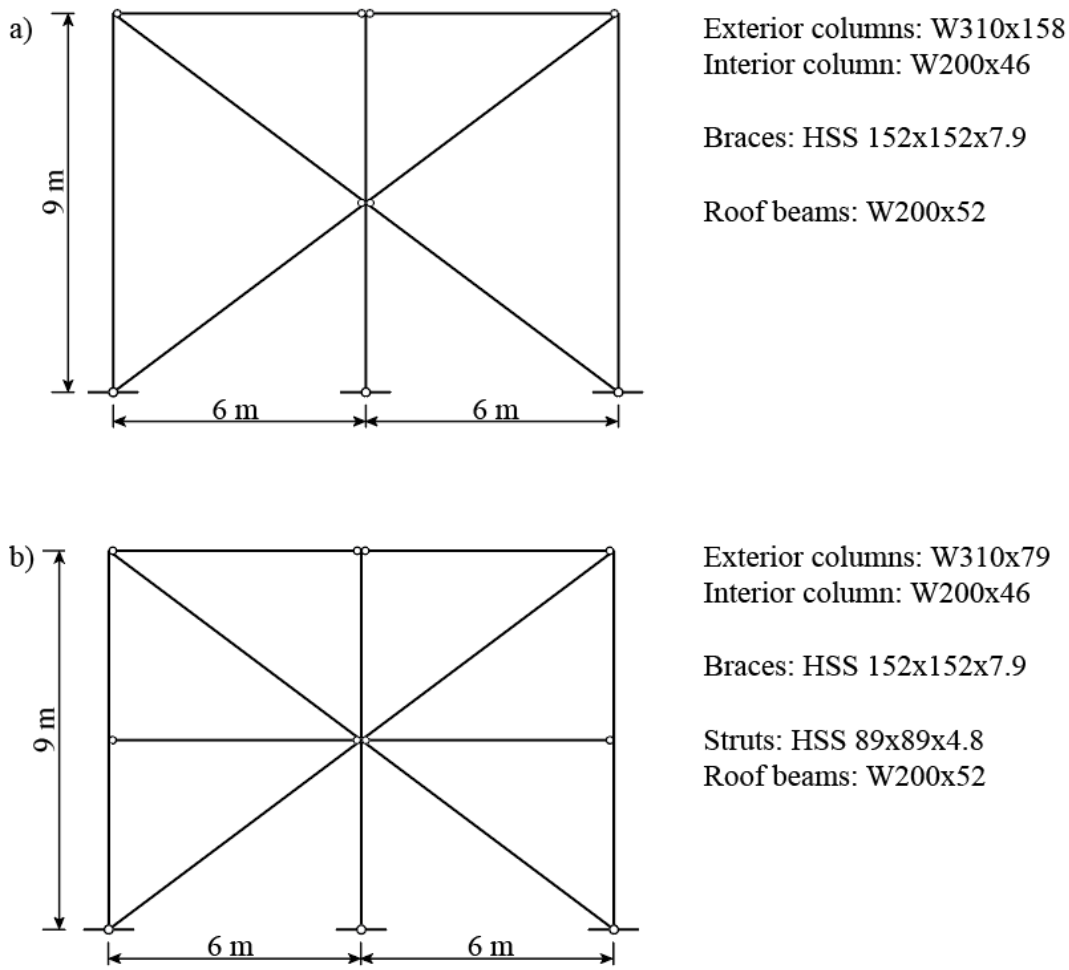

Figure 7.3 Geometry and sections of the studied two-bay X-CBFs: a) without strut; and b) with strut

7.2 Nonlinear response history analysis

NLRH analyses were realized using the model and ground motions presented in Chapter 4. The columns are considered pinned at their base for both in-plane and out-of-plane bending. At their tops, they are considered braced in the out-of-plane direction and for torsion. The yield strength of the braces is taken equal to R_yF_y = 460 MPa. As discussed previously, this ensures that the maximum loads are transferred to the columns after brace yielding. The columns are capacity-protected elements, and their specified yield strength is F_y = 345 MPa. Peak values presented in this section are obtained from the mean of the five most demanding ground motions for a given parameter.

7.2.1 Two-bay X-CBF without strut

The results from the configuration without an intermediate strut are first presented. Figure 7.4 shows the frame deformed shape at the yielding of the tension braces. For this frame, the period calculated manually is equal to 0.375 s while the period obtained from the *OpenSees* numerical model is equal to 0.366 s. This 2.4% difference is attributed to the inclusion of rigid elements representing brace gusset plates in the numerical model, thus making each brace shorter and stiffer.

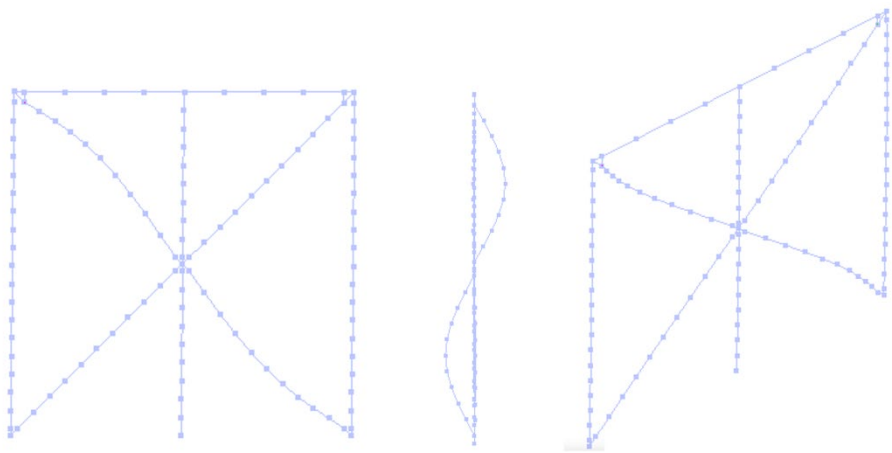

Figure 7.4 Deformed shape of the OpenSees numerical model at tension brace yielding of a two-bay X-CBF without strut (leaning column not shown)

Even though the frame has reached its maximum roof displacement, all three columns remain relatively straight and no disparity can be visually observed between the top and bottom brace segments. Table 7.1 shows peak values of key response parameters for the frame.

Table 7.1 Peak frame response for the two-bay X-CBF without strut

		Exterior Columns		Interior Column	
$\delta_{roof,NLRH}$ (% h_s)	$\delta_{roof,NLRH}/R_dR_o\delta_e$	M_{cy} / M_{py}	M_{cx} / M_{px}	M_{cy} / M_{py}	M_{cx} / M_{px}
0.57	1.30	0.05	0.022	0.05	0.056

As observed for the two-bay MT-CBFs examined previously, the maximum storey drift from NLRHA ($\delta_{roof,NLRH}$) is approximately 30% higher than that predicted in design ($R_dR_o\delta_e$). However, this did not cause any undesirable response or column instability. In fact, both in-plane and out-of-plane moments in the columns remained small. All moment values are taken at mid-height of the frame (M_{cy}, M_{cx}). Although no strut is present to impose a horizontal load to the columns, some flexure is still observed in the columns. This is attributed to the initial geometric imperfections and P-δ effects. As the frame is pushed towards its maximum lateral displacement, in-plane and out-of-plane initial geometric imperfections are amplified because of the axial loads and, with them, the bending moment. Strong axis moments are also produced at mid-height of the interior column by the out-of-plane buckling of the compression braces.

To further illustrate the frame behaviour, Figure 7.5 shows the frame response under the 1983 Coalinga 1983 ground motion. This ground motion was selected because it produces the largest displacement demand for both two-bay X-CBFs: with and without strut members. The largest drift peaks occur between 8 s and 9 s, when maximum brace axial force demand as well as the maximum in-plane bending demand in all three columns occur. The inclusion of a middle column does not negatively influence brace response, as top and bottom braces exhibit the same behaviour throughout the ground motion. Tension brace yielding occurs at 8.7 s, producing an axial force of 1528 kN in the compression column, which correlates well with the design prediction of 1504 kN. This 1.6% difference is mainly explained by strain hardening in the tension brace.

As explained above, maximum flexural demand in the columns occurs when peak displacement values are reached. The middle column curvature depends on the direction of the storey displacement, whereas the exterior columns tend to maintain the curvature imposed by the initial geometric imperfections. This can be seen by the negative in-plane bending moments for these columns.

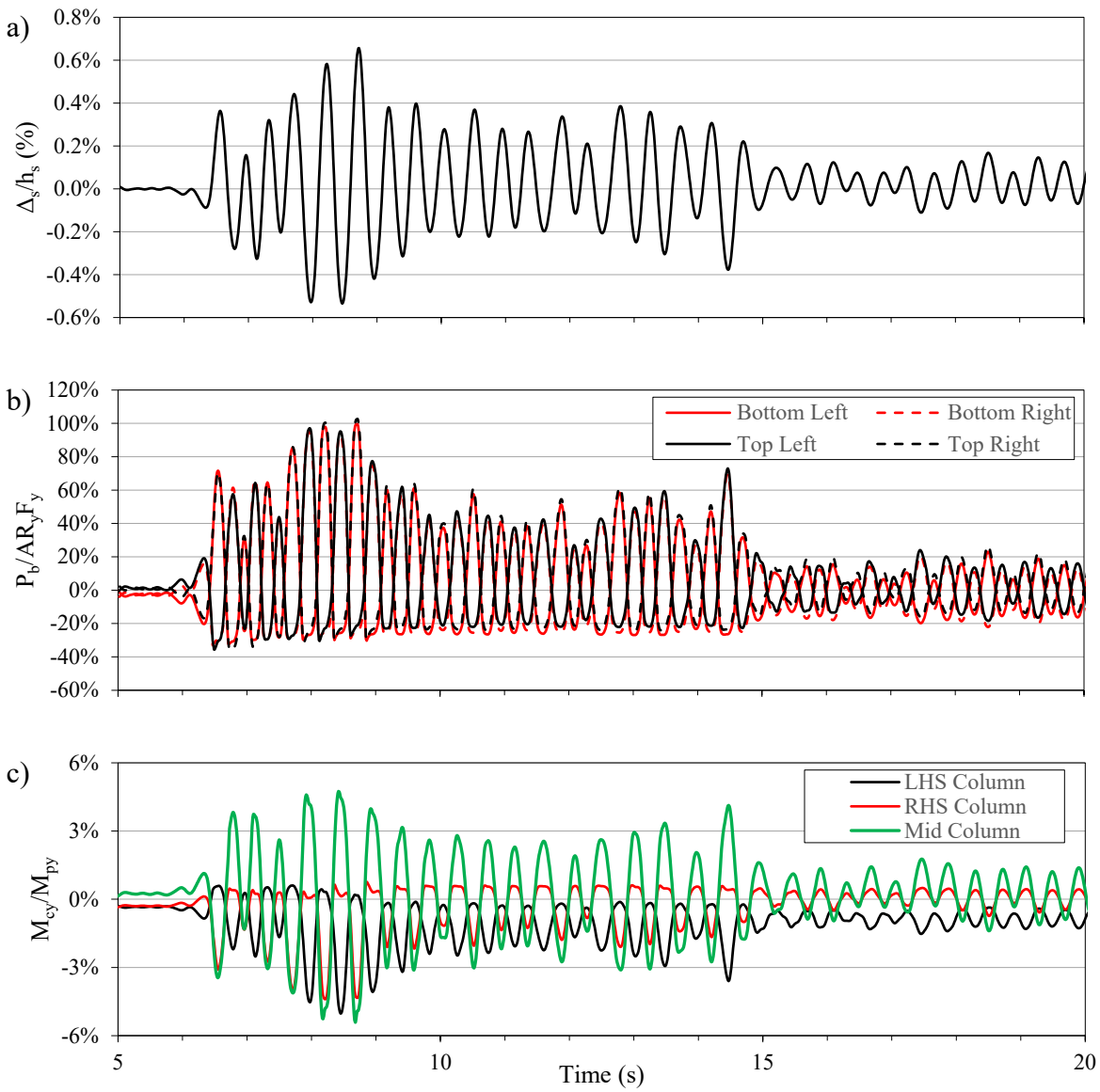

Figure 7.5 Two-bay X-CBF without strut response under 1983 Coalinga earthquake, Cantua Creek School record: a) storey drift; b) brace normalized forces; and c) in-plane column normalized moments

In summary, the seismic response of the frame corresponds well to a multi-storey CBF, where the addition of an intermediate column does not significantly affect the seismic behaviour. The design method underestimates the peak storey displacement, but member force demands remain at acceptable levels even though some bending moment is seen in the columns.

7.2.2 Two-bay X-CBF with strut

This section presents the seismic behaviour of a two-bay X-CBF with strut, as described above. This horizontal strut allows the column section to be reduced from a W310x158 to a W310x79, a 50% weight reduction. The fundamental period of the frame is slightly higher, due to the more flexible columns, and is equal to 0.39 s by hand calculation. *OpenSees* yields a similar result with a period of 0.38 s.

Figure 7.6 shows the deformed shape of the frame at brace buckling and at maximum lateral storey displacement. At brace buckling, the columns remain straight whereas at maximum lateral storey displacement some bending can be visually observed, more so in the compression column.

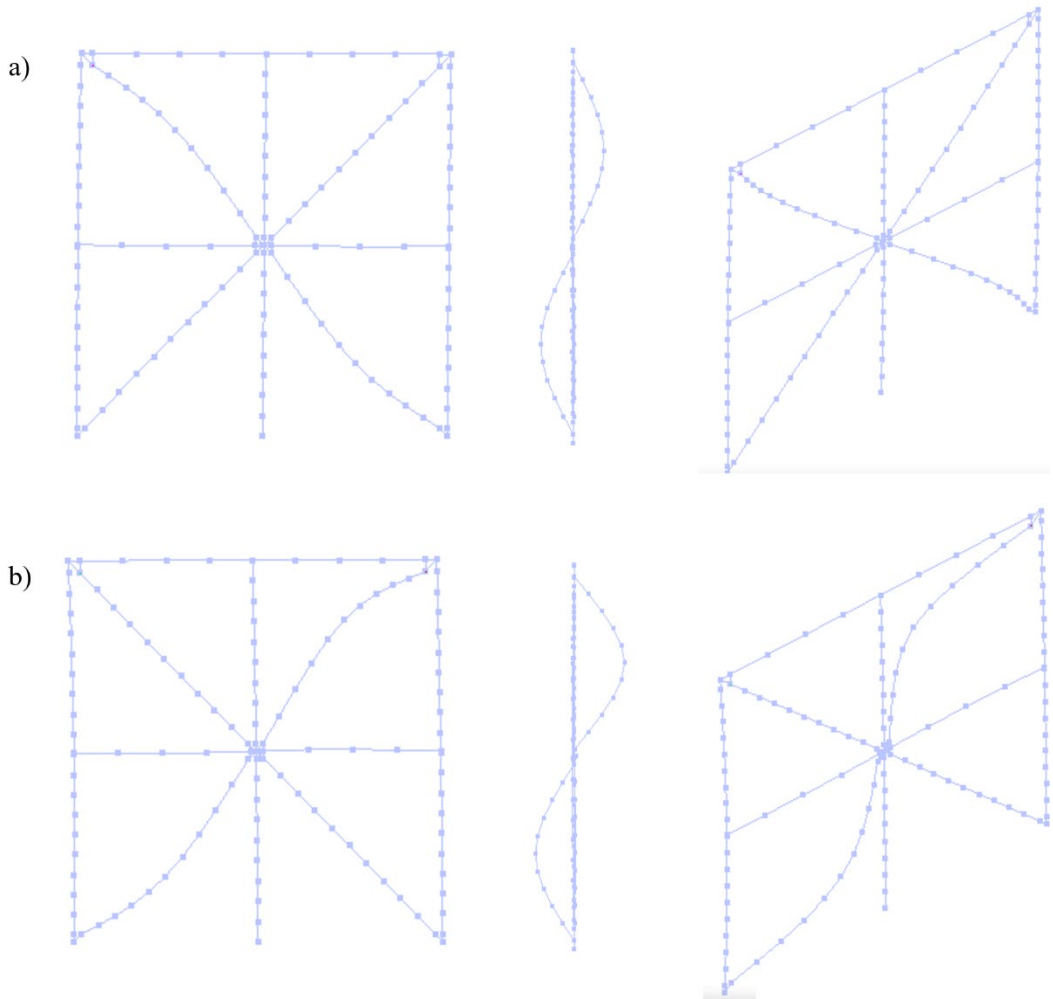

Figure 7.6 Deformed shape of the OpenSees numerical model of a two-bay X-CBF with strut: a) at first brace buckling; and b) at maximum roof displacement

Table 7.2 shows the maximum peak values from NLRH analyses for the two-bay X-CBF with intermediate strut. Peak drift demand is similar to that observed in the previous frame, since drifts are mainly governed by brace response and stiffness. As the deformed shape suggests, significant in-plane flexure occurs in the exterior columns (M_{cy}). For this frame geometry and configuration, the design assumption of $0.2M_{py}$ correlates very well with the bending moments from NLRHA.

Table 7.2 Peak frame response parameters for the two-bay X-CBF with strut

		Exterior Columns		Interior Column	
$\delta_{roof,NLRH}$ (% h_s)	$\delta_{roof,NLRH}/R_dR_o\delta_e$	M_{cy} / M_{py}	M_{cx} / M_{px}	M_{cy} / M_{py}	M_{cx} / M_{px}
0.59	1.29	0.20	0.058	0.033	0.055

The interior column is not heavily loaded in bending, since it is placed at the neutral axis of the frame and the top and bottom brace responses are nearly the same. Furthermore, the addition of the intermediate strut contributes to reducing the in-plane bending in this column. Because the strut is relatively rigid axially, all column nodes at mid-height of the frame move together and experience very close horizontal displacement values. This benefits the interior column, which has significantly lower flexural stiffness than the exterior columns.

Figure 7.7 presents the frame response under the 1983 Coalinga earthquake for drifts, brace forces and in-plane moments.

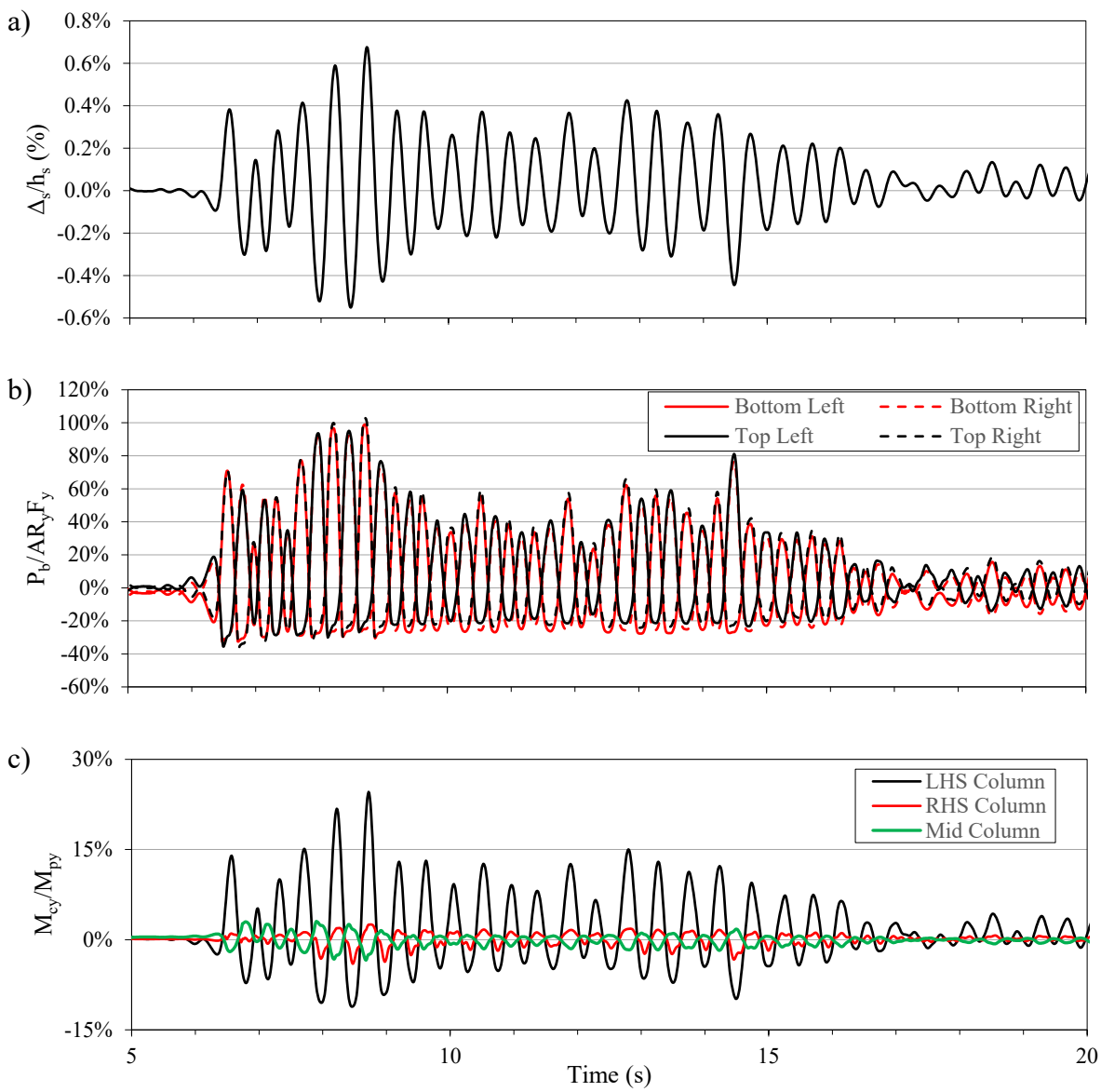

Figure 7.7 Two-bay X-CBF with strut response under 1983 Coalinga earthquake, Cantua Creek School record: a) storey drift; b) brace normalized forces; and c) column in-plane normalized moments

Peak drift values reaching a maximum value of 0.66% of the storey height are observed between 8 s and 9 s. Brace response is again very similar in bottom and top braces, with no significant portion of the effort being transferred to the strut or interior column. One yielding cycle can be seen at maximum roof displacement, which coincides with the maximum in-plane bending demand in the columns. Although moments remain similar in the interior and right hand-side columns, the

left-hand side column reaches 25% of its plastic moment when in compression. This load case is critical for column stability. This higher flexural demand in the left-hand side column can be partly explained by the initial geometric imperfections that correspond to the deformed shape shown in Figure 7.6 b. This higher bending demand in the left-hand side column is also attributable to the Coalinga 1983 earthquake, as other records showed in-plane moments concentrated in the right-hand side column. Figure 7.8 shows the axial deformation of the top right and bottom left braces for the Coalinga 1983 earthquake.

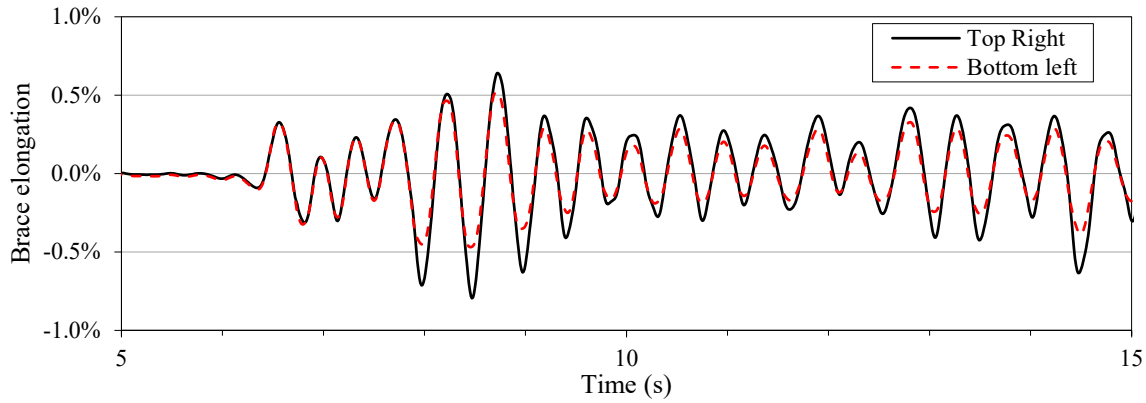

Figure 7.8 Two-bay X-CBF with strut response under Coalinga 1983 earthquake, Cantua Creek School record: brace axial elongation

The top braces in the two-bay X-CBF with an intermediate strut buckle first, resulting in more out-of-plane displacement than the bottom braces. Over a couple cycles, the top braces axial deformation is larger than for the bottom braces. This induces an additional displacement at the frame center, which the tension braces and the middle column are capable to counteract slightly. Some of this displacement, however, is transferred by the strut to the exterior columns. Furthermore, when the frame reaches large roof displacements towards the left, the intermediate strut acts as a support for the column in compression. In consequence, a parallel can be made between this column and a beam on two supports with an overhang. The mass applied at the roof level represents a load on the beam overhang and in-plane bending develops because of the non-linear deformed shape. At these peak displacements, the intermediate strut is loaded in tension, supporting the column at mid-height against larger displacements.

The flexural demands sustained by the columns of the studied frame are larger when an intermediate strut is included. The average peak value of $0.20M_{py}$ is significant and must be considered in the design phase to ensure the stability of the columns following the philosophy of capacity-based design. In this study, an approximation of the in-plane moments in the exterior columns was made based on existing provisions for multi-storey CBFs. This assumption needs to be refined by studying additional frame geometries. Potentially, in-plane moment values could be extracted from averages observed in these different frames. Finally, the interior column did not exhibit any significant in-plane or out-of-plane bending, similar to the two-bay X-CBF without an intermediate strut. It is not anticipated that any additional design requirements are needed for this member.

7.2.3 Accounting for brace yield strength variability in two-bay X-CBFs

The two two-bay X-CBFs studied above were analyzed again bi assigning 90% R_yF_y to the bottom brace halves. Table 7.3 presents the peak results for the two configurations. For bending moments, only in-plane demand is presented as the out-of-plane moments remained similar to the previous analyses.

Table 7.3 Peak response from NLRHA of the two-bay X-CBF with and without strut when using 90% of R_yF_y in bottom braces

Frame	$\delta_{roof,NLRH}$ (% h_s)	$\delta_{roof,NLRH}/R_dR_o\delta_e$	Exterior column M_{cy} / M_{py}	Interior column M_{cy} / M_{py}
Without strut	0.58	1.32	0.04	0.092
With strut	0.59	1.29	0.18	0.063

Storey drifts see a slight increase compared to the analyses where R_yF_y was specified to the braces due to earlier yielding of the bottom braces. Compared to the previous analyses, the flexural demand on exterior columns is 16% and 13% lower for the frame without an intermediate strut and the frame with an intermediate strut respectively. This is due to the lower probable brace resistances, which produces lower axial loads in the columns and higher flexural stiffness because of smaller P-δ effects.

In contrast, in-plane flexural demand is increased in the interior column by 84% and 91% for the configuration without strut and the one with strut, respectively. At peak storey displacement, the bottom tension brace yields first, resulting in a large inelastic deformation in this tier. Then, the top tension brace, as well as the interior column, contribute to the in-plane lateral stiffness in limiting the inelastic deformations in the bottom tension brace. This increase in flexural demand on the interior column is not deemed critical for its stability, as it remains laterally restrained by the elastic tension brace and the strut when present. In an extreme scenario, if a plastic hinge was to develop in the interior column at mid-height of the frame, the gravity axial load could still be carried by the member. The column would effectively become pinned at its mid-height, while still benefitting from the restraint of an elastic spring provided by the struts and braces.

CHAPTER 8 SEISMIC BEHAVIOUR OF A SPLIT-X CBF

This chapter presents the results obtained from the NLRH analysis of the split-X CBF. This bracing system is commonly used for tall single-storey buildings, as it often becomes economical to laterally brace the columns at their mid-height to reduce their weak axis buckling length about their section weak axis. Similar to the MT-CBFs and the two-bay X-CBFs studied in Chapter 6 and Chapter 7, respectively, it is anticipated that non-uniform yielding of the tension braces will occur and produce in-plane bending demand in the columns through an horizontal load carried by the strut. The frame geometry was selected and used in design. The design procedure and assumptions are first presented, followed by the observations and the interpretation of the results from NLRH analyses.

8.1 Split-X CBF design

The prototype building studied for the split-X CBF is the same as what was considered for two-bay 2T-CBFs in Chapter 6. Its dimensions are 85 m by 35 m, with the split-X CBF placed on the long side. The building is located in Vancouver, BC, on a Class E site. The total building seismic weight is 6803 kN and the calculated fundamental period with the final sections is equal to 0.41 s. As such, the design seismic force acting on one split-X braced bay is 489 kN.

The braces must resist a factored compression load of 424 kN, including 20 kN from gravity loads. With a length of 11.4 m and a K factor of 0.45, an HSS 127x127x7.9 section was selected. The factored axial compression load in the columns is 1546 kN, and an in-plane bending moment equal to $0.2Z_yF_y$ was considered in anticipation of a non-uniform brace yielding. The strut provides in-plane lateral bracing to the columns, resulting in a W310x79 section. The strut itself is designed to provide the required stiffness and strength to laterally brace the column, and an HSS 76x76x4.8 is selected. Figure 7.2 illustrates the geometry and final sections of the designed split-X CBF.

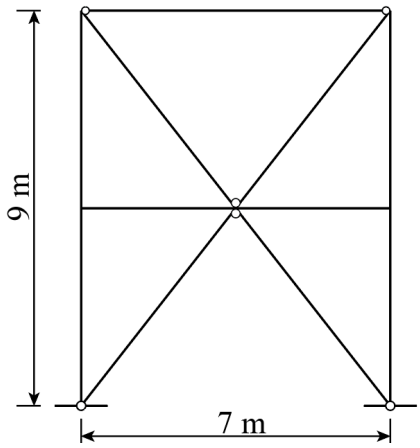

Columns: W310x79

Braces: HSS 127x127x7.9

Strut: HSS 76x76x4.8
Roof beam: W200x52

Figure 8.1 Geometry and sections of the studied split-X CBF

8.2 Nonlinear response history analysis

The numerical model and ground motions presented in Chapter 4 were used to conduct the following NLRH analyses. The columns are considered pinned at their base for both in-plane and out-of-plane bending. The columns are considered braced in the out-of-plane direction and for torsion. The yield strength of the braces is taken equal to R_yF_y = 460 MPa, while columns are specified with F_y = 345 MPa. Peak values presented in this section are obtained from the mean of the five most demanding ground motions for a given parameter.

The fundamental period of the frame obtained by hand calculation is 0.413 s, while the *OpenSees* model has a fundamental period of 0.406 s. Figure 8.2 shows the frame deformed shape at various points during the 1989 Loma Prieta earthquake. This record was selected because it is representative of the overall frame behaviour and produces the highest peak drifts.

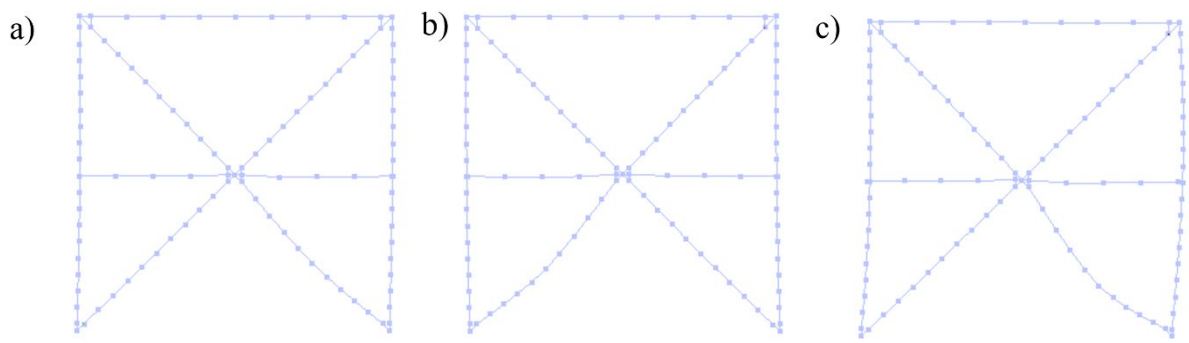

Figure 8.2 Deformed shape of the OpenSees numerical model of a split-X CBF under the Loma Prieta 1989 earthquake, Hollister Differential Array: a) at first discontinuous brace buckling, b) at first discontinuous brace buckling; c) at maximum roof displacement

Out-of-plane deformations of braces after buckling are more pronounced in the bottom two braces. The bottom braces are slightly longer than the top ones and they do not intersect with the roof beam. It can also be observed that significant in-plane bending of the columns occurs during the seismic event, when the frame reaches peak displacement values. Table 8.1 presents peak drift and moment values for the frame.

Table 8.1 NLRHA mean values for the studied split-X CBF

Parameter	Value
$\delta_{roof,NLRH}$ (% h_s)	0.61
$\delta_{roof,NLRH}/R_dR_o\delta_e$	1.22
$M_{cy,\ NLRH}$ / M_{py}	0.19
$M_{cx,\ NLRH}$ / M_{px}	0.068

As already observed for other bracing configurations, the peak storey drift is underestimated in design. For this split-X CBF, the peak storey drift remains well below the 2.5% code limit at 0.67% of storey height, but this still represents an increase of 26% over the predicted values. Out-of-plane moments in the columns correlate with what was noted for other bracing systems, with the most

probable explanation attributed to the amplification of the initial deformed shape at large storey displacement. The plastic hinge forming in the gusset plates at brace buckling also produces out-of-plane moments at the column extremities.

The in-plane flexural demand on the column reached 18.5% of the member's plastic moment. To further examine the frame response and determine the points at which this demand occurs, response histories the 1989 Loma Prieta earthquake are plotted in Figure 8.3.

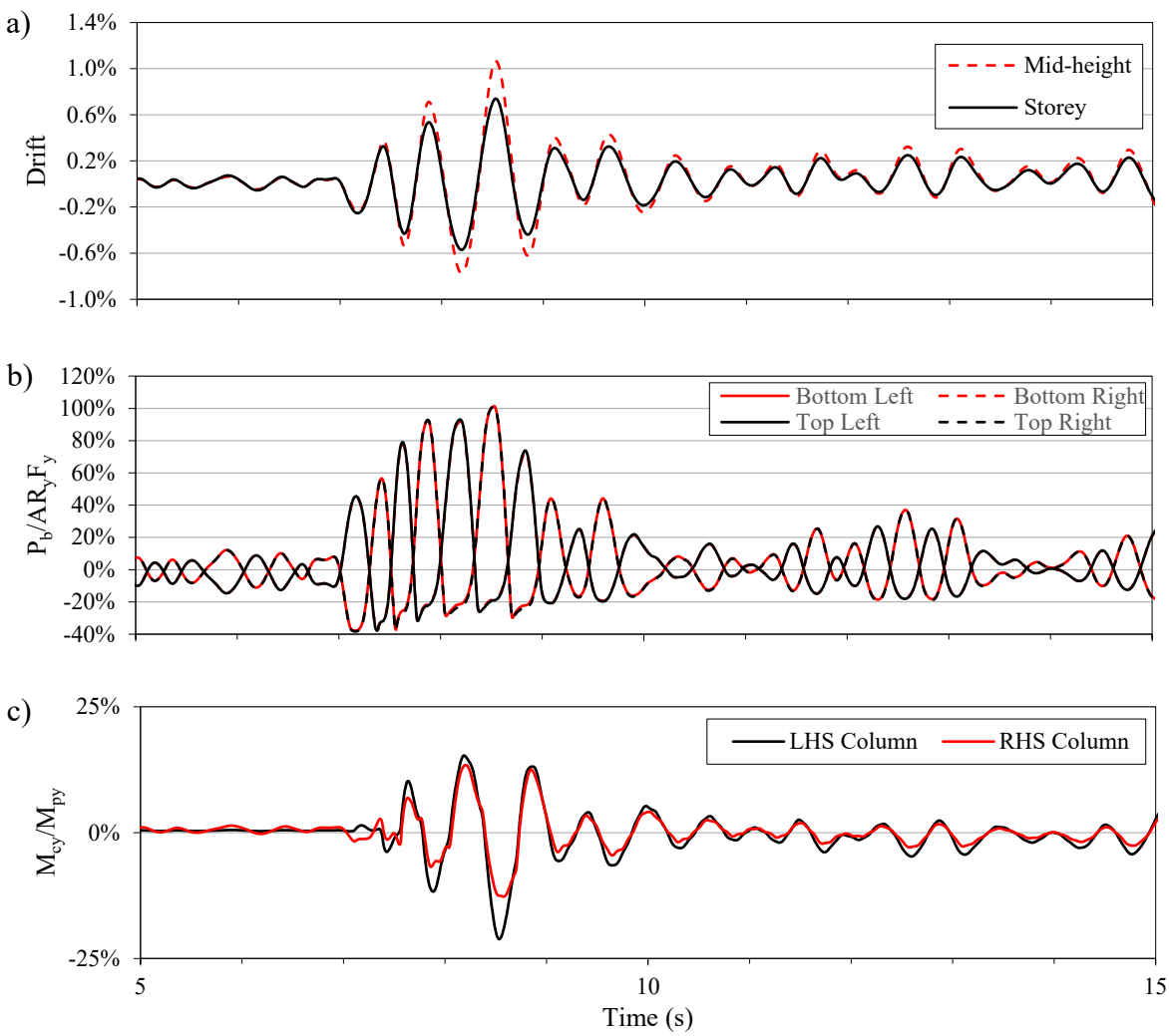

Figure 8.3 Split-X response under the 1989 Loma Prieta earthquake, Hollister Differential Array: a) drifts; b) braces normalized forces; and c) column in-plane normalized moments

Peak in-plane flexural demand is induced in the compression column at t = 8.6 s, in combination with a 1559 kN column axial load. This agrees well with the design axial load of 1546 kN. This peak flexural demand is well approximated by $0.2M_{py}$ considered in design. In contrast to the two-bay X-CBF with an intermediate strut studied in Chapter 7, most of the column deformation is concentrated in the lower half of the frame. This can be observed on Figure 8.3 a) where the drift at mid-height of the frame is larger than the storey drift. For the split-X CBF, the strut does not act as a support for the column in compression. Conversely, it pushes the column further creating a non-uniformity over the frame height. To further analyse this behaviour, Figure 8.4 shows the displacement of the brace intersection node. This node is located at the center of the frame, representing the middle of the through plate connecting the braces to the strut. Out-of-plane displacement is traced relative to the frame center-line. In-plane displacement is plotted relative to the expected displacement at mid-height if the deformation was linear using:

$$\partial_{relative,in-plane} = \partial_{in-plane} - \frac{\partial_{roof}}{2} \qquad \text{(Eq. 8-1)}$$

The relative in-plane displacement calculated with (Eq. 8-1 highlights the additional displacement caused by the concentration of drift in the bottom half of the frame. If drift was well distributed throughout the frame height, the deformed shape would be linear and the relative in-plane displacements in Figure 8.4 a) would remain close to null.

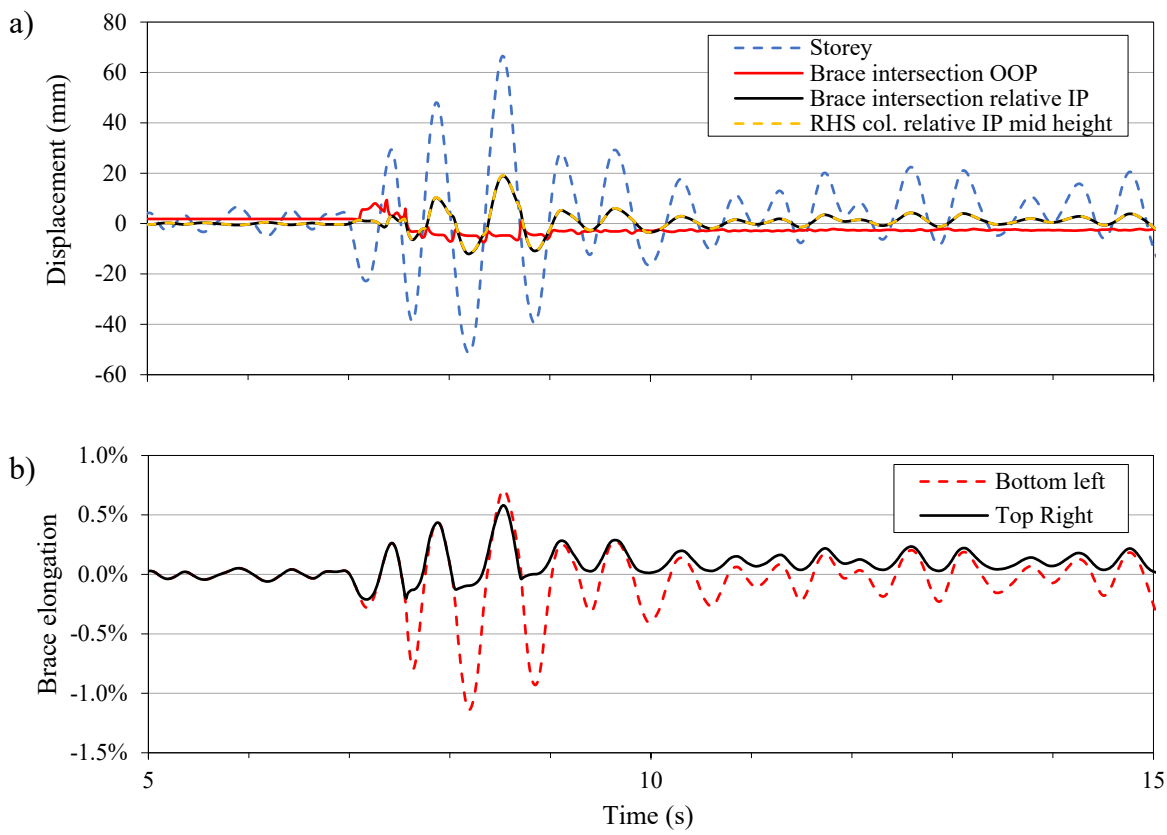

Figure 8.4 Split-X response under the 1989 Loma Prieta earthquake: a) in-plane and out-of-plane displacement of the brace intersection node; and b) brace elongation

In the out-of-plane direction, the brace intersection node starts to veer towards the positive *Z* direction, but after the first cycle of brace buckling at 7.6 s it is reversed in the negative *Z* direction and oscillates around a residual displacement of -5 mm. Throughout the ground motion, the center node never comes back to its precise location, as residual deformations exist in the braces due to buckling and elongation upon yielding in tension. This out-of-plane displacement produces in-plane and out-of-plane flexural demand in the columns. At the end of the record, residual in-plane moments are present in the columns and are partly due to the residual displacement remains at the brace intersection.

In the in-plane horizontal direction, the intersection of the braces follows the global movement of the frame but is pushed further than half of the storey displacement when large axial demands are produced in the braces. Because of the strut, the brace intersection point undergoes the same

displacement as the column at mid-height, as seen in Figure 8.4. As discussed above, this creates an effect where the strut pushes the column in compression, producing in-plane flexure. This effect is larger than in two-bay X-CBFs, as the interior column was able to contribute to the stabilization of the brace intersection point. In this split-X CBF, difference in brace axial deformation induces an additional horizontal load in the strut, which is transferred to the columns at their mid-height. Figure 8.4 b) shows the axial deformation for the bottom left and top right braces, which are in tension when the right-hand side column is loaded in compression. Because of its higher length, the bottom left brace buckles first, resulting in overall higher elongation over multiple cycles. The top right brace does not buckle as much, and its overall axial deformation is limited. This differed buckling induces in-plane displacements of the brace intersection connection and uneven drifts in the bottom and top half of the frame. Thus, the frame does not benefit from the inclusion of an intermediate strut, as it produces unwanted flexural demand. However, if adjacent gravity columns were to be similarly braced at mid height, this horizontal load would be transferred to adjacent struts. This would allow for the gravity column to participate in the overall lateral stiffness, reducing the bending demand in a single braced frame column, as studied previously by Imanpour, Auger, and Tremblay (2016). This would have to be explicitly considered in design to satisfy the requirements for members loaded in axial compression and bending. Additional studies on different split-X CBF configuration would allow to quantify the effect of differed buckling of the top and bottom compression buckling. This could help improve the prediction of the in-plane flexural demand sustained by the columns.

Finally, reducing the specified yield stress of the bottom braces to 90% R_yF_y did not have a significant impact on the analyses results. Drifts remained similar, while in-plane and out-of-plane moments in the columns were slightly reduced. When the bottom tension brace yielded at a stress of $0.9R_yF_y$, the top tension brace did not develop additional axial forces as it was limited to the bottom brace resistance. Contrary to what was observed for two-bay MT-CBFs, considering the variation in brace yield stress did not yield to additional critical scenarios in regard of the column flexural demands.

CHAPTER 9 CONCLUSIONS AND RECOMMENDATIONS

In this chapter, the main findings of the study are summarized, and areas that would benefit from additional research are introduced.

9.1 Summary

This research project concentrated on the design and study of the seismic behaviour of two-bay multi-tiered concentrically braced frames, as well as two-bay X-CBFs and split-X CBFs. Such bracing systems are commonly used in tall single-storey buildings in North America and entail characteristics that can require additional attention in design. Namely, the formation of a critical tier can produce non-uniform drift response along the frame height and concentrate inelastic deformation in certain bracing members. A critical tier refers to the tier in which a bracing member yields in tension before the other ones in the braced frame. This bracing member can undergo large inelastic deformation, which leads to in-plane flexural demand on the frame columns in the case of traditional MT-CBFs.

The main purpose of this study was to evaluate the seismic response of the aforementioned bracing systems in regard to what is currently provided in the Canadian seismic provisions. The presented frame designs and nonlinear response history analyses aimed at providing a better understanding of these systems, by highlighting their similarities and differences with current knowledge of MT-CBF seismic response.

This objective was achieved by conducting a thorough literature review, followed by the design of a two-tiered CBF according to the Canadian and American design standards. The two design approaches were compared to highlight the differences in design approach. A numerical model was then elaborated using the *OpenSees* program and validated against an *Abaqus* numerical. Six two-bay MT-CBFs were designed, varying the bay widths and the number of tiers. NLRH analyses were conducted on the six frames to assess their seismic behaviour. Two-bay X-CBFs with and without an intermediate strut were also studied in the same manner, followed by a split-X CBF.

9.2 Limitations of the study

Numerical models in this research project were constructed using the *OpenSees* program to further the understanding of MT-CBFs. The ability of this numerical program to simulate inelastic

behaviour of steel structures has been demonstrated in the past (Imanpour, Tremblay, Fahnestock, et al., 2016), but still comprises its limitations. Namely, the inability of fiber-based elements to recreate local buckling emphasizes the need for adequate material calibration and validation of inelastic behaviour. As an added consequence, lateral-torsional buckling can not be simulated. This type of failure is known to be a possibility in MT-CBF columns (Imanpour, Tremblay, Davaran, et al., 2016).

The selected geometries and buildings studied in this thesis were based on assumptions concerning current practice. This research work did not aim at drawing conclusions for bracing systems with geometries and sections other than the ones studied, as the seismic response can vary significantly depending on the frame geometry, location and practical considerations.

9.3 Conclusions

First, the design of a two-tiered CBF in accordance with the Canadian steel design standard and the U.S. Seismic Provisions for Structural Steel Buildings allowed to point out key differences between the two methods. It was first determined that bracing members for an identical building would not be the same because of the large difference in force modification factors, in the American (R = 6.0) and Canadian (R_dR_o = 3.9) codes. Also, the design earthquake is different in both approaches, as the American provisions require that two-thirds of the risk-targeted maximum considered earthquake be considered (ASCE, 2016). Furthermore, the CSA S16-19 specifies that gravity contribution must be included for the selection of the braces. These previous factors, added to the slight difference in compression strength calculation, modifies brace selection for the same design base shear. In other words, for the same brace section, a braced frame designed following the American provisions will have a higher tributary seismic load than its Canadian counterpart. Next, the calculation of in-plane and out-of-plane bending moments in the columns differs between the two standards. CSA S16-19 requires a progressive yielding analysis of the frame to be realized, where the tension braces in non-critical tiers are considered elastic. On the contrary, AISC 341-16 provides a calculation method that assumes that tension braces in both tiers have reached their probable tensile resistances. For the studied 2T-CBF, the second approach resulted in significantly higher in-plane moments. Both approaches use out-of-plane notional loads to represent the influence of brace buckling on the columns, but the calculation methods. For the 2T-CBF studied in Chapter 3, the resulting out-of-plane bending moment in the columns from the American design

was 90% than the Canadian design. Despite this, the difference in calculation of the in-plane bending moment has a more significant impact on member selection for the columns and typically leads to heavier sections when using the American design method.

Second, the current CSA S16-19 design method for MT-CBFs was applied for a two-bay MT-CBF. This method considered progressive yielding possibilities in tiers and adjacent bays. NLRH analyses were conducted on two-tiered and three-tiered prototype frames. The main findings from these analyses are summarized as follows:

- For all frames studied, storey drifts from NLRHA remained below the limit of 2.5% prescribed in the NBCC. However, drifts predicted in design were consistently underestimated by a factor of 1.29 on average.
- Progressive yielding mechanisms were well captured in design. The multiple critical tier scenarios considered in the design procedure were well reproduced by varying brace yield stress in the analyses.
- In single-bay MT-CBFs, progressive yielding mechanisms can be propagated between tiers. This was noted in Chapter 5 where yielding of the bottom tier occurred first, followed by the top tier. In two-bay MT-CBFs, this same phenomenon was observed. However, the horizontal propagation of tier yielding was also introduced. In these frames, yielding of tension braces can be propagated from the critical tier to any adjacent tier, depending on their probable shear resistances. To ensure an appropriate selection of column sections, these multiple critical tier scenarios must be considered in the design phase.
- In-plane bending demands in the columns were accurately predicted when using an appropriate roof displacement in design. However, for the designed frames, the CSA S16 design procedure consistently overestimated in-plane flexural demand. It was identified that this discrepancy was due to the compression brace forces in the non-yielded tiers reaching values close to the post-buckling probable brace resistances (C'_{prob}), whereas the design method assumes a value equal to the probable resistance at brace buckling (C_{prob}). The considered design procedure is deemed efficient, yet conservatory. In fact, using exact values from NLRHA for the compression braces can be time consuming since nonlinear models similar to the one used in this thesis are not a common occurrence in practice for buildings such as the ones presented in this study.

- Out-of-plane flexural demand in the columns was largely overestimated in design. NLRH analyses showed, however, that this demand reached its maximum value at brace buckling, as predicted in design.
- For the two-bay two-tiered non-uniform 6- and 8-m bays configuration, no tier yielding was observed as the shear demand in the braces was being well distributed among the different tiers. This was attributed to a design coincidence and can not be applied to all two-bay MT-CBFs. Scaling up one critical ground motion produced yielding in the critical tier and showed that the anticipated design scenarios are likely to occur under higher seismic loading. Therefore, the design procedure that was used to design this frame is still deemed appropriate to capture the possible yielding mechanisms in the braced tiers. However, to ensure that these mechanisms can be captured in design without conduction NLRHA, the brace yield stress in tiers adjacent to the critical tier could be reduced. For example, to remain conservatory, these frames could be designed assuming a 10% reduction in brace yield stress for the non-critical tiers.
- The overall seismic behaviour is satisfactory, with drift demands, brace axial load demands, and column flexural demands remaining under acceptable levels and accurately predicted by the design method.
- In view of the previous conclusions, two-bay MT-CBFs represent a viable bracing system that can provide sufficient seismic resistance when using a design method that considers progressive yielding between tiers and bays. This was the case for all bracing configurations studied, including those using uneven bay width and different bracing members. From the results of this research project, it does not seem that there is any contraindication to their usage in seismic resisting bracing systems in Canada.

Third, the design and study of the seismic behaviour of two-bay X-CBFs was realized. Configurations with and without an intermediate strut were studied. The main findings for this bracing configuration are as follows:

- Both frames showed an acceptable drift response. Top and bottom braces showed largely the same axial forces values and no unbalanced load due to different brace axial forces was transferred to the strut when it was included.

- The two-bay X-CBF without strut showed satisfactory seismic behaviour, with little in-plane flexural demand being induced in the exterior and interior columns. As a result, no additional design provision is required for this frame, as it is currently the case in CSA S16-19.
- The two-bay X-CBF with an intermediate strut exhibited peak in-plane bending moments in the exterior columns reaching 20% of the member's plastic moment about its weak axis. This was due to the strut acting as a horizontal support for the exterior columns at their mid-height, inducing a non-uniform in-plane deformed shape. Non-uniform brace axial deformation in the top and bottom half of the frame further increased the in-plane flexural demand in the columns. In current Canadian design provisions, no special design provision is present for this system. However, in view of the studied frame, in-plane bending must be considered when selecting a column section as it might be critical for member stability. Further geometries should be studied to provide appropriate design requirements for two-bay X-CBFs using intermediate struts.
- The interior column of the two-bay X-CBF with an intermediate strut did not exhibit significant in-plane or out-of-plane bending demand. As a result, it is not deemed necessary to include any special design consideration for this column.
- Accounting for variability in brace yield stress showed an increase in the in-plane flexural demand for both interior and exterior columns. This bending moment demand was considered for exterior columns in design, but not for the interior column. For the configuration without an intermediate strut, the intersection of the braces with the interior column produced large in-plane displacements after tension brace yielding, which led to in-plane bending of that column.

Last, a split-X CBF was designed and studied through NLRH analyses. The main findings for the split-X CBF studied are as follows:

- Storey drifts are found to be acceptable. Drifts remained under the 2.5% limit found in the NBCC. Brace behaviour resembles to the one typically observed for CBFs, where there is no major discrepancy in axial forces between top and bottom braces.
- A significant amount of in-plane flexural demand is induced in the columns with peaks reaching 19% of M_{py}. This is attributed to the difference in brace axial deformation in top

and bottom members. The bottom braces exhibited larger deformations following large out-of-plane displacement at buckling than the top braces. This led to the brace intersection sustaining in-plane lateral displacements. Axial loads were thus transferred to the strut, and subsequently to the columns. It is found important to assess the magnitude of the in-plane flexural demand on the columns using different split-X CBF configurations in the aim to propose updated design provisions which would ensure appropriate column resistance and stability.

9.4 Recommendations for future research

Following the conclusions made for the structures studied, the following recommendations can be made for future research on MT-CBFs:

- The frames studied in this thesis have similar widths and heights, as well as similar bracing members. Broader parametric studies should be performed to cover a wider range of frame geometries and brace sizes to improve our understanding of all three studied systems: two-bay MT-CBFs, two-bay X-CBFs and split-X CBFs. Such extended parametric studies should permit the development of design recommendations for future revisions of the current seismic provisions.
- Multi-tiered frames in CSA S16 provisions are currently limited to three tiers in height. For tall structures such as lighting towers or bridge piers, configurations with four or more tiers can be preferable from a practical standpoint, and future parametric studies could be extended to frames with a larger number of tiers, to examine their seismic performance and validate design methods.
- The buildings considered in this research project were all located in western Canada. Eastern Canada is also a zone of seismic activity, with earthquake ground motions richer in high frequency. Conducting NLRH analyses using designs and ground motions from eastern Canada would also broaden the conclusions on the seismic response and design of MT-CBFs.
- The proposed design method for two-bay MT-CBFs could be refined to consider the reduced forces in compression braces in the non-critical tiers. This would lead to a better approximation of the column flexural demands, and more economical designs.

- The *OpenSees* software could be improved to include elements that are able to capture local buckling and lateral torsional buckling, as it is not currently the case. This would significantly improve the dependability of the *OpenSees* models.
- Conducting an experimental program on individual bracing members and full-scale MT-CBF specimens would permit the validation of the numerical models developed in this project. The calibration of the *Steel02* material, as well as the base conditions for the columns represent two of the main factors that can heavily influence braced frame response. A thorough experimental program would permit to refining assumptions made in analysis and design.

BIBLIOGRAPHY

American Institute of Steel Construction. (2010a). *Seismic Provisions for Structural Steel Buildings (ANSI/AISC 341-10)*. Chicago, Ill.: American Institute of Steel Construction.

American Institute of Steel Construction. (2010b). *Specification for Structural Steel Buildings (ANSI/AISC 360-10)*. Chicago, Ill.: American Institute of Steel Construction.

American Institute of Steel Construction. (2016a). *Seismic Provisions for Structural Steel Buildings (ANSI/AISC 341-16)*. Chicago, Ill.: American Institute of Steel Construction.

American Institute of Steel Construction. (2016b). *Specification for Structural Steel Buildings (ANSI/AISC 360-16)*. Chicago, Ill.: American Institute of Steel Construction.

ASCE. (2016). *SEI/ASCE 7-16 Minimum Design Loads for Buildings and Other Structures*: American Society of Civil Engineers.

ASTM. (2015). *ASTM A1085, Standard Specification for Cold-Formed Welded Carbon Steel Hollow Structural Sections (HSS)*. West Conshohocken, PA: ASTM International.

ASTM. (2020). *ASTM A992, Standard Specification for Structural Steel Shapes*. West Conshohocken, PA: ASTM International.

Auger, K. (2017). *Conception parasismique des contreventements concentriques en treillis à segments multiples combinés aux poteaux gravitaires*.

Beaulieu, D., Picard, A., Tremblay, R., Grondin, G., & Massicotte, B. (2008). *Calcul des charpentes d'acier. Tome 1* (2e éd., 2e tirage revu. -- ed.). Markham, Ont.: Institut canadien de la construction en acier.

Beaulieu, D., Picard, A., Tremblay, R., Grondin, G., & Massicotte, B. (2010). *Calcul des charpentes d'acier. Tome 2* ([2e éd.?]. -- ed.). Markham, Ont.: Institut canadien de la construction en acier.

Canadian Standards Association. (2014). *Design of Steel Structures (S16-14)*. Toronto, ON: CSA Group.

Canadian Standards Association. (2019). *Design of Steel Structures (S16-19)*. Toronto, ON: CSA Group.

Cano, P., & Imanpour, A. (2018). *Evaluation of Seismic Design Methods for Steel Multi-Tiered Special Concentrically Braced Frames*.

Cano, P., & Imanpour, A. (2019). *Dynamic Analysis of Steel Multi-Tiered Special Concentrically Braced Frames*.

Cano, P. A. (2019). *Evaluation of the seismic design methods for steel multi-tiered concentrically braced frames*.

Chopra, A. K. (2007). *Dynamics of structures : theory and applications to earthquake engineering* (3rd ed.). Upper Saddle River, N.J.: Pearson Prentice Hall.

CSI. (2019). SAP2000 (Version 21.0.1). Berkeley, CA: Computers & Structures Inc. Retrieved from www.csiamerica.com

Dehghani, M., & Tremblay, R. (2015). Robust Period-Independent Ground Motion Selection and Scaling for Effective Seismic Design and Assessment. *Journal of Earthquake Engineering, 20* 1-34. doi:10.1080/13632469.2015.1051635

Fell, B., Kanvinde, A., Deierlein, G., & Myers, A. (2009). Experimental Investigation of Inelastic Cyclic Buckling and Fracture of Steel Braces. *Journal of Structural Engineering-asce - J STRUCT ENG-ASCE, 135*. doi:10.1061/(ASCE)0733-9445(2009)135:1(19)

Filiatrault, A. (2013). *Elements of earthquake engineering and structural dynamics* (3e édition. -- ed.). Montréal: Presses internationales Polytechnique.

Galambos, T. V., & Ketter, R. L. (1961). Columns under combined bending and thrust, Proc. ASCE, 85 (EM2), p. 1, (1959), (also ASCE

Trans. Vol. 126, (1961), Reprint No. 136 (61-22). *Fritz Laboratory Reports, 29*.

Gélinas, A. (2013). Étude expérimentale du comportement sismique des assemblages utilisés dans les contreventements en X en acier.

Helwig, T., & Yura, J. (1999). Torsional Bracing of Columns. *Journal of Structural Engineering-asce - J STRUCT ENG-ASCE, 125*. doi:10.1061/(ASCE)0733-9445(1999)125:5(547)

Heo, Y., Kunnath, S. K., & Abrahamson, N. (2011). Amplitude-Scaled versus Spectrum-Matched Ground Motions for Seismic Performance Assessment. *Journal of Structural Engineering, 137*(3), 278-288. doi:doi:10.1061/(ASCE)ST.1943-541X.0000340

Imanpour, A. (2015). *Seismic response and design of steel multi-tiered concentrically braced frames*.

Imanpour, A., Auger, K., & Tremblay, R. (2016). Seismic design and performance of multi-tiered steel braced frames including the contribution from gravity columns under in-plane seismic demand. *Advances in Engineering Software, 101*. doi:10.1016/j.advengsoft.2016.01.021

Imanpour, A., Stoakes, C., Tremblay, R., Fahnestock, L., & Davaran, A. (2013). *Seismic Stability Response of Columns in Multi-Tiered Braced Steel Frames for Industrial Applications*.

Imanpour, A., & Tremblay, R. (2012). *Analytical Assessment of Stability of Unbraced Column in Two-Panel Concentrically Braced Frames* (Vol. 4).

Imanpour, A., & Tremblay, R. (2016). Seismic design and response of steel multi-tiered concentrically braced frames in Canada. *Canadian Journal of Civil Engineering, 43*(10), 908-919. doi:10.1139/cjce-2015-0399

Imanpour, A., Tremblay, R., & Davaran, A. (2012). *Seismic performance of steel concentrically braced frames with bracing members intersecting columns between floors*.

Imanpour, A., Tremblay, R., & Davaran, A. (2014). *A New Seismic Design Method for Steel Multi-Tiered Braced Frames*.

Imanpour, A., Tremblay, R., Davaran, A., Stoakes, C., & Fahnestock, L. A. (2016). Seismic Performance Assessment of Multitiered Steel Concentrically Braced Frames Designed in Accordance with the 2010 AISC Seismic Provisions. *Journal of Structural Engineering, 142*(12). doi:10.1061/(asce)st.1943-541x.0001561

Imanpour, A., Tremblay, R., Fahnestock, L. A., & Stoakes, C. (2016). Analysis and Design of Two-Tiered Steel Braced Frames under In-Plane Seismic Demand. *Journal of Structural Engineering, 142*(11). doi:10.1061/(asce)st.1943-541x.0001568

Izvernari, C., & Tremblay, R. (2007). Modeling of the seismic response of concentrically braced steel frames using the OpenSees analysis environment. *Advanced Steel Construction, 2* 242.

Koval, I. (2019). Accounting for cold working and residual stress effects on the axial strength of HSS bracing members.

Lamarche, C.-P., & Tremblay, R. (2011). Seismically induced cyclic buckling of steel columns including residual-stress and strain-rate effects. *Journal of Constructional Steel Research, 67*(9), 1401-1410. doi:10.1016/j.jcsr.2010.10.008

McKenna, F., & Fenves, G. L. (2016). Open System For Earthquake Engineering Simulation (Version 2.5.0). University of California, Berkeley, CA: Pacific Earthquake Engineering Research Center (PEER). Retrieved from http://opensees.berkeley.edu/

National Research Council Canada. (2015). *National building code of Canada 2015*. (Fourteenth Edition. ed., pp. 1 online resource).

NRCC. (2017). *Structural commentaries (User's guide - NBC 2015: Part 4 of Division B)*: Ottawa : National Research Council of Canada, 2017.

Simulia. (2011). Abaqus (Version 6.14). Retrieved from www.simulia.com

Stevens, D., & Wiebe, L. (2019). Experimental Testing of a Replaceable Brace Module for Seismically Designed Concentrically Braced Steel Frames. *Journal of Structural Engineering (United States), 145*. doi:10.1061/(ASCE)ST.1943-541X.0002283

Tremblay, R., Archambault, M. H., & Filiatrault, A. (2003). Seismic Response of Concentrically Braced Steel Frames Made with Rectangular Hollow Bracing Members. *Journal of Structural Engineering-asce - J STRUCT ENG-ASCE, 129*. doi:10.1061/(ASCE)0733-9445(2003)129:12(1626)

Uriz, P., Filippou, F., & Mahin, S. (2008). Model for Cyclic Inelastic Buckling of Steel Braces. *Journal of Structural Engineering-asce - J STRUCT ENG-ASCE, 134*. doi:10.1061/(ASCE)0733-9445(2008)134:4(619)

Yura, J. A. (2001). Fundamentals of beam bracing. *Engineering Journal, 38* 11-26.

APPENDIX A LIST OF THE GROUND MOTION RECORDS USED IN NLRH ANALYSES

Table A.9.1 List of the ground motion records used in NLRH analyses

Ground motion file name	M	R (km)	Soil type	Event name	Record Station	Date	SF1	SF2
RSN778_LOMAP_HDA255	6.93	24.82	D	Loma Prieta	Hollister Differential Array	1989-01-01	1.286	1.052
RSN322_COALINGA.H_H-CAK270	6.36	24.02	D	Coalinga-01	Cantua Creek School	1983-01-01	1.859	1.052
RSN615_WHITTIER.A_A-DWN180	5.99	20.82	D	Whittier Narrows-01	Downey - Co Maint Bldg	1987-01-01	1.783	1.052
RSN614_WHITTIER.A_A-BIR180	5.99	20.79	D	Whittier Narrows-01	Downey - Birchdale	1987-01-01	1.168	1.052
RSN6959_DARFIELD_REHSS88E	7	19.48	E	Darfield_ New Zealand	Christchurch Resthaven	2010-01-01	1.394	1.052
EHM0160103241528_NS	6.8	47	D	Japan, Geiyo	IYO	2001-03-24	1.858	1.000
4354c_a.acc	7.7	137	D	El Salvador,	Ahuachapán	2001-01-13	2.297	1.000
YMG0180103241528_EW.acc	6.8	56	D	Japan, Geiyo	TOHWA	2001-03-24	1.513	1.000
BA01003u.smc.F1.a.acc	7.7	87.4103	E	El Salvador,	San Bartolo	2001-01-13	1.838	1.000
EHM0080103241528_EW.acc	6.8	44	D	Japan, Geiyo	MATSUYAMA	2001-03-24	1.445	1.000

Table A.9.1 List of the ground motion records used in NLRH analyses (cont.)

Ground motion file name	M	R (km)	Soil type	Event name	Record Station	Date	SF1	SF2
CHB0191103111446_NS.acc	9.1	227	E	Japan, Tohoku	KYONAN	2011-03-11	1.907	1.000
CHB0161103111446_EW.acc	9.1	190	E	Japan, Tohoku	MISAKI	2011-03-11	2.132	1.000
CHB0081103111446_NS.acc	9.1	186	E	Japan, Tohoku	URAYASU	2011-03-11	1.932	1.000
CHB0241103111446_NS.acc	9.1	179	D	Japan, Tohoku	INAGE	2011-03-11	1.990	1.000
NIGH081103111446_NS2.acc	9.1	203	D	Japan, Tohoku	TSUGAWA	2011-03-11	3.292	1.000

APPENDIX B CRITICAL GROUND MOTIONS STUDIED IN THIS THESIS

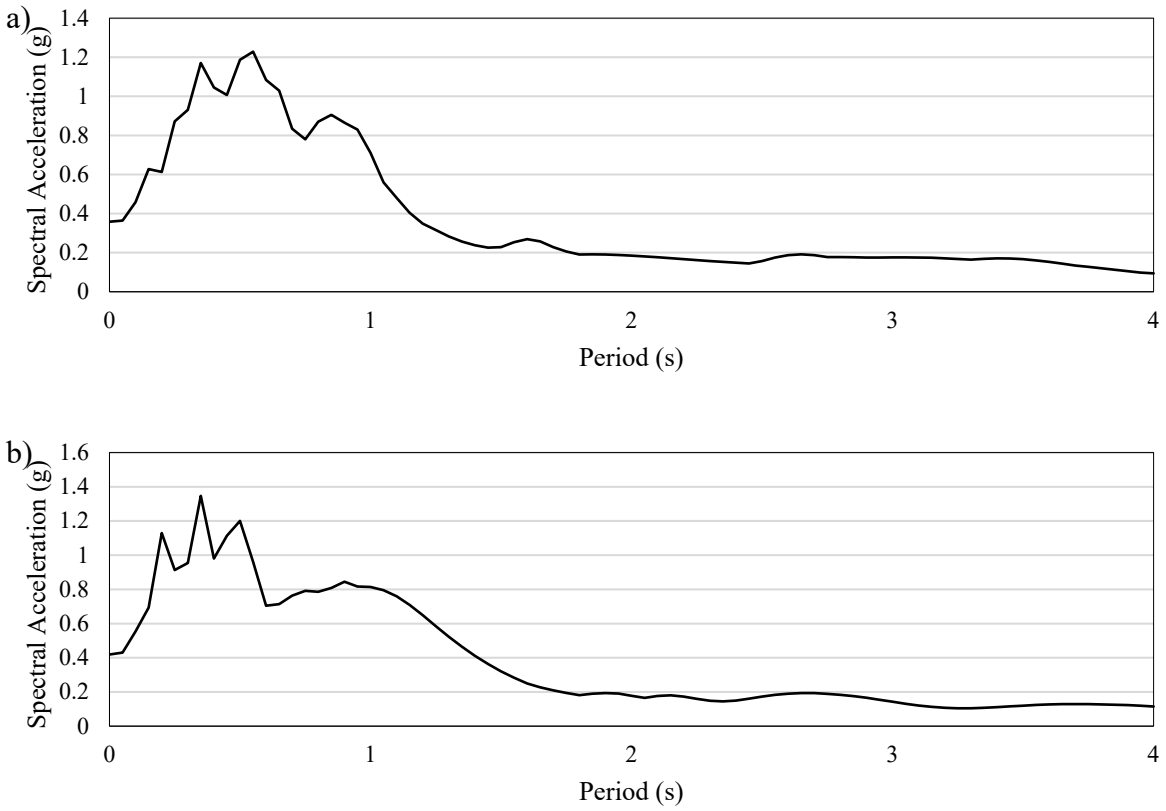

Figure B.9.1 Spectral accelerations of the critical ground motions: a) Loma Prieta 1989 earthquake, Hollister Differential Array record; and b) Coalinga 1983 earthquake, Cantua Creek School record

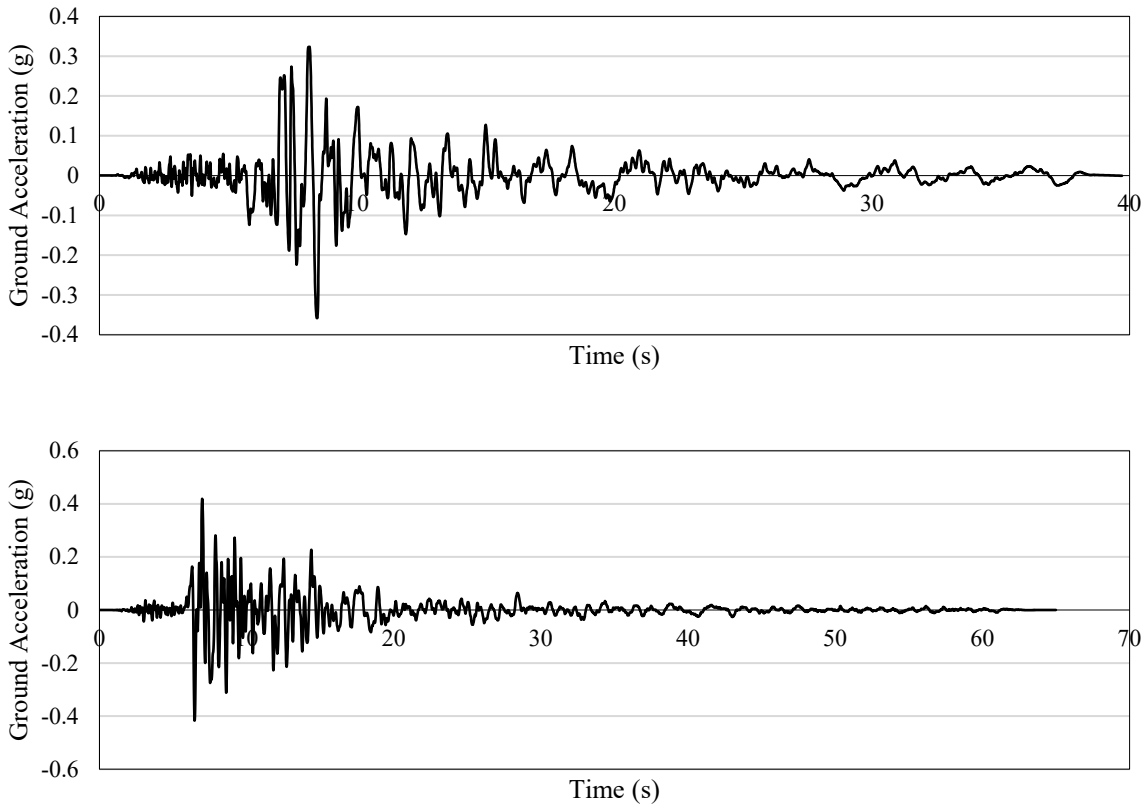

Figure B.9.2 Ground accelerations of the critical ground motions: a) Loma Prieta 1989 earthquake, Hollister Differential Array record; and b) Coalinga 1983 earthquake, Cantua Creek School record